



Lukas Rosenberger, BSc

Evaluation and Further Optimization of a Railway Axle Production Process

MASTER'S THESIS

for the purpose of obtaining the academic degree

Diplom-Ingenieur

Master's Degree Program Mechanical Engineering and Business Economics

submitted at

Graz University of Technology

Supervisor

Univ.-Prof. Dipl.-Ing. Dr.techn., Franz Haas

Dipl.-Ing., Matthias Steffan

Institute of Production Engineering

Graz, May 11, 2017

STATUTORY DECLARATION

I declare that I have authored this Thesis independently, that I have not used other than the declared sources/resources, and that I have explicitly marked all material which has been quoted either literally or by content from the used sources. The document uploaded in TUGRAZonline is identical with the Master's Thesis at hand.

EIDESSTATTLICHE ERKLÄRUNG

Ich erkläre an Eides statt, dass ich die vorliegende Arbeit selbstständig verfasst, andere als die angegebenen Quellen/Hilfsmittel nicht benutzt, und die den benutzten Quellen wörtlich und inhaltlich entnommenen Stellen als solche kenntlich gemacht habe. Das in TUGRAZonline hochgeladene Textdokument ist mit der vorliegenden Masterarbeit identisch.

May 11, 2017

(Date/Datum)



(Signature/Unterschrift)

Note of Thanks

I would like to thank

Institute of Production Engineering, especially

Mr. Univ.-Prof. Dipl.-Ing. Dr.techn. Franz Haas,

Mr. Dipl.-Ing. Matthias Steffan and

Mr. Ass. Prof. Dipl.-Ing. Dr.techn. Jörg Edler

for supervising this Master's Thesis and their encouragement and support.

Siemens MO MLT BG for enabling this Master's Thesis. Special thanks to

Mr. Dipl.-Ing. Gottfried Janisch for the care of this Thesis and

Mr. Dr. Ing. Bernd Jerzembek for his support and help.

Lucchini RS for the agreement to join this project, for the provision of production-related data and the great support throughout the whole project. Special thanks to

Mr. Dipl.-Ing. Stefano Cantini,

Mr. Dipl.-Ing. Andrea Colla and

Mr. Ing. Michele Portesi

for the great cooperation.

Abstract/Kurzfassung

The evaluation and further optimization of a railway axle production process of a key supplier of Siemens MO MLT BG is the topic of the presented Master's Thesis. The evaluation is based on assorted product characteristics of a specific wheelset axle type.

Supplier's production systems and machining procedures are analyzed regarding their capability of meeting defined quality requirements. Furthermore, measuring data for the selected product characteristics of seven different production batches are collected and statistically analyzed in order to assess current process performance (before process optimization).

Based on these analyses, the most influencing factors on the product quality are determined. Subsequently, extensive investigations are performed in order to find out what the root causes for not fully satisfying results are. In this context, investigations are mainly focused on the centering process and the grinding machining process, as these machining steps have the most influence on the final product quality. Moreover, the process step of final dimensional inspection is investigated.

Finally, improvement proposals are worked out. These measures are presented as recommendations for the supplier to ensure further improvement of the process performance (process quality) and the productivity.

Das Thema dieser Masterarbeit ist die Bewertung und weitere Optimierung des Fertigungsprozesses von Radsatzwellen eines strategisch wichtigen Lieferanten von Siemens MO MLT BG. Die Bewertung erfolgt anhand ausgewählter Produktmerkmale eines spezifischen Wellentyps.

Die vom Lieferanten eingesetzten Produktionssysteme und Fertigungstechnologien werden hinsichtlich der Fähigkeit, definierte Qualitätsanforderungen erfüllen zu können, analysiert. Um die grundsätzliche Prozessleistung (vor der Prozessoptimierung) ermitteln und bewerten zu können, werden über einen bestimmten Zeitraum Messdaten zu den definierten Produktmerkmalen erhoben und anschließend statistisch ausgewertet.

Basierend auf diesen Analysen erfolgt die Bestimmung von Haupteinflussfaktoren auf die erreichte Produktqualität. Anschließend werden umfangreiche Untersuchungen durchgeführt, um die tatsächlichen Ursachen für nicht vollständig zufriedenstellende Bearbeitungsergebnisse zu ermitteln. Der Fokus liegt dabei auf den Fertigungsschritten Zentrierbohren und Schleifen, da diese den größten Einfluss auf die schlussendlich erreichte Produktqualität darstellen. Weiters wird der Prozess der geometrischen Produktprüfung untersucht.

Schlussendlich erfolgt die Ausarbeitung potenzieller Prozessoptimierungsmaßnahmen, welche dem Lieferanten als Empfehlungen präsentiert werden. Durch die Implementierung dieser Maßnahmen sollen die Leistung beziehungsweise die Qualität des Fertigungsprozesses sowie die Produktivität verbessert werden.

List of Abbreviations

ANOVA	Analysis of Variance
ARM	Average-Range-Method
AV	Appraiser Variation
EV	Equipment Variation
GG	Global Gauß
GN	Global Minimum
GPS	Geometrical Product Specifications
GX	Global Maximum
LP	Local Point
LRS	Lucchini Rolling Stock
LSC	Least Square Circle
LSL	Lower Specification Limit
MCC	Minimum Circumscribed Circle
MCD	Mono-Crystalline Diamond
MIC	Maximum Inscribed Circle
MSA	Measurement System Analysis
R&R	Repeatability and Reproducibility
Siemens MO MLT BG	Siemens Mobility, Mainline Transport, Bogies Graz
SQE	Supplier Quality Engineer
USL	Upper Specification Limit

List of Symbols

Symbol	Designation	Unit
α_l	Linear expansion coefficient	K^{-1}
μ	“Real” or actual mean	m
σ	“Real” or actual standard deviation	m
σ_{obs}	Observed standard deviation	m
σ_{actual}	Actual standard deviation of production process	m
σ_{ms}	Measurement system’s standard deviation	m
(a, b)	Center point coordinates of LSC	–
a_{ed}	Cutting depth of dressing tool (per stroke)	m
$a_{ed ges}$	Overall cutting depth	m
a_{pd}	Effective contact width of dressing diamond	m
B_i	Bias (systematic measurement system error)	m
C_g	Measurement system capability index, only considers measurement system’s variation	–
C_{gk}	Measurement system capability index, considers measurement system’s variation and bias	–
C_p	Process capability index, only considers process variation	–
C_{pk}	Process capability index, considers variation and location of process output	–
D_0	Initial diameter	m
d_2^*	Statistical factor for MSA	–
ΔD	Diameter change	m
d_j	Distance between a single measuring point and LSC	m
d_w	Workpiece diameter	m
f_{ad}	Dressing tool feed in axial direction	m
k	Number of different appraisers	–
K_1	Statistical factor for unbiased estimation (EV)	–
K_2	Statistical factor for unbiased estimation (AV)	–
L_0	Initial length	m

Symbol	Designation	Unit
ΔL	Length change	m
l	Number of readings for type-1 study	–
m	Number of points for determining LSC	–
n	Number of different measurement objects	–
p	Pressure	MPa
q_d	Dressing velocity ratio	–
q_s	Velocity ratio	–
Q_w	Metal removal rate	$\text{m}^3 \cdot \text{s}^{-1}$
Q'_w	Specific metal removal rate	$\text{m}^3 \cdot \text{m}^{-1} \cdot \text{s}^{-1}$
r	Number of repeated measurements	–
R	Range of a dataset	m
\bar{R}	Average range	m
$\bar{\bar{R}}$	Average of average ranges (type-2 study)	m
R_{LSC}	Radius of LSC	m
R_m	Tensile strength	MPa
r_p	Profile radius of form roll	m
R_{ts}	Effective grinding wheel roughness	μm
s	Standard deviation (calculated from present measurement values)	m
s_g	Standard deviation (statistical characteristic for MSA)	m
T_0	Initial temperature	K
ΔT	Temperature change	K
TR	Characteristic's tolerance range	m
$ \Delta U $	Induced voltage	V
u_d	Coverage ratio	–
\dot{V}'	Specific volume flow	$\text{l} \cdot \text{s}^{-1} \cdot \text{m}^{-1}$
v_{KSS}	Velocity of cooling liquid jet	$\text{m} \cdot \text{s}^{-1}$
v_{fad}	Dressing tool feed rate in axial direction	$\text{m} \cdot \text{s}^{-1}$
v_{fr}	Feed ratio in radial direction	$\text{m} \cdot \text{s}^{-1}$
v_R	Circumferential speed of rotational dressing tool	$\text{m} \cdot \text{s}^{-1}$
v_s	Circumferential speed of grinding wheel	$\text{m} \cdot \text{s}^{-1}$
(x_j, y_j)	Coordinates of a single measuring point	–

Symbol	Designation	Unit
\bar{x}	Mean (calculated from present measurement values)	m
X_{diff}	Range of means (type-2 study)	m
\bar{x}_g	Mean (statistical characteristic for MSA)	m
x_j	Represents the individual readings	m
x_{ref}	Reference value	m
$\%AV$	Evaluation parameter for appraiser variation	—
$\%EV$	Evaluation parameter for equipment variation	—
$\%RE$	Evaluation parameter for measurement device resolution	—
$\%R\&R$	Evaluation parameter for repeatability & reproducibility	—

Table of Contents

1	Introduction.....	1
1.1	Production Process.....	3
2	Theoretical Background.....	6
2.1	Quality Control.....	6
2.1.1	Seven Fundamental Quality Control Tools.....	6
2.1.2	Process Control.....	9
2.2	Grinding Machining.....	13
2.2.1	Grinding Wheel.....	15
2.2.2	Reconditioning.....	16
2.2.3	Cooling System.....	21
2.2.4	Machining Parameters.....	23
2.3	Measurement Systems.....	24
2.3.1	Dimension Measurement Methods.....	25
2.3.2	Determination of Characteristics on Geometry Elements.....	28
2.3.3	Thermal Expansion of Solids.....	30
2.3.4	Measurement System Analysis.....	32
2.3.5	Procedures for Measurement System Analysis.....	34
3	Measurement System Investigation.....	36
3.1	Measurement System Description.....	36
3.2	Measurement System Analysis.....	38
3.2.1	Basic Assessment.....	38
3.2.2	Type-1 Study.....	38
3.2.3	Type-3 Study.....	40
3.2.4	Root Cause Analysis.....	42
3.3	Interpretation of Results.....	47
4	Machining Process Investigation.....	49
4.1	Axle Centering.....	52
4.2	Grinding Machining.....	54
4.2.1	Operator Influence.....	56
4.2.2	In-Process Measurement System.....	59
4.2.3	Machining Process Control.....	66
4.2.4	Reconditioning.....	67
4.2.5	Grinding Parameters.....	72

4.2.6	Cooling System	73
5	Summary and Outlook.....	75
5.1	Measurement System for Final Inspection	75
5.2	Grinding Machining Process	75
6	Bibliography.....	78
7	List of Figures.....	81
8	List of Tables.....	83
9	Appendix	84

1 Introduction

Siemens Mobility, Mainline Transport, Bogies Graz (Siemens MO MLT BG) as a world competence center for bogies receives a large part of the bogie components from global suppliers. To ensure the availability of top-quality purchased parts, and coupled with this, the own readiness for delivery of reliable and safe solutions for the end customer, a close collaboration with suppliers is indispensable. After a well prepared and analysis based selection of key suppliers, Siemens MO MLT BG is highly interested in how these partners cope with set requirements in the serial production of ordered components. In the present pilot project, Lucchini Rolling Stock's (Lucchini RS') innovative and highly automated machining process for wheelset axles is going to be analyzed and further optimized. Lucchini RS, located in Lovere (Italy), is the world leader in design and manufacturing of high speed wheelsets and a key supplier of axles and wheels for Siemens MO MLT BG.

In a previous Bachelor's Thesis, which was finished in September 2015, a basic evaluation of supplier's production process regarding process performance was carried out. The evaluation of the machining process showed a great potential for further improvement. Therefore, the project was extended. Information and findings gathered in the Bachelor's Project built the basis for setting up the present Master's Thesis.

Analyses and investigations within the scope of this Master's Project are based on assorted product characteristics of a specific wheelset axle type. One particular axle type had to be chosen for conducting investigations since the supplier produces a great variety of different axle types. Lucchini RS manufactures various kinds of wheelset axles for Siemens MO MLT BG as well as for other customers in the railway industry. All the production processes for different axle types have basic steps and activities in common. But considered in detail, no manufacturing process for one specific axle type is completely the same as for another. There is even a difference between trailer and motor axles of one axle type for a single customer.

For the investigations, motor axles of the "Thameslink" project (London) were chosen because of the importance of this assignment for Siemens MO MLT BG as well as for the end customer. Another reason for this selection is the great extent of this project and thus the great quantity of produced parts.

Representative product characteristics were chosen based on the experience from the previous Bachelor's Project. It was a common decision with the supplier as well as with Supplier Quality Engineers (SQE) and employees from Engineering Department of Siemens MO MLT BG. The Thesis' main focus lies on the diameter, the cylindricity and the surface roughness of the wheel seat, because the fulfillment of requirements for these characteristics is of great importance. The conformance of these characteristics is essential for the wheelset assembly at the Siemens MO MLT BG site in Graz as well as for the safety of the train in operation, in which the axle is going to be built in.

To get a basic understanding for the purpose of a wheelset axle, the terms bogie and wheelset have to be explained. In this context, Figure 1 is presented in order to show the axle's integration in the complete rail vehicle (bottom-up).



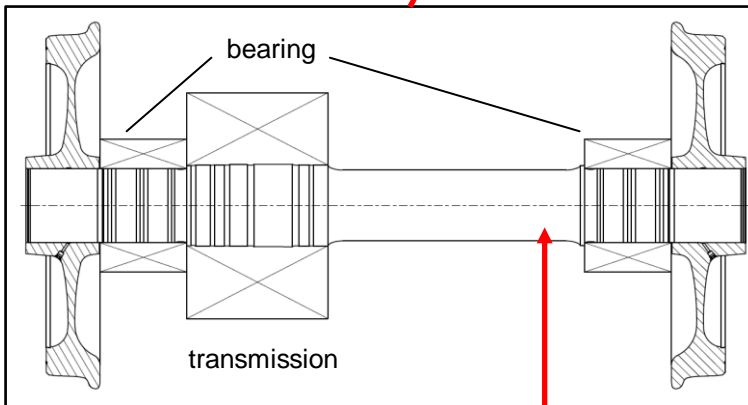
Rail Vehicle
(Desiro City Thameslink)

Source:
Siemens Mobility



Motor Bogie

Source:
Siemens Mobility



Wheelset

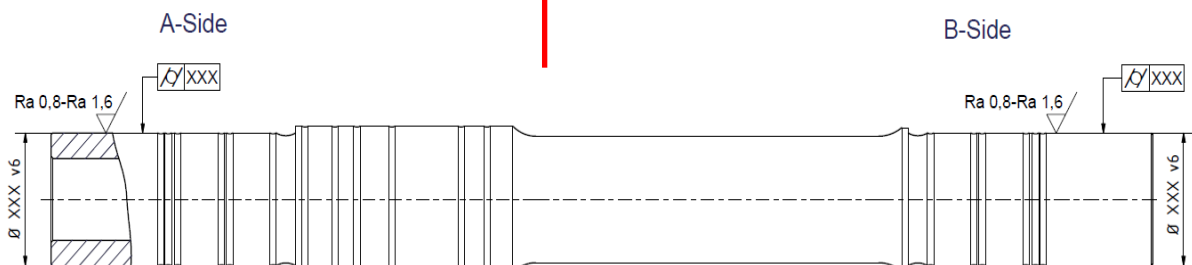


Figure 1: Integration of wheelset axle in complete rail vehicle, Source: Rail Vehicle: Based on Siemens Mobility (2016); Bogie: Siemens AG (2013), p. 11; Wheelset: Own illustration; Axle: Own illustration.

In the lower part of Figure 1, the “Thameslink” motor axle, which is special because of its inboard bearings, and the selected product characteristics, are shown. For privacy reasons, the exact value of the journal diameter as well as of the cylindricity tolerance is encrypted. In order to be able to understand analyses and investigations within the scope of this Thesis, it has to be explained that every wheelset axle has an A- and a B-side. As for this project a motor axle is used, the allocation of the two sides is rather easy. In general, the axle’s A-side is closer to the transmission seat, like it is depicted.

Each axle is built into a wheelset. In its basic and simplest form, a wheelset consists of an axle and two wheels which are fixed on it by a longitudinal interference fit. As for the project a motor axle was chosen and due to the special design of the selected wheelset axle type, a transmission and bearings along with bearing shells and attachment parts have to be mounted on the axle before the wheels can be assembled. After pressing the wheels onto the axle, the wheelset assembly is completed.

As shown in Figure 1, the axle journal serves as bearing seat and as seat for pressing on the wheels. Due to the special design of the selected project’s bogie, an inboard bearing concept is used. This means, the wheels are mounted on the outer part of the journal. In most cases the arrangement is different, as normally the bearings are fixed on the outer section of the journal.

In general, two wheelsets are built into each bogie. A bogie is the connecting part between the rails and the train body and transmits driving and breaking forces.¹

1.1 Production Process

In 2011, a new axle finish machining line (shown in Figure 2) was installed at Lucchini RS’ production site in Lovere. This innovative and highly automated production line consists of nine machines in sequence, whereat all the machines are connected by an automated part transfer system. This system consists of transfer units which are responsible for loading the axles into the different machines and for the transfer between them. The transfer units, one of which is highlighted in Figure 2, are transferring the parts from one machine to another along the straightforward production flow. This happens in a height of about four meters over the shop floor ground.



Figure 2: Automated finish machining line, Source: Own illustration.

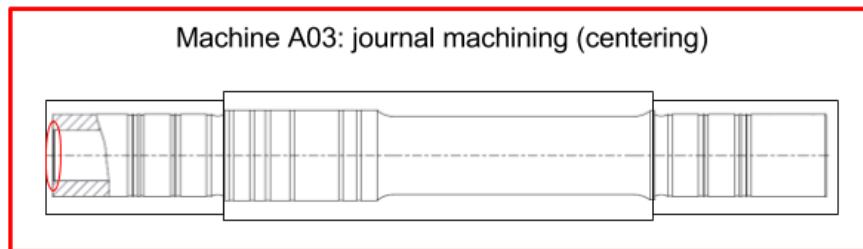
¹ Conf. Haigermoser (2005), p. 183.

The present project focuses on three main process steps, which are highlighted in Figure 3. One of them is the journal machining operation in A03, in particular the machining of the axle centering (highlighted in the first part of Figure 3), which is a part of the process performed in that machine. Furthermore, the grinding operations performed in machines A07 and A08 were selected due to their criticality as well as their huge impact on the final product quality. In A10 (automated 3D measuring machine), the final dimensional inspection is performed. These measurement values are taken into account for the decision whether an axle meets the requirements, has to be reworked or has to be scrapped due to smaller dimensions than required. Furthermore, the readings gathered by the measuring machine build the basis for the machining process evaluation. Based on these facts, the final dimensional inspection step in A10 is also a subject of investigation. Additional information about the grinding process has to be given as a basis for further considerations in this Thesis. The axle enters the automated finish machining line always in the same alignment, in which the A-side of the product is on the left side in the top view. This alignment is maintained for all machines up to A07. In A07, the B-side of the axle is finish machined by grinding. After that process step, the axle is rotated 180° by the automated transfer system between the two machines A07 and A08. Then it is loaded into A08. In this machine, the axle's A-side is machined. After finishing this grinding operation, the axle is rotated back in its initial position for the following process steps. This machining approach is used due to cycle time reasons.

As Lucchini RS produces a great number of different axle types for various customers, not all the production steps and machines are used for every axle. In Figure 3, the finish machining process of the selected axle type with its constituent steps is shown, in which machine A06 is skipped because cold rolling is not required for this axle type. For machine A03 and A04, the machining allowance for these process steps is additionally indicated. The dark lines around the axle constitute the axle geometry after the machining operation in these machines. Machine A10 is followed by A11 and A12, in which the magnetic particle inspection and the stamping of the axle respectively are performed.

Before the axles enter the automated production line for finish machining, a great deal of previous production steps has to be carried out. The production cycle of a wheelset axle begins in Lucchini RS' own steel production in the Lovere site. This stage is followed by an open-die forging operation in order to obtain the basic shape of the axle. After this step, the axle material gets heat treated. The axle type, on which the focus of this Thesis lies, is made of EA1N. This low-alloy steel with a carbon content of maximal 0.4% is one of the most important materials for wheelset axles in the European railway industry. The 'N' in the material designation indicates that the axle is normalized. Before performing the first rough machining step of the blanks, mechanical, chemical and metallographic tests are carried out.

The machining process starts with blank axles, which have the basic shape and a rough surface as a result of open-die forging and heat treatment. The first rough machining operation is performed in order to remove great quantity of material as well as to prepare the axle surface for the ultrasonic examination which is carried out as a next step. After assurance, that no volume defects are present in the axle material, the hollow bore is produced by deep-hole boring. The honing process, which guarantees that the high quality requirements for the hollow bore surface are met, is the last machining step before the axle enters the automated finish machining line described above.



Machine A04: horizontal turning machine for rough machining



Machine A05: horizontal turning machine for finish machining

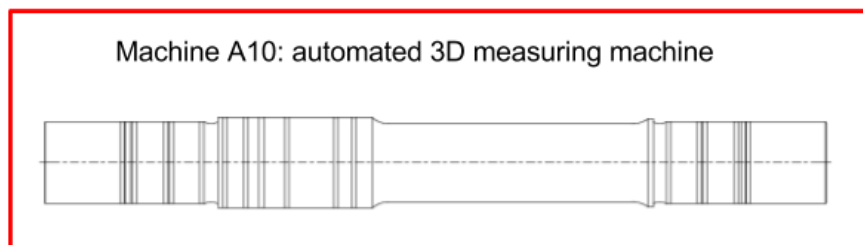
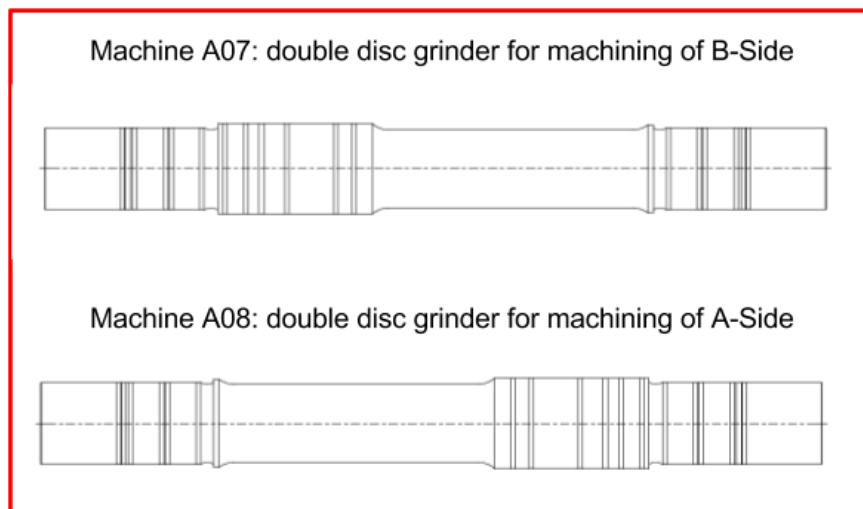


Figure 3: Axle finish machining process (top view), Source: Own illustration.

2 Theoretical Background

In this chapter theoretical background of different fields is presented. It builds the basis for performed evaluations, analyses and investigations within the scope of the present Thesis.

2.1 Quality Control

To be successful in today's economic climate, companies must be dedicated to continual improvement. They have to constantly seek more efficient ways to produce products and services. Furthermore, organizations must focus upon their customers and make customer satisfaction a primary business goal. To accomplish this, everyone in an organization must be committed to improvement and to the usage of effective methods for quality control.²

Some of these methods are presented in the following sections.

2.1.1 Seven Fundamental Quality Control Tools

Basic information about quality control tools is given in this chapter:³

A great deal of different methods and tools for quality control are available. One of these methodologies is the set of Q7-tools, or also named the seven fundamental quality control tools. Figure 4 gives an overview of the single techniques.

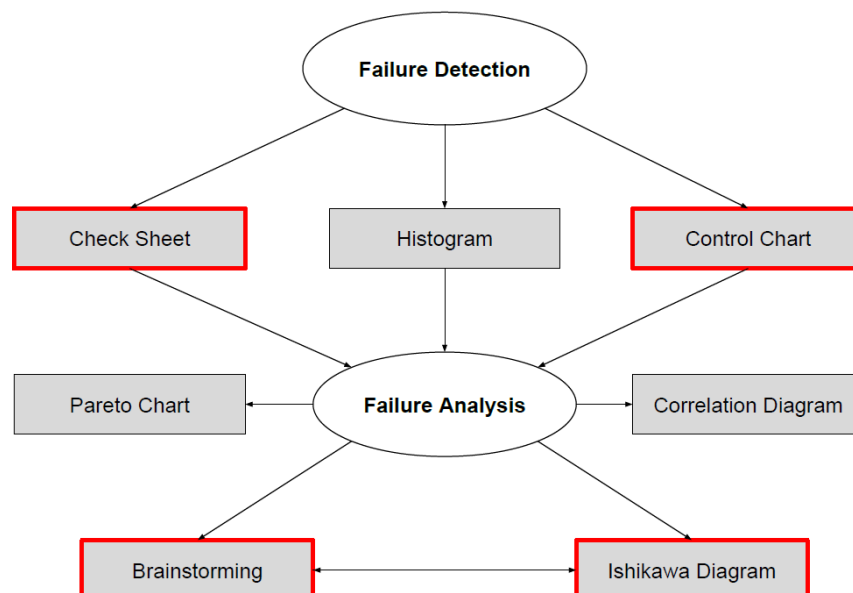


Figure 4: Interaction of Q7-Tools, Source: Based on Hehenberger (2011), p. 211.

² Conf. Daimler Chrysler Corporation et al. (2005), p.3;

³ Conf. Hehenberger (2011), p. 210-216.

The seven tools were defined and collected by Kaoru Ishikawa, who also developed the cause-and-effect diagram. Ishikawa was a Japanese chemist and he is said to be the founding father of the well-known Japanese quality control campaign.

Most of the Q7-Tools are based on mathematic background and were especially prepared for usage in shop floor areas without violating statistical rules. With these easy to use methods, a great variety of different problems in production areas can be solved.

Figure 4 shows the interaction of the single Q7-tools. Tools which were used in the course of this project are highlighted by red frames and are described in more detail in following chapters.

2.1.1.1 Control Chart

A control chart is a graphical display of a quality characteristic that has been measured from a sample versus the sample number or time. It is a tool that is frequently used in statistical process control (SPC) in order to monitor a stable process. For this purpose, control limits are calculated by applying statistical formulas to data from the process. By using control charts with control limits, it is possible to determine whether special causes of variation are present in the process or not. More information about special and common causes of variation is provided in chapter 2.1.2.

In contrast, a control chart can also be used to get a basic idea of how a process basically works by simply plotting original values in a control chart. The specification limits (upper and lower specification limit; USL and LSL) can be indicated in such control charts, to determine whether the process produces conformance parts or not. An example for an original value chart is shown in Figure 5, in which the middle of the tolerance range is represented by an interrupted line.

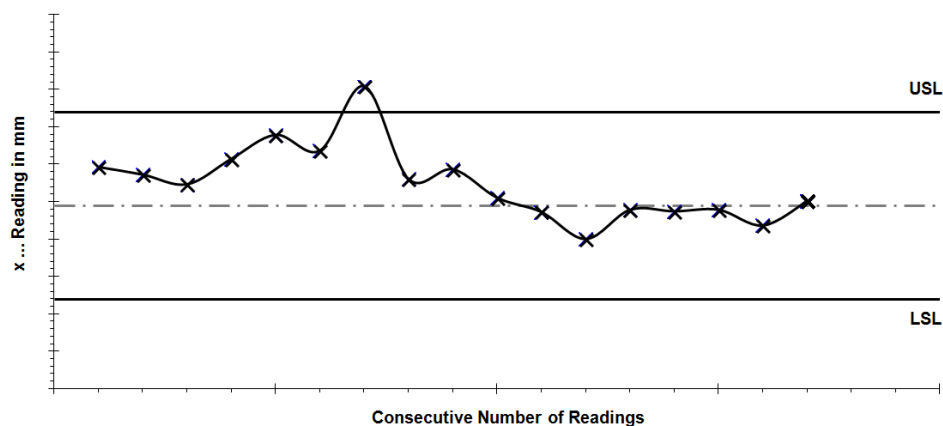


Figure 5: Original value chart, Source: Based on Hehenberger (2011), p. 212.

2.1.1.2 Check Sheet

By the use of check sheets, observed and determined failures can easily be counted and recorded. The representation by failure type and quantity enables the determination of trends as well as regularities in order to get a clear depiction of the reality. The precise information collected in a check sheet is the basis for further analyses. An example of a check sheet is presented in Figure 6.

Check Sheet	
Failure	Quantity
# 1	
# 2	
# 3	
# 4	

Figure 6: Check sheet, Source: Based on Hehenberger (2011), p. 212.

2.1.1.3 Cause-and-Effect Diagram

The cause-and-effect diagram is also named fishbone diagram due to its look or Ishikawa diagram after its developer. According to Ishikawa, a dedicated effect is mostly not based on a single cause, especially not on a cause which seems to be evident at first glance, but rather on a combination of causes from different fields like operators (man power), machines (equipment), methods and material. These four 'Ms' are the basic categories of influencing factors for a production process, but also diagrams with up to six or even more categories are common today. An Ishikawa diagram has to be adapted to the problem or application for which it is used. Examples for additional influencing factors are measurement, management or environment (milieu). Figure 7 shows an Ishikawa diagram with six main influencing factors, also called categories or simply 'Ms'. Additionally, one main and one secondary cause are inserted in this diagram.

When creating an Ishikawa diagram, the first step to be done is to place a concise problem description at the point of a horizontal arrow. After that, arrows with the main influencing factors (categories), which are pointing diagonally to the horizontal arrow drawn first, are added. When the main influencing factors, which are relevant for the present problem, are selected, potential causes for the problem or effect have to be explored by using creativity techniques. For each category, potential main and secondary causes are inserted in the diagram, which were collected by brainstorming. Once the exploration is completed, every single cause has to be weighted by a team regarding its importance and its impact to the problem. In the end, the potential causes with the highest probability of being the real root causes are selected.

This quality control tool is mostly used for systematic and complete determination of causes for problems or specific states as well as for process analyses. Because of the graphical representation of a problem and its potential causes, an Ishikawa diagram is a good discussion basis for team work and it helps to gain a greater understanding of a problem and its various causes.

A disadvantage of Ishikawa diagrams is that they can get really confusing when they are used for investigation of complex problems.

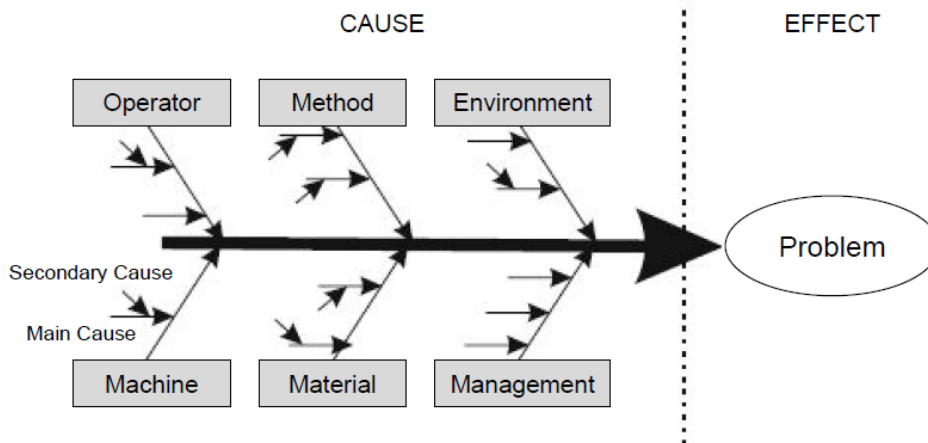


Figure 7: Ishikawa diagram, Source: Based on Hehenberger (2011), p. 215.

2.1.2 Process Control

Various aspects regarding process control are presented in this chapter.

At first, it has to be explained what is meant by the terms “process under statistical control” and “capable process” respectively:⁴

A process is referred to as being under statistical control if all special causes of variation have been eliminated and only common causes are remaining. In this case, the output of the process is predictable, as its location and variation are stable over time. This circumstance is shown in Figure 8.

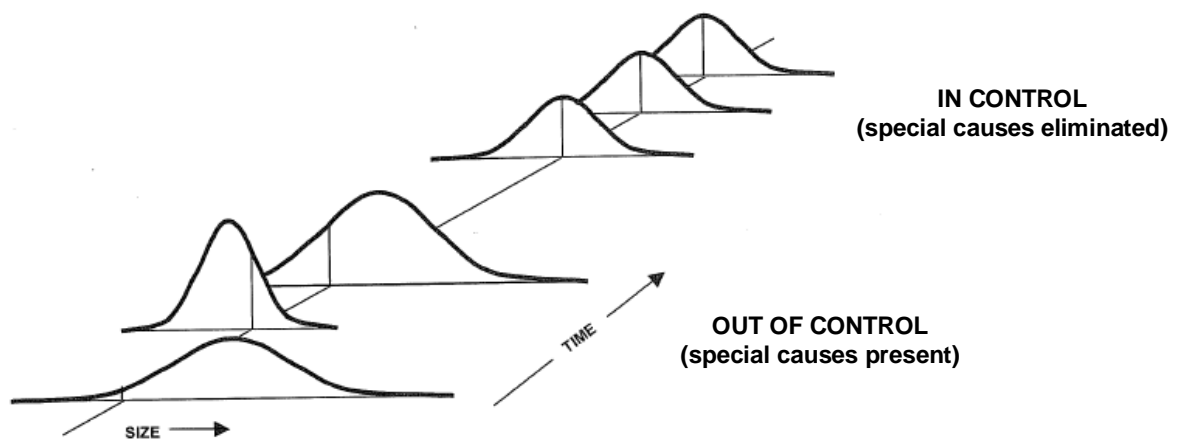


Figure 8: Process control, Source: Daimler Chrysler Corporation et al. (2005), p. 18.

In this context, a distinction between special and common causes of variation has to be made:⁵

⁴ Conf. Daimler Chrysler Corporation et al. (2005), p.19, 20;

⁵ Conf. Daimler Chrysler Corporation et al. (2005), p.12-14.

Special causes, also often called assignable causes, are a source of variation which affects only some of the process output. It is often intermittent and unpredictable. Special causes are signaled by one or more points beyond the control limits or a non-random pattern of points within the control limits. Unless all the special causes of variation are identified and acted upon, they may continuously affect the process output in unpredictable ways. If special causes of variation are present, the process output will not be stable over time. Tool fracture or operator failures, like a change of machine settings in a wrong way, are examples for special causes of variation.

Common causes, also named chance causes, are a source of variation that affects all the individual values of the process output. Therefore, it is the source of the inherent process variation. If only common causes of variation are present and do not change over time, the process' output is predictable. Examples for common causes of variation are wear in normal extent or wrong settings of the machine.

Once a process is brought under statistical control, its capability to meet customer expectations can be assessed. If a high level of variation from common causes is present in the process' output (bottom half of Figure 9), measures have to be taken in order to reduce this variation.

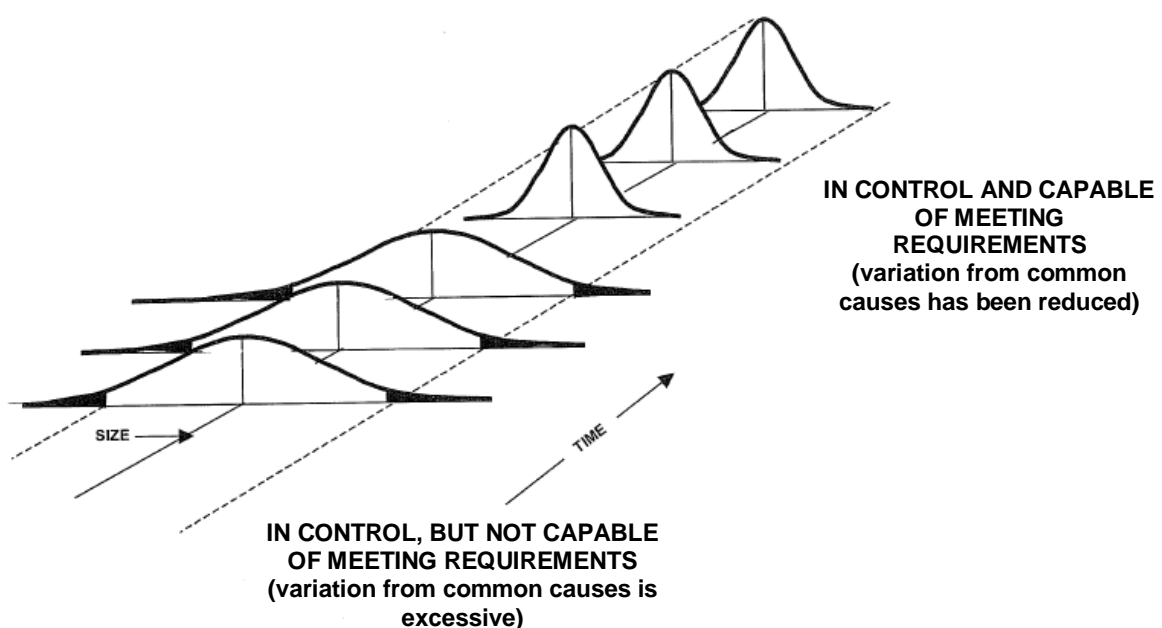


Figure 9: Process capability, Source: Daimler Chrysler Corporation et al. (2005), p. 18.

A capable process meets the requirement $C_{pk} \geq 1.33$. In this context, the capability indices C_p and C_{pk} have to be explained. The C_p -index only takes into account the variation s , whereas C_{pk} also considers the location of process output's distribution. The relations for calculation of stated indices are presented in formula (2.1).⁶

⁶ Conf. Danzer (2016), p. 126-128.

$$C_p = \frac{T}{6s} \qquad C_{pk} = \frac{\Delta_{krit.}}{3s} \qquad (2.1)$$

In formula (2.1), $\Delta_{krit.}$ stands for the distance between the actual mean of process output \bar{x} and the specification limit which is closer to \bar{x} . This situation is depicted in Figure 10 and is formulated mathematically in formula (2.2).⁶

$$C_{pk} = \min \left[\frac{USL - \bar{x}}{3s} ; \frac{\bar{x} - LSL}{3s} \right] \qquad (2.2)$$

By means of C_p , only the basic suitability of a technology can be assessed, as the variation of the process is set in relationship to the investigated characteristic's tolerance range T . An actual evaluation regarding process capability can only be made by determining the C_{pk} -index.⁶

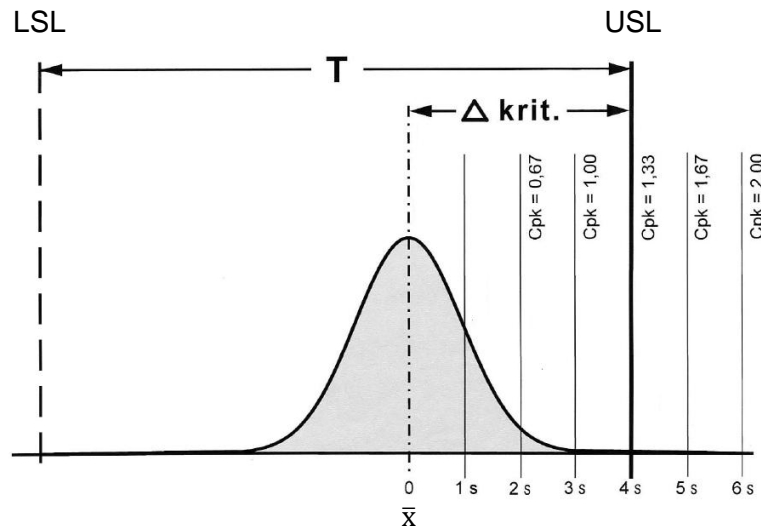


Figure 10: Normal distribution of process output, Source: Based on Danzer (2016), p. 127.

It is very important to reach and maintain a process which is under statistical control and capable of meeting requirements. To verify this statement, the concept of Taguchi loss function is considered in the following chapter.

2.1.2.1 Taguchi Loss Function

In this section, Taguchi's loss function approach is presented.⁷

According to Taguchi, each deviation from the target value (design intent) leads to a deterioration of overall results. The so-called loss function (Figure 11 (b)) is a quadratic form. This means that an increasing loss is incurred, the further a particular characteristic gets from the target value. Beside an increasing risk of producing non-conformance production parts, each deviation from the target value has negative effects on the reliability of the product in use as well as on its attractiveness on the market.

⁷ Conf. Daimler Chrysler Corporation et al. (2005), p. 148-150.

In former times, a concept called “Goal Post Mentality” (Figure 11 (a)) was used to assess the product quality. In this model, all parts in tolerance, regardless of their location within the specification range, are called equally “good” and all parts beyond specification are called equally “bad”. It does not matter how far they are beyond specification. In the course of this concept, “good” means that no additional costs arise.

Taguchi’s approach is totally different; additional costs - in form of rework or scrap - do not arise only when specification limits are exceeded. Each deviation from the target value leads to a deterioration in form of additional costs and an increasing failure risk.

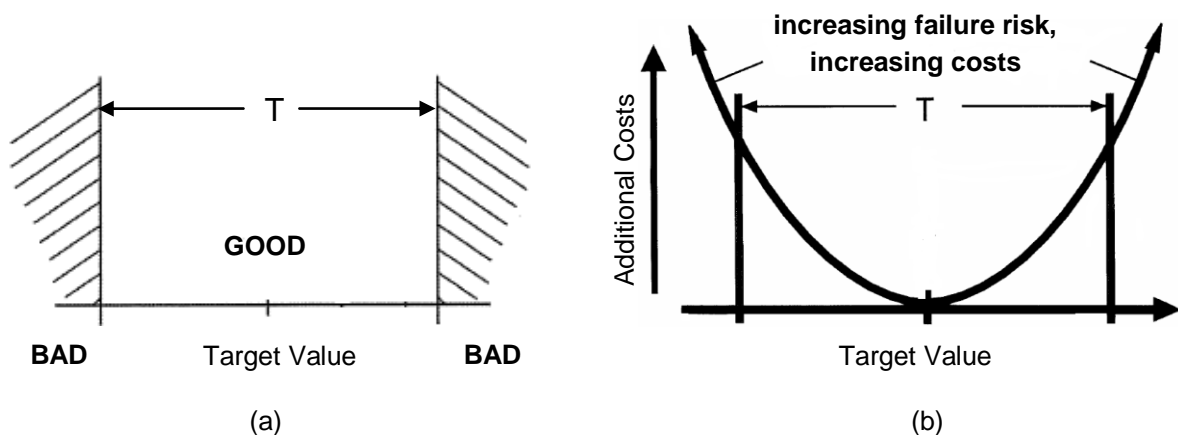


Figure 11: Comparison “Goal Post Mentality” and Taguchi Loss Function, Source: Based on Daimler Chrysler Corporation et al. (2005), p. 148.

2.1.2.2 Production Control Plan

A production control plan constitutes an instruction regarding process control, which should be available on each workstation in production and assembly areas. By means of this document, the operators should be able to ensure a process which is under statistical control and capable of meeting requirements.⁸ Subsequently, the content of a control plan is presented:⁸

- Important Product Characteristics

Part characteristics which may have a decisive impact on the reliability and safety of the final product can be seen as important in this context. These characteristics are provided in the control plan as input for operator’s responsible task. Their conformance has to be ensured.

- Important Process Parameters

In order to ensure satisfying results, some main process parameters have to be controlled in each process step. These parameters are presented in the control plan. Furthermore, the ranges of these parameters, in which the best results can be achieved, are indicated.

⁸ Conf. Danzer (2013), p. 94.

- Required Inspection Activities and Measures

The inspection plan for a certain workstation is also a part of the control plan. Important information regarding required inspections is presented in this section. These are for instance characteristics which have to be inspected, gages and tools which have to be used and the frequency of specific tests.

- Procedures in Case of Unexpected Events

In this section of the control plan, the operator gets instructions regarding appropriate actions in case of emergency. Information is given in order to prevent physical harm and to enable the operator to trigger the right measures in critical situations.

After this introduction into the topic of quality control, theoretical background of grinding machining has to be given due to its importance for the present Thesis.

2.2 Grinding Machining

As the grinding operation is the process step which has the main influence on the achieved product quality, an extensive overview of theoretical background is given in this chapter.

According to the classification of manufacturing processes of DIN 8580, grinding machining is assigned to the major group “cutting”. Particularly, it is associated to the subgroup of “cutting with geometrically undefined cutting edges”. The procedure is characterized by cutting mechanisms which are a result of the operation of a huge amount of geometrically undefined cutting edges.⁹

In a grinding machining process, grinding wheels are used as tools for material removal. Figure 12 shows a grinding wheel with its typical components: grinding grains, bonding material and pores.

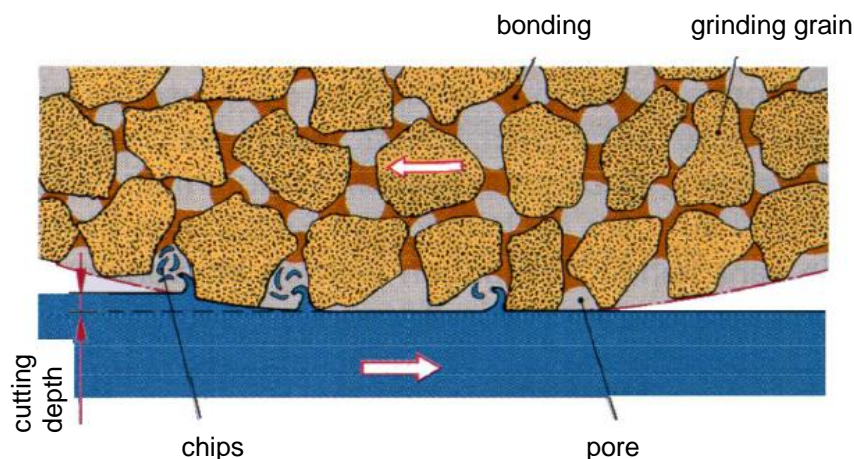


Figure 12: Grinding wheel, Source: Based on Dillinger et al. (2007), p. 175.

⁹ Conf. Uhlmann (2014(a)), p. 531.

Compared to other cutting processes like turning or milling, there are a few characteristics which differentiate grinding from these procedures:¹⁰

- Small chip thickness
- Varying distance of the cutting edges from the grinding wheel center and therefore varying chip thickness
- Cutting edges possess different geometries and mainly high negative chip angles
- High velocity of the cutting edges during operation in the material
- Tool (grinding wheel) consists of three components
 - Grain
 - Bonding
 - Pores

Depending on workpiece geometry, machined workpiece area, active grinding wheel area and the main feed direction, different grinding techniques according to DIN 8589 can be distinguished¹¹. In the following sections, the grinding technique which is relevant for this project gets described in more detail.

Figure 13 shows the principle of straight line cylindrical plunge grinding. In there, v_s and v_w represent the rotational speed of the grinding wheel and the workpiece respectively. Furthermore, the feed rate in radial direction v_{fr} is indicated.

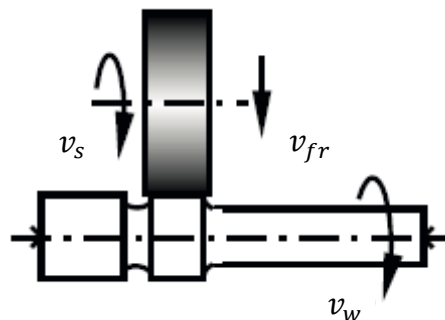


Figure 13: Straight line cylindrical plunge grinding, Source: DIN 8589-11 (2003), n.p., quoted from Uhlmann (2014(b)), p. 539.

The procedure of cylindrical plunge grinding is used for machining of narrow function surfaces on rotationally symmetric workpieces. Generally, a distinction between the procedures of straight line and diagonally external cylindrical grinding can be made. This classification refers to the alignment of the grinding wheel relative to the workpiece. The rotational axis of the grinding wheel is parallel to the workpiece ones in Figure 13 which shows the straight line cylindrical plunge grinding. In this arrangement, the profile of the grinding wheel gets depicted on the workpiece. This procedure is mostly used to produce highly accurate seats on shafts and axles. On the other hand, the grinding technique is termed diagonally external cylindrical grinding if the rotational axis of the grinding wheel is inclined referring to the axis of the workpiece.¹²

¹⁰ Conf. Klocke (n.d.), p. 6;

¹¹ Conf. Klocke (n.d.), p. 13;

¹² Conf. Rowe (2009), n.p., quoted from Uhlmann (2014(b)), p. 539.

Basically, a grinding system is characterized by various parameters which can be classified into input-, process- and result parameters¹³. This differentiation is shown in Figure 14.

Selected elements or parameters of a grinding system are theoretically considered in the following chapters. The sequence of the parameters in the following description is based on the categorization shown in Figure 14.

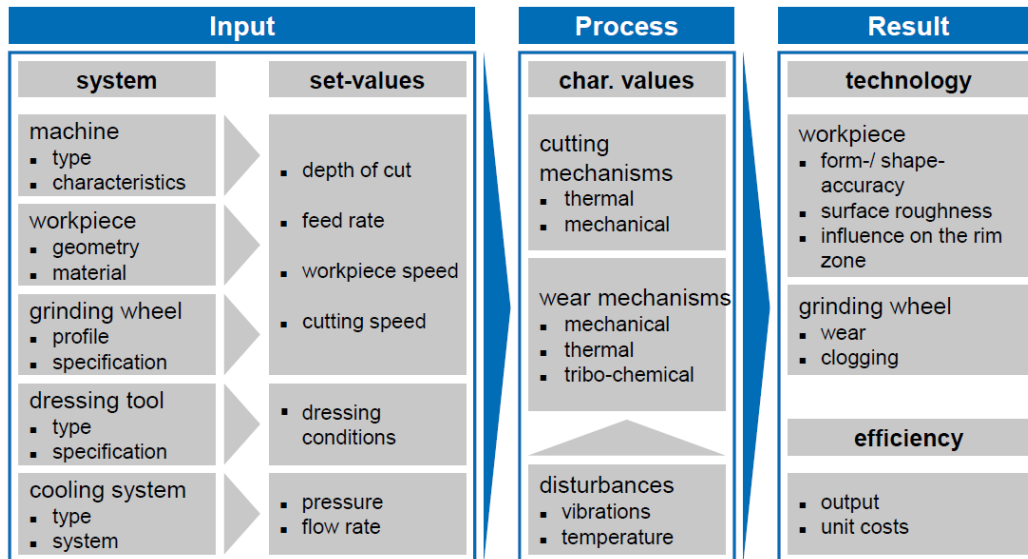


Figure 14: Parameters of grinding system, Source: Based on Klocke, König (2005), p. 186

In the following paragraphs, different input parameters are considered. In general, input parameters are describing the geometry and the kinematics of the workpiece and the tool as well as system descriptive parameters like the kind of cooling liquid¹³.

2.2.1 Grinding Wheel

In the following three paragraphs, the grinding wheel and abrasives are discussed:¹⁴

In the grinding process, the material gets cut by grinding grains which are the most important component of the grinding wheel.

There is a great deal of requirements for grinding grain materials:

- High hardness as well as high toughness in order to enable machining and for retaining the sharpness of the cutting edges for longer periods
- Thermal resistance against high machining temperatures and fast temperature changes
- Chemical resistance to avoid undesired reactions of the grain material with surrounding air, cooling lubricant or the workpiece material. Such reactions may weaken the grain.

¹³ Conf. Klocke, König (2005), p.186;

¹⁴ Conf. Klocke, König (2005), p. 19.

Additionally, there are requirements to the fracture behavior of the abrasives which depend on specific applications. As no abrasive can completely meet all these requirements, different natural or synthetic grain materials are used in grinding machining processes.

Nowadays, natural abrasives like quartz or emery are of little importance in industrial applications because of their insufficient strength properties. Another reason for using synthetic abrasives instead of natural ones is that the grain quality of these natural products can only be controlled and reproduced insufficiently. The only natural abrasive which still is in use for industrial applications is natural diamond.

Synthetic abrasives can be classified into conventional- and superabrasives. The following list gives an overview of the most important synthetic grain materials:

- Corundum (Al_2O_3)
- Silicon carbide (SiC)
- Cubic boron nitride (cBN)
- (synthetic) Diamond

Corundum and silicon carbide can be assigned to the group of conventional abrasives.

As shown in Figure 12, grinding wheels consist of bonding and enclosed pores in addition to the grinding grain.

The bonding interconnects the individual grains and is also responsible for connecting the grains to the body of the grinding wheel. In addition, it has the important task of holding the grains until they are blunted by the grinding process. Blunted grains should then be released by the bonding so that sharp grains can come into operation. The bonding needs to have sufficient strength properties to fulfill the holding function. In addition to that, small cavities in the bonding material are required to provide space for cut material as well as for the cooling lubricant. These cavities are called pores which were described above. Basically, it has to be distinguished between resin-, ceramic-, metal- and galvanic bond.¹⁵ It can be said in general that the choice of grain and bonding material strongly depends on the application.

When talking about grinding wheels, the required reconditioning operation has to be considered. This is done in the subsequent chapter.

2.2.2 Reconditioning

Generally, grinding tools are in an unusable condition right after delivery as well as after a certain time of usage in the grinding operation. Grinding machining is a temporal non-stationary process because of the appearance of wear at the grinding grain as well as at the bonding material. This circumstance leads to a change of the macro- and micro-geometry of the grinding wheel. In this stage, complete grains or parts of grains can break out of the bonding and microcrystalline splintering can occur. These mechanisms change the cutting edge structure of the grinding wheel which influences the grinding process

¹⁵ Conf. Klocke, König (2005), p. 43.

forces as well as the quality of the surface and the geometrical accuracy of the workpiece. Therefore, a reconditioning procedure between different machining steps is required in order to achieve acceptable results.¹⁶

Basically, the reconditioning procedure is performed in order to obtain the right geometric form, adequate run-out properties as well as sufficient cutting ability of the grinding wheel. In this context, the effective surface roughness of the grinding wheel plays a decisive role, because the roughness of the production part can strongly be influenced by this characteristic. For example, a grinding wheel with a rough surface has a good cutting ability and acts aggressive in the process. But it also leads to a rough surface on the machined part.¹⁷

The targets of reconditioning, which can be divided into the subtasks profiling, sharpening and cleaning, are presented in Table 1.

Table 1: Reconditioning of grinding wheels, Source: Uhlmann (1994), n.p., quoted from Uhlmann (2014(c)), p. 570.

Reconditioning of grinding wheels		
<i>Dressing</i>		<i>Cleaning</i>
<i>Profiling</i>	<i>Sharpening</i>	
Macro-structure	Micro-structure	Micro-structure
Creation of: - radial run-out - profile of grinding wheel	Creation of topography	Removal of chips from chip space
Changes to grain and bonding are intended.	Removal of bonding material is intended.	Changes to grinding wheel are not intended.

In subsequent sections, basic information about grinding wheel reconditioning is given:¹⁸ The required dimension- and shape accuracy of the grinding wheel profile is achieved by profiling. Whereas the micro geometrical cutting edge structure is created by sharpening. These two subtasks of the reconditioning process are amalgamated under the name dressing. Depending on the bonding material, the profiling operation may not only be responsible for creation of the desired profile but also for achievement of sharp cutting edges as well as sufficient chip space. In most cases in industrial practice, the sharpening operation is included in the profiling process. Due to that, profiling is often used as a synonym for dressing. On the other hand, rests of chips, grain or bonding material are removed by the cleaning process in order to prevent clogging of pores. In practice, this step is also included in the dressing operation.

The applied dressing strategy depends on qualitative and economical requirements as well as the available machine concept. Whereas the possible dressing tools and procedures are determined by the type of abrasive, kind of bonding material and grinding

¹⁶ Conf. Uhlmann (2014(c)), p. 569-571;

¹⁷ Conf. Studer (n.d.), p. 1;

¹⁸ Conf. Klocke, König (2005), p. 155-157.

wheel profile. In general, the dressing tool needs to be harder than the material of the grinding wheel. Otherwise sufficient sharpening would not be possible and the wear of the dressing tool would exceed acceptable limits.

An automated dressing process is desired in general. Therefore, additional equipment in the grinding machine is required. During the reconditioning operation, the grinding wheel ought to stay on the grinding spindle in order to reduce clamping errors as well as time effort. Reproducible reconditioning results are the basis for an automated grinding process.

In the following section, information about different dressing procedures is provided:^{19,20}

Dressing procedures can be distinguished by different aspects. One of them is the kinematics, which divides the procedures into dressing with non-rotational tools and dressing with rotating tools. This distinction is important for the present Thesis.

Dressing with non-rotational tools is comparable to a turning process. The dressing tool is moved along the rotating grinding wheel in axial direction in order to produce the desired topography. It is set in radial direction after a dressing stroke. These dressing tools can easily be applied in different kind of grinding machines without the need of a separate dressing spindle. Therefore, non-rotating tools constitute a cost-effective alternative.

Figure 15 (a) shows a non-rotational dressing tool which looks similar to a device used in a traditional turning process. The main part of the tool is made of steel; only a plane at the tip of the tool is equipped with diamond material.

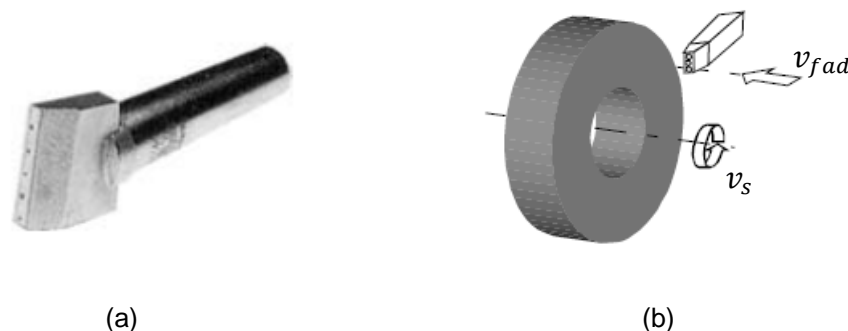


Figure 15: Non-rotational dressing tool, Source: Klocke, König (2005), p. 158.

Figure 15 (b) shows the principle and the kinematics of the dressing process. In there, v_s stands for the rotational speed of the grinding wheel and v_{fad} represents the velocity by which the tool moves along the grinding wheel surface.

In the group of rotating dressing tools, two main types can be distinguished. By using dressing tools which have the negative shape of the grinding wheel, only feed in radial direction is required in the reconditioning process. Such tools are called profile rolls and enable high depicting accuracy at short dressing times. Because of their little flexibility, they are mainly used for mass production.

Tools which do not operate over the whole grinding wheel width require additional tool movement in axial direction and are named form rolls. The advantage in using such tools

¹⁹ Conf. Klocke, König (2005), p. 157-160;

²⁰ Conf. Dr. Kaiser Diamantwerkzeuge (2012), p. 6-9.

is their flexibility. These rolls can be used for different grinding wheel profiles. On the other hand, the higher effort for moving the tool along the grinding wheel in order to produce the desired profile as well as higher time demand, have to be mentioned.

Figure 16 (a) shows a form roll, which is driven by a dressing spindle in operation. Figure 16 (b) shows the principle and the kinematics of the dressing process. Parameters v_s and v_{fad} have the same meaning as in Figure 15. In addition, v_R represents the rotational speed of the form roll.

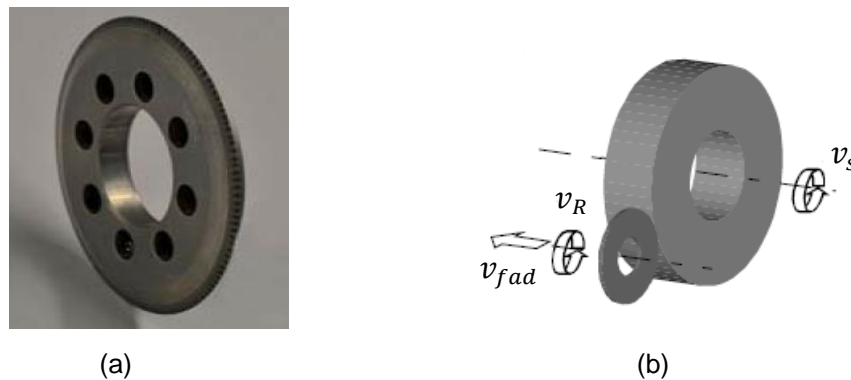


Figure 16: Rotating dressing tool (form roll), Source: Klocke, König (2005), p. 160.

The main body of the reconditioning tool is made of steel. Only a thin layer on the surface is equipped with diamond material.

In general, different types of diamond material can be applied in dressing tools. The selection should be based on the grinding grain material.

Beside the used procedure, the dressing parameters have a decisive impact on the dressing operation and thus on the behavior of the grinding wheel in the machining process.

2.2.2.1 Dressing Parameters

The results of the dressing process are strongly influenced by the depth of cut a_{ed} as well as by the feed per grinding wheel rotation f_{ad} in axial direction. In connection with the axial feed, the effective contact width of the dressing tool (Figure 17 (b)) is another important factor in the reconditioning system. In this context, the coverage ratio u_d , as a characterizing parameter for a reconditioning process, has to be considered. It strongly influences the effective roughness of the grinding wheel R_{ts} . When using rotating form rolls for dressing, the results are additionally influenced by the dressing velocity ratio q_d as well as by the rotation direction of the dressing tool relative to the grinding wheel.²¹

On the following two pages, more detailed considerations of different parameters are presented:^{21,22}

²¹ Conf. Saint-Gobain (2014/2015), p. 108-112;

²² Conf. Klocke, König (2005), p. 177-183.

In a dressing process, the tool's radial position is adjusted after each dressing stroke. Therefore, the tool is moved by the distance a_{ed} in the grinding wheel direction. That means, a_{ed} represents the cutting depth of the dressing tool. In general, the effective roughness of the grinding wheel R_{ts} increases by an increase of the cutting depth a_{ed} . This further implies that the surface roughness of the machined part also increases. The coverage ratio u_d (formula (2.3)) defines the number of grinding wheel revolutions while the dressing tool moves the distance of one times the effective contact width of the dressing diamond a_{pd} in axial direction (Figure 17 (b)). In general, a high coverage ration leads to a small effective roughness of the grinding wheel, which is followed by a low roughness value of the machined surface. The relationship between the coverage ratio and the obtained effective roughness of the grinding wheel R_{ts} is depicted in Figure 17 (a) for better understanding. Three different dressing situations are shown in this picture, in which the coverage ration continually decreases from the top situation to the bottom one because of an increasing axial feed f_{ad} .

$$u_d = \frac{a_{pd}}{f_{ad}} = \frac{a_{pd} \cdot n_s}{v_{fad}} \tag{2.3}$$

$$v_{fad} = f_{ad} \cdot n_s \tag{2.4}$$

In formula (2.3), a_{pd} represents the effective contact width of the dressing tool in operation and f_{ad} stands for the feed in axial direction during one grinding wheel revolution. The contact width of a form roll with a circular profile at the circumference can be calculated by the profile radius r_p and the cutting depth a_{ed} . The feed rate v_{fad} represents the velocity of the reconditioning tool by which it moves along the rotating grinding wheel in axial direction. It is calculated by the product of the axial feed per grinding wheel revolution f_{ad} and the grinding wheel rotational speed n_s (formula (2.4)). Mentioned characteristics can be seen in Figure 17 (b).

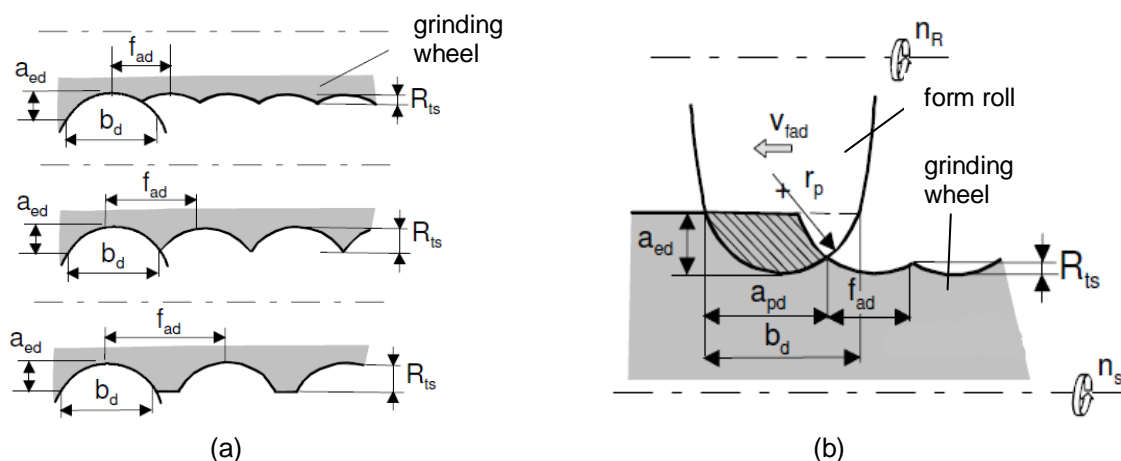
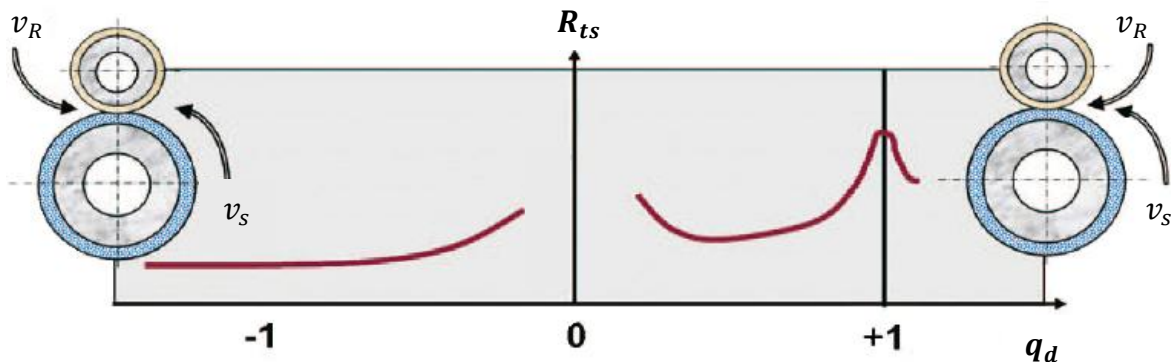


Figure 17: Contact conditions of a form roll dressing procedure, Source: Based on Klocke, König (2005), p. 177,178.

The velocity ratio for dressing q_d (defined in formula (2.5)) represents the ratio between the circumferential speeds of the dressing roll v_R and the grinding wheel v_S . It constitutes an important regulation variable in reconditioning processes using a rotating dressing tool. When climb dressing is performed (dressing tool and grinding wheel are moving in same direction in contact zone), q_d has a positive value, otherwise it has a negative one.

$$q_d = \frac{v_R}{v_S} \quad (2.5)$$

It has to be considered that q_d has a high level of influence on the grinding wheel topography and therefore, on the dressing and grinding machining result. The relation between the dressing velocity ratio q_d and obtained effective roughness of the grinding wheel R_{ts} is shown in Figure 18.



**Figure 18: Relation between velocity ratio q_d and effective grinding wheel roughness R_{ts} ,
Source: Saint-Gobain (2014/2015), p. 111.**

In order to obtain satisfying dressing results, it is recommended to choose a value between +0.5 and +0.85 for q_d when performing climb dressing and a value q_d between -0.2 and -0.5 for up-cut dressing. A dressing velocity ratio of +1 should be avoided because the grinding wheel structure is crushed due to extremely high process forces at this value.

Furthermore, it is required to use cooling lubricants in the dressing and the grinding process in order to obtain satisfying results. This topic is considered in detail in the subsequent chapter.

2.2.3 Cooling System

The reasons for applying cooling lubricants in the machining operation as well as their tasks in the grinding process are presented in the following sections:²³

²³ Conf. Klocke, König (2005), p. 15-16;127-129.

Generally, the majority of the supplied energy is converted into heat energy in the grinding process because of friction and the cutting operation. Therefore, all system components involved in the chip formation are exposed to thermal stress.

Without the usage of cooling lubricants, a high heat flow into the workpiece as well as into the grinding tool is present. This has a negative impact on these components. The heat which is received by the workpiece may lead to local structural changes in the fringes due to a strong temperature increase. By the use of cooling lubricants, adverse effects to the workpiece material and the grinding tool can be avoided.

Beside coolant's importance for the heat transfer, it also has a great impact on the friction conditions between grinding tool and workpiece. Thus, the cooling lubricant influences the process of chip formation as well as the wear of the grinding wheel.

Basically, the cooling lubricant has to fulfill primary and secondary tasks in the grinding process.

The most important tasks of the cooling lubricant, which already were named, are:

- The reduction of friction between grinding grain and workpiece as well as between bonding and workpiece by producing a stable lubricant film
- Cooling of the contact zone and the workpiece surface by heat absorption and heat transport

The secondary tasks can be classified into:

- Cleaning of workpiece and grinding wheel
- Chip transport out of the machining zone
- Corrosion protection of grinding machine parts and workpiece

The physical, chemical and biological properties of the cooling lubricant have a decisive impact on the machining process. Therefore, the choice of the right coolant type is very important and strongly depends on the application. Additionally, the environmental and human compatibility of the coolant have to be considered.

2.2.3.1 Classification of Coolants

As numerous different cooling lubricant types are available for industrial applications, a basic classification is given in this chapter:²⁴

In general, cooling lubricants can be distinguished by their basis liquid into oil or water based coolants.

Due to their importance for the present project, water based cooling liquids are further considered in the following section.

The group of water based cooling liquids is further subdivided into emulsions and aqueous solutions. These types are engaged if the cooling effect is of higher importance compared to the lubricating effect. This choice is based on the fact that water based cooling lubricants have a much better cooling effect but worse lubrication characteristics compared to oil based ones.

Beside the selection of the right cooling liquid type, an appropriate coolant supply of the grinding zone is of great importance.

²⁴ Conf. Klocke, König (2005), p. 129-135.

2.2.3.2 Coolant Supply

Basic information about the cooling system is presented in this chapter.²⁵

In order to provide satisfying machining results, the pressure and the flow rate of the coolant jet have to be perfectly adapted to the present machining conditions. Generally, cooling liquid's velocity v_{KSS} should have nearly the same value as the surface rotational speed of the grinding wheel v_s when it passes the outlet nozzle. If this requirement is met, the transport of cooling liquid into the grinding zone is ensured as the liquid "sticks" to the grinding wheel for about 10% of one wheel revolution. This situation is called equal velocity fluid delivery (according to H.W. Ott) and is shown in Figure 19 (b).

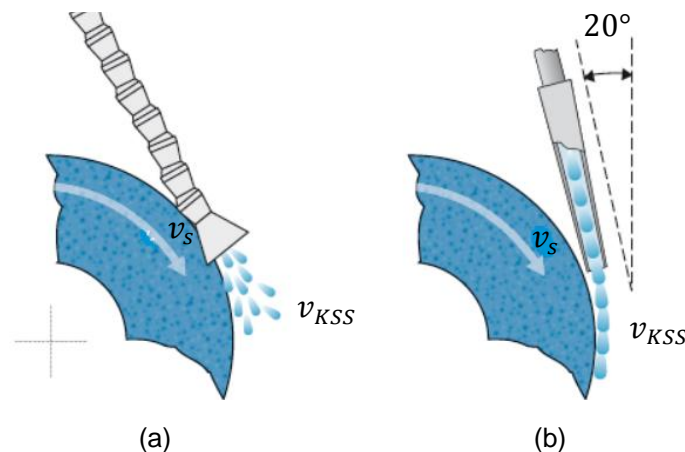


Figure 19: Coolant supply, Source: Winterthur Technology Group (2006), p. 98.

Furthermore, the design of the cooling liquid nozzle plays a decisive role.

Plastic nozzles, which are assembled from pluggable elements (Figure 19 (a)), may be a solution which provides great variability, but it does not meet the requirements for precision machining. These nozzles are often not able to maintain the set position and lead to turbulences in the coolant jet. For securing the principle of equal velocity fluid delivery, the setting angle of the nozzle should have a value of about 20° . Additionally, the outlet area should be a straight section, like it is shown in Figure 19 (b).

2.2.4 Machining Parameters

In the following three paragraphs, the parameters specific metal removal rate and velocity ratio are considered:²⁶

The specific metal removal rate Q'_w stands for the workpiece volume which is removed per second and per mm. To obtain this parameter, the metal removal rate Q_w is divided by the grinding wheel width in order to be able to compare different grinding tools. Formula (2.6) shows how Q'_w is calculated.

$$Q'_w = v_{fr} \cdot \pi \cdot d_w \quad (2.6)$$

²⁵ Conf. Winterthur Technology Group (2006), p. 98,99;

²⁶ Conf. Klocke, König (2005), p. 186,187,191.

In this relation, v_{fr} stands for the radial feed ratio which represents the quotient of the machining allowance and the grinding time. The variable d_w stands for the workpiece diameter, which represents the circumference of the machined seat in connection with π . Beside the machining time, the wear of the grinding wheel and the obtainable surface roughness of machined parts are inter alia influenced by this parameter. The cycle time of grinding machining can be reduced by an increase of Q'_w . Furthermore, this measure would lead to an increase of surface roughness on the machined part as well as to an increase of grinding wheel wear.

Another characterizing parameter of a grinding process is the velocity ratio q_s , which is the quotient of the circumferential speeds of the grinding wheel v_s and the workpiece v_w . This relation is presented in formula (2.7).

$$q_s = \frac{v_s}{v_w} \quad (2.7)$$

In general, obtained topography of a grinding machined part is a kinematic distorted depiction of the grinding wheel topography. It can be said that obtained surface roughness of machined parts slightly decreases by an increase of q_s . This can be explained by the overlap of grinding wheel cutting profile depictions on each part of the axle surface. Generally, a higher velocity ratio leads to a stronger overlap.²⁷

Usually, a spark-out operation has to be performed in the end of the machining cycle in order to ensure high surface quality as well as shape accuracy of machined parts. The spark-out action can be seen as a special form of a finishing operation in which the radial feed ratio v_{fr} has the value 0. This means, the grinding wheel does not change its position throughout this operation. In this final stage of the grinding process, elastic deformations of the system (workpiece, machine, tool) caused by grinding forces, dissipate. The spark-out time, more precisely the number of workpiece revolutions during the spark-out operation, plays a decisive role in this context and can be seen as another grinding process parameter.²⁸

Besides grinding machining, measuring technology constitutes an important part of the present project. Therefore, theoretical background of this topic is given in the next section.

2.3 Measurement Systems

In this chapter, theoretical basics about different methods of dimension measurement and about measurement system analysis (MSA) are given. As environmental conditions, especially temperature, have a great influence on the measuring process, the effect of thermal expansion of solids is also considered.

²⁷ Conf. Frühling (1976), n.p., quoted from Uhlmann (2014(d)), p. 556;

²⁸ Conf. Klocke, König (2005), p. 314.

Before theoretical background of the topic measurement systems (or also measuring systems) is given, the term is defined according to the Measurement System Analysis Reference Manual.

“Measurement System is the collection of instruments or gages, standards, operations, methods, fixtures, software, personnel, environment and assumptions used to quantify a unit of measure or fix assessment to the feature characteristic being measured; the complete process used to obtain measurements.”²⁹

2.3.1 Dimension Measurement Methods

A variety of different measuring principles is used in modern dimension measuring technology. Various principles provide different advantages and disadvantages regarding measuring range, uncertainty and robustness. For further usage of gathered measuring signals in control and feedback control systems, electric signals are required. Therefore, the non-electric signal from the environment (which describes the non-electric physical value) has to be transformed into an electric signal. It is essential that the measuring information is not distorted by the transformation process. One further step has to be done for application in modern measuring technology and automation; the measuring information has to be provided in digital form. This is required for data usage in computers or high-performance automation solutions.³⁰

2.3.1.1 Inductive Sensors

Theoretical basics about inductive sensors are presented in this chapter.³¹

In general, electric dimension measuring devices with analog and incremental measurement systems respectively have to be distinguished. Inductive sensors belong to the group of electric measuring devices with an analog measurement system.

Inductive dimension measurement is based on the principle that voltage is induced in a coil by alternating current. The group of inductive sensors can be divided into contactless devices, which only can be deployed for ferromagnetic materials, and contact measuring equipment. Latter ones are mostly used for precision dimension measuring applications.

For the present Thesis, inductive contact measuring technology, in particular the half bridge linear variable differential transducer (LVDT), is of great importance. Figure 20 shows the basic structure of the LVDT-methodology, in which the measuring pin is directly attached to the armature.

In this measuring principle, the movement of the measuring pin influences the field line length of a magnetic circle. The primary coil is provided with high carrier frequency in this arrangement.

The analog measuring signal provided by the sensor can directly be transferred to an analog display or it can be transformed into a digital one for further processing. The latter option is shown in Figure 20 in which the signal transformation is included in the step of signal processing.

²⁹ Chrysler Group LLC et al. (2010), p. 5;

³⁰ Conf. Parthier (2008), p. 111;

³¹ Conf. Keferstein, Marxer (2015), p. 141-143.

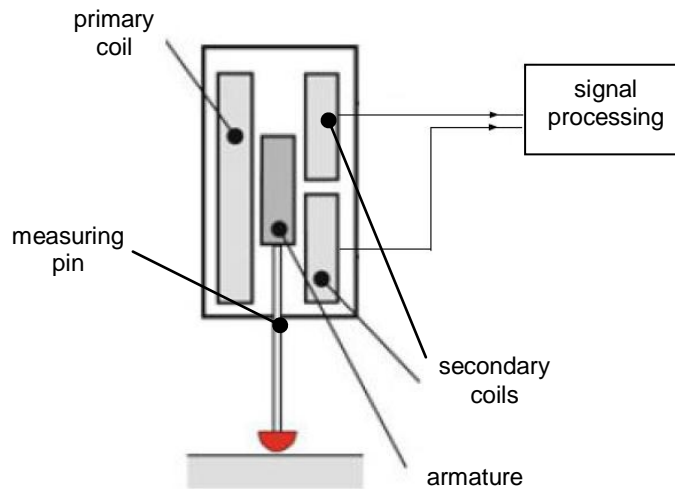


Figure 20: Linear variable differential transducer, Source: Based on Keferstein, Marxer (2015), p. 142.

Basically, the relation between displacement and induced voltage in a coil is non-linear. But if the armature moves between two symmetrically arranged coils (secondary coils in Figure 20) which are connected in a bridge circuit, the output signal is nearly linear in a range around the middle position after phase-controlled rectification. This circumstance is shown in Figure 21, in which x represents the displacement of the measuring pin and $|\Delta U|$ stands for the induced voltage.

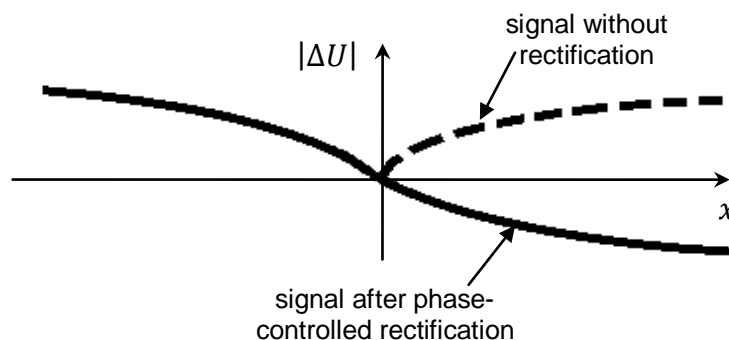


Figure 21: Relation between measuring pin displacement x and induced voltage $|\Delta U|$, Source: Based on Tränkler, Fischerauer (2014), p. 24.

Inductive precision indicators are on the one hand characterized by a high sensitivity level but on the other hand by only a small measuring range with a linearity error on a low level. This range is around the middle position, as Figure 21 shows. Usual linearity errors around the middle position of about $\pm 1\%$ lead to deviations of $\pm 0.1 \mu\text{m}$ in a measuring range of $20 \mu\text{m}$, for instance. Another important characteristic is the zero offset, which is stated in $\mu\text{m}/\text{K}$ and shows how the displayed measurement value changes with temperature when measuring the same measurand.

2.3.1.2 Incremental Sensors

Incremental sensors belong to the group of direct digital sensors. This implies that they provide a digital value directly without an analog-digital transformation. The measurement value given by an incremental system is the result of a counting operation. Beside optical incremental sensors, one of which is shown in Figure 22, measuring rulers with different magnetization levels are used in measuring technology.³²

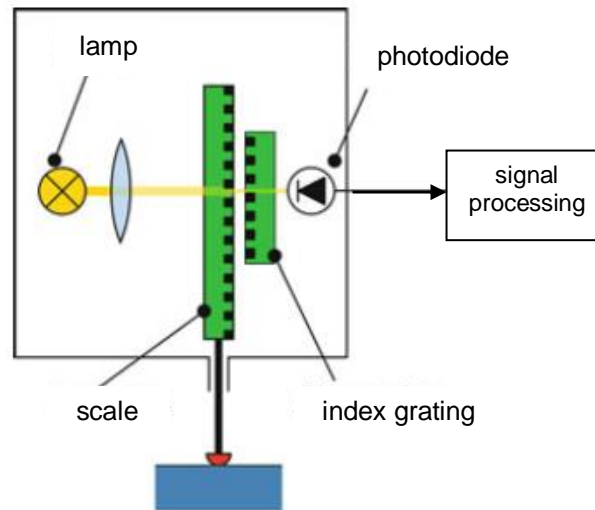


Figure 22: Optical incremental transducer, Source: Based on Keferstein, Marxer (2015), p. 144.

In the following paragraph, optical incremental transducers are described due to their relevance for this project:³³

The accuracy of such sensors is mainly determined by the measuring ruler. It represents the solid measure and is divided into quantization intervals of same size. By a displacement Δs of the measuring ruler against its initial position, impulses occur which are counted and displayed or transmitted to a computer for further usage. The magnitude of displacement can be calculated by multiplying the quantization unit of the ruler by the quantity of counted impulses. This implies that only displacements of the ruler, which means position changes, can be measured. For obtaining absolute dimension values, the incremental sensor has to be aware of its initial position, also called start point.

Precision digital sensors with optical scales are available for a measuring range between 10 and 100 mm and quantization intervals down to 0.01 μm . In general, the resolution of optical incremental transducers is finer than corresponding to their quantization intervals. This is enabled by interpolation procedures, which are based on phase shifted signals.

³² Conf. Parthier (2008), p. 129, 130;

³³ Conf. Parthier (2008), p. 128.

2.3.2 Determination of Characteristics on Geometry Elements

In this chapter, information about determination of circle diameters in a measuring plane as well as about evaluation of deviations from the cylinder shape is presented.

2.3.2.1 Diameter Determination

Different procedures and methodologies for determination of diameter values on geometry elements are available. Figure 23 shows four common approaches for diameter determination of a circle in a measuring plane. It is evident that all these methodologies provide different results. Furthermore, each approach is suitable for different applications.³⁴

These approaches are standardized according to DIN EN ISO 14405-1. This standard is an element of the GPS (Geometrical Product Specifications) system.

The GPS system provides the basics for industrial measurement technology and comprises a variety of different standards and specifications. By the implementation of this system, a complete, uniform and consistent standard for industrial measurement was created.³⁵

In general, information has to be provided on the drawing near the dimension specification regarding which of the four approaches has to be applied for a specific characteristic. This statement provides transparency for the machining and inspection operation. If no further information is provided near the dimension specification on the drawing, the Local Point (LP) method has to be applied for default. The receiver of the drawing (specification) is responsible for the selection of the right inspection method in order to fulfill stated requirements.³⁶

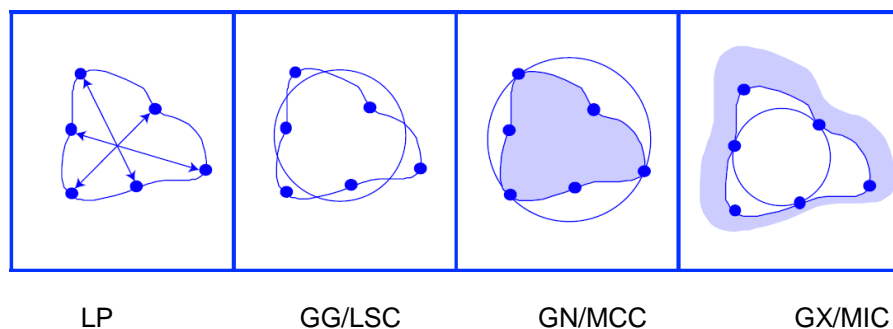


Figure 23: Approaches for diameter determination, Source: Carl Zeiss Industrielle Messtechnik (2017), p. 8.

In the following paragraphs, the four different methods are described.

When applying the Local Point method, the distance between two exactly opposite points is determined³⁷.

³⁴ Conf. Keferstein, Marxer (2015), p. 91, 92;

³⁵ Conf. Keferstein, Marxer (2015), p. 17;

³⁶ Conf. DIN EN ISO 8015 (2011), p.9;

³⁷ Conf. DIN EN ISO 14405-1 (2011), p. 10.

The Minimum Circumscribed Circle (MCC), which is determined by the Global Minimum (GN) method, is the smallest possible circle which comprises all the measuring points. This approach is used when the pairing capability of a shaft has to be checked.³⁴

The Maximum Inscribed Circle (MIC) is a circle having the greatest possible diameter value which can be placed in the center of the point cloud ensuring that each point is located outside the circle. This approach is used when the pairing capability of a bore has to be checked and is called the Global Maximum method.³⁴

The Global Gauß (GG) or Least Square Circle (LSC) method is described in the following sections.³⁸

By this methodology, the circle of least squared deviations, or in other words, the circle which best represents the data, is determined. For practical reasons, it has to be considered that the pairing capability is not ensured by this approach.

The method is based on minimizing the mean square distance from the fitting curve (least square circle) to data points. When having m points (x_j, y_j) , $1 \leq j \leq m$ in a measuring plane, the objective function is defined by formula (2.8). In there, d_j represents the (geometric) distance between the point (x_j, y_j) and the curve (circle) which best fits the data.

$$F = \sum_{j=1}^m d_j^2 \quad (2.8)$$

In this context, the basic equation of a circle has to be taken into account, which is presented in formula (2.9).

$$(x - a)^2 + (y - b)^2 = R_{LSC}^2 \quad (2.9)$$

In this relationship, (a, b) represents circle's center point and R_{LSC} stands for the radius. The distance d_j between a single point (x_j, y_j) and the index circle can be determined by formula (2.10).

$$d_j = \sqrt{(x_j - a)^2 + (y_j - b)^2} - R_{LSC} \quad (2.10)$$

In the end, the circle parameters a, b and R_{LSC} are determined in a way, so that condition (2.11) is met.

$$F = \sum_{j=1}^m d_j^2 = \text{minimal} \quad (2.11)$$

³⁸ Conf. Chernov, Lesort (2005), p. 239, 240.

2.3.2.2 Cylindricity Evaluation

Information about cylindricity evaluation of geometry elements is presented in this chapter:³⁹

The cylindricity of a geometry element corresponds with requirements, if the element is located between two coaxial cylinders with a radius difference equal to or smaller than the specified tolerance range. The location of the rotational axis and the cylinder radii should be selected in a way that the smallest possible radius difference between the two cylinders is ensured. In this context, Figure 24 is presented for further explanation.

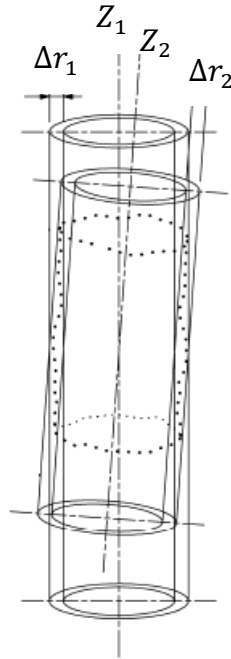


Figure 24: Cylindricity evaluation, Source: DIN EN ISO 1101 (2008), p. 60.

The dotted cylinder represents the actual shape of the geometry element. Different approaches for determination of the actual geometry are available and standardized in DIN EN ISO 12180-2.

In the example presented in Figure 24, two possible locations of the coaxial cylinders, which enclose the actual geometry element, are indicated by the rotational axes Z_1 and Z_2 . As the radius difference Δr_2 is smaller than Δr_1 , the correct location of the coaxial cylinders is the one which is defined by Z_2 . In order to fulfill the requirements, Δr_2 has to be equal to or smaller than the specified tolerance range.

2.3.3 Thermal Expansion of Solids

As the measuring process implemented in Lucchini RS' finishing line is influenced by environmental conditions, especially by temperature changes, the effect of thermal expansion has to be considered.

³⁹ Conf. DIN EN ISO 1101 (2008), p. 60.

Theoretical basics about the mathematical description of this effect are given in this chapter:⁴⁰

Thermal expansion is the tendency of matter to change in shape, area, and volume in response to a change in temperature. Due to its relevance for the project at hand, linear thermal expansion of solids is considered in the following section.

The effect of linear thermal expansion only takes into account the change of one dimension like the length for example. In this context, the linear expansion coefficient α_l has to be described. The linear expansion coefficient α_l of a solid body (a bar in this general description) with a length L constitutes the constant of proportionality between a temperature change ΔT and the relative length change $\Delta L/L$. According to that, α_l describes the relative length change as a consequence of a temperature change.

The material specific parameter, which is also temperature-dependent in general, is defined by formula (2.12).

$$\alpha_l = \frac{\Delta L}{L \cdot \Delta T} \quad (2.12)$$

After solving this differential equation by separation of variables, the temperature-dependent length of a bar can be calculated by relation (2.13).

$$L(T) = L(T_0) \cdot \exp\left(\int_{T_0}^T \alpha_l(T) dT\right) \quad (2.13)$$

The linear expansion coefficient can be assumed as a constant in the temperature range which is relevant for this project. This assumption connected with the definitions $L_0 = L(T_0)$ and $\Delta T = T - T_0$ lead to relation (2.14). Uniform warming or cooling of the whole bar is assumed for this relation.

$$L = L_0 \cdot \exp(\alpha_l \cdot \Delta T) \quad (2.14)$$

For most applications it is adequate to use the approximation shown in formula (2.15), in which the exponential function is approximated by an aborted Taylor series.

$$L \approx L_0(1 + \alpha_l \cdot \Delta T) \quad (2.15)$$

According to that, the length change $\Delta L = L - L_0$ can be approximated by relation (2.16).

$$\Delta L \approx \alpha_l \cdot L_0 \cdot \Delta T \quad (2.16)$$

Within the scope of the present project, diameter variations of axle seats due to temperature changes are analyzed. The approach to this task is the same as for calculation of temperature caused elongation of a bar. In this context, the initial circumference of the axle seat is taken for L_0 , which easily can be computed from the diameter. This implies that a temperature caused change of the circumference is

⁴⁰ Conf. Böge, Eichler (2008), p. 77-79.

determined by this approach, which easily can be back-calculated to a diameter change. When considering this procedure, it is getting evident that the diameter change ΔD can be calculated directly from the initial diameter D_0 . This relation is shown in formula (2.17).

$$\Delta D \approx \alpha_l \cdot D_0 \cdot \Delta T \quad (2.17)$$

2.3.4 Measurement System Analysis

Presented information in the following four paragraphs is derived from the Measurement System Analysis (MSA) Reference Manual:⁴¹

In modern production processes, measurement data are of great importance and are used in different ways. Basically, decisions about the product or the process are based on measuring data. For instance, the decision whether a product meets the specified requirements is commonly based on measurement data. Furthermore, the decision to adjust a manufacturing process is also often based on measurement data. Readings, or some statistics calculated from them, are compared with statistical control limits for the process. If the comparison indicates that the process is out of statistical control, adjustments to the process are made.

The benefit of such data-based procedures is strongly determined by the quality of used measuring data. If the data quality is low, the benefit of statistical procedures is likely to be low as well. On the other hand, if the quality of gathered data is high, the benefit is also likely to be high. The quality of measurement data is defined by the statistical properties of multiple measurements obtained from a measurement system operating under stable conditions.

The statistical properties most commonly used to characterize measuring data quality are the bias Bi and the variation of the measurement system s_g . The property called bias refers to the location of gathered data relative to a reference (actual) value. This circumstance is shown in Figure 25. When talking about bias, once is talking about a systematic error of the measurement system.

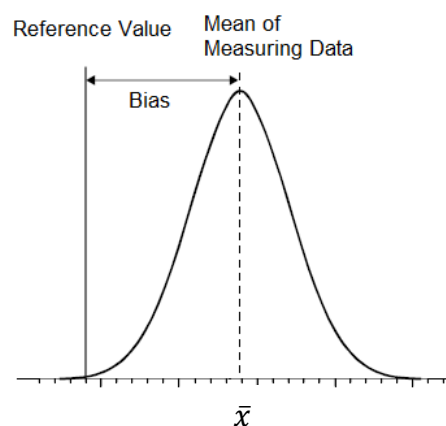


Figure 25: Systematic error of measurement system, Source: Based on Chrysler Group LLC et al. (2010), p. 6.

⁴¹ Conf. Chrysler Group LLC et al. (2010), p. 3, 4.

The property called variation refers to the spread of the data around its mean \bar{x} . The bigger the variation in a data set is, the wider is the Gaussian distribution curve. For this consideration a normal distribution of the data is assumed. In Figure 26, the variation of measuring data from two different measurement systems is compared. In this example, the variation (standard deviation s_g) of the measurement values from the red measurement system is smaller. Thus, the repeatability of this measurement system is higher compared to the blue ones.

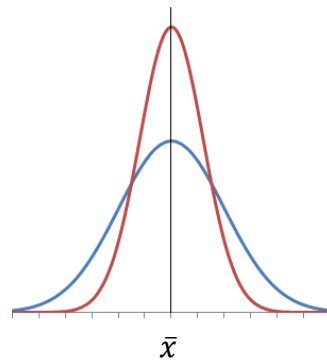


Figure 26: Variation of a measurement system, Source: Based on Chrysler Group LLC et al. (2010), p. 7.

For theoretical considerations in this chapter, basic statistical background has to be provided.

The “real” or actual mean μ and the “real” or actual standard deviation σ of a process are unknown in most cases. Therefore, values for the mean and the deviation (\bar{x} and s) are calculated from the present readings. In statistical language this is called “estimating”.⁴² As the following considerations about different forms of variation are of general nature, the actual standard deviation σ is used.

If the measurement system generates too much variation, the quality of gathered data is low. This may lead to unusable data. This circumstance is described in detail in the following consideration:⁴³

The basic relation between the measuring process variation and the actual variation of the investigated manufacturing process is shown in formula (2.18).

$$\sigma_{obs}^2 = \sigma_{actual}^2 + \sigma_{ms}^2 \quad (2.18)$$

In formula (2.18), σ_{obs} stands for the observed process variation, which is the result obtained from measurement values gathered by a measurement system. Squared observed process variation is the sum of squared manufacturing process’ actual variation and squared variation of the measurement system itself. The actual variation of the manufacturing process σ_{actual} is the parameter which should be determined in order to be able to assess the process performance. In this context, a measurement system with a high level of variation σ_{ms} may not be appropriate for use in analyzing a manufacturing process because its variation may mask the actual variation in the manufacturing process.

⁴² Conf. Bredner (2014), p. 3-5;

⁴³ Conf. Chrysler Group LLC et al. (2010), p. 20, 21.

2.3.5 Procedures for Measurement System Analysis

In this chapter, a short overview of procedures for performing a measurement system analysis is given:⁴⁴

Figure 27 shows the approach for conducting a measurement system analysis. Before one of the studies can be carried out, the resolution of the measurement system has to be checked. The resolution is said to be sufficient for measuring a certain characteristic, if it is finer than five percent of a specific reference figure. In most cases, characteristic's specified tolerance range is taken as reference for this evaluation.

In the scope of the type-1 study, the capability indices C_g and C_{gk} are used to determine whether the measurement device is capable for its intended use under actual operating conditions. For this study, a standard has to be utilized whose true value lies within the tolerance range of the test characteristic. If for technical reasons no measurement standard is available, the calculation of C_{gk} is omitted. In this case, only the repeatability can be determined by using a suitable measuring object. The repeatability describes the variation in measurements obtained with one measuring instrument when used several times by one appraiser while measuring the identical characteristic on the same part. By performing the repeatability study, the equipment variation or within-system variation is determined.

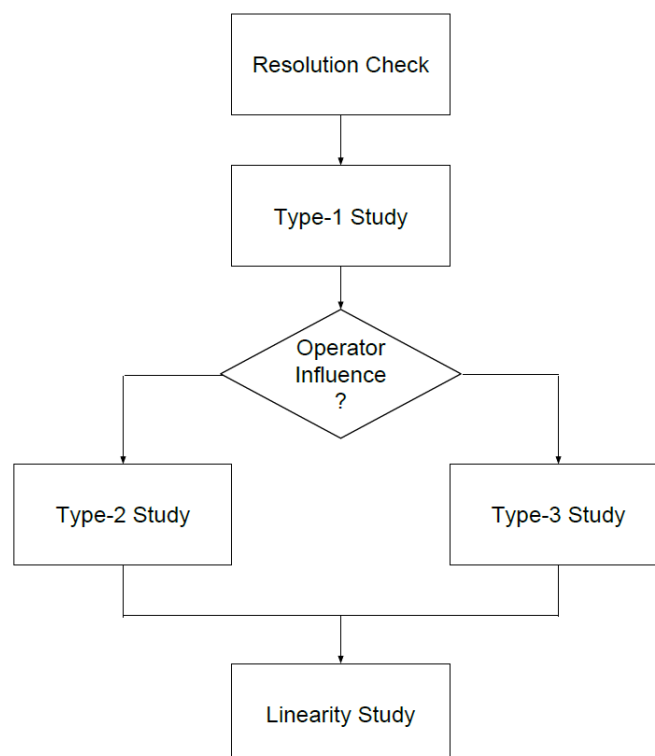


Figure 27: Approach for measurement system analysis, Source: Based on Audi AG et al. (2002), p. 18.

⁴⁴ Conf. Audi AG et al. (2002), p. 16-18.

For the type-1 study, 50 measurements have to be taken from the measurement standard at short intervals under repeatable conditions. The standard has to be reinserted in the same position before each measurement. If a single measuring process requires a lot of time, the quantity of taken measurements can be reduced. Nevertheless, a minimum of 20 taken measurements must not be undershot.

When the type-1 study is completed with satisfactory results, further course of action depends on the fact whether operator influence is present in the investigated measurement system or not. It is only possible to exclude user influence entirely, if the measuring process works completely automated including an automated loading operation of the part into the measuring machine. If an operator influences measuring results, the type-2 study has to be conducted which determines the appraiser influence. In this study, the index $\%R\&R$ (repeatability and reproducibility) is used to assess whether a measurement device is suitable for a certain measuring task, taking into account all the influences. In contrast to the type-1 study, the R&R-investigation is not conducted under repeatable conditions. That means, not only the influence of the measurement equipment is present. Different factors which basically influence a measuring process are shown in the Ishikawa diagram for the automated 3D measurement system (Figure 31).

If operator influence can totally be excluded, the type-3 study has to be performed instead. It can be seen as a special form of the type-2 study. Objective of this study is to determine whether a measuring device is suitable for the measuring task at hand, taking into account the operating conditions and any influences originated from different production parts. The system can be assessed by means of the index $\%EV$. EV stands for equipment variation.

In this context, it has to be mentioned that basically two different approaches for measuring data analysis exist for the type-2 and type-3 study. These are namely the ARM (Average-Range-Method) and the ANOVA-method (Analysis Of Variance). Basically, ARM can be carried out without the need of special statistics software and constitutes a method which is appropriate for a basic measurement system evaluation. Therefore, this approach is used for the performed MSA within the scope of this project.

A linearity study constitutes the last step to the acceptance of the measurement system. Thereby, the relationship between the output variable and the input variable (measurand) is determined as the input variable changes within the operating range of the measurement system. In other words, the change in bias over the normal operating range of the measurement system is determined. As well as bias, a linearity inaccuracy constitutes a systematic error component of the measurement system.

3 Measurement System Investigation

In this chapter, the performed MSA of the automated 3D measurement system, which is responsible for final dimensional inspection, is described. Associated results and derived measures are considered in the end of this section.

3.1 Measurement System Description

Before going into more detail about the MSA, the measurement device itself has to be considered. By this measurement system, all important product characteristics like lengths, diameters as well as the shape and the radial run-out of different axle seats are checked. The axles are loaded into loading prisms by automatic handling equipment to obtain the measuring position. Thus, the whole measuring process is performed automatically without any operator influence. Operators only have to interfere when problems occur in the measuring process or for the calibration action of the system. Once the axle is positioned in the loading prisms, centering pins, one of which is powered by a servo drive, are inserted in the centering of each axle side to rotate the axle. The 3D measuring machine, which is shown in Figure 28, is based on the principle of contact measurement. It is set up with four rests, lying next to each other on a linear guidance system. Each rest has its own servo drive, which enables it to move longitudinally to the crosscut which has to be measured, and contains two measuring units (1).

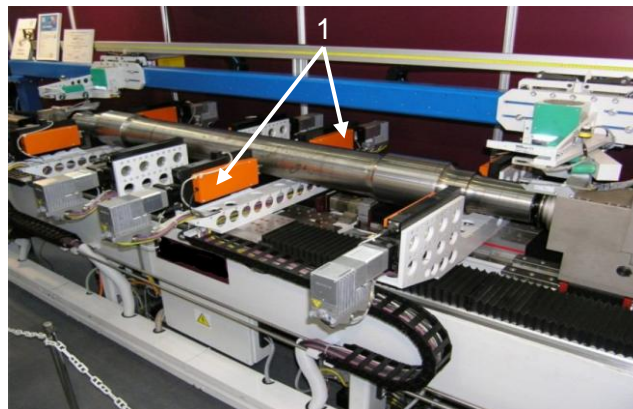


Figure 28: 3D measuring machine, Source: AMEST (2008).

Information presented in the following three paragraphs is based on the manufacturer of the measuring machine (personal contact):

Each measuring unit comprises a pair of linear guideways for positioning the measuring head on the axle surface. In measuring unit's body (shown in Figure 29), optical incremental transducers (considered in chapter 2.3.1.2) are responsible for determining the exact position of the measuring head. Once the measuring sphere touches the axle surface, the axle gets rotated and the inductive measuring head determines a huge amount of points around its circumference. For data point acquisition, the half bridge inductive probes technology (LVDT, described in chapter 2.3.1.1) is used. In the end, each point gathered by the measuring machine is the result of combination of the values

detected by the inductive measuring heads and the fixed position of optical incremental transducers inside the body of the rests. The diameter value is then determined by the machine control out of the set of points around the circumference by using the GG method (chapter 2.3.2).

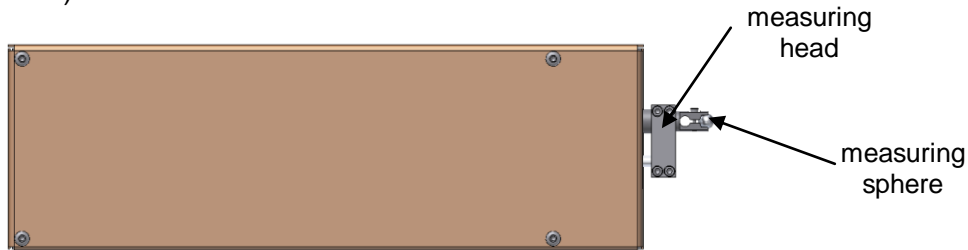


Figure 29: Measuring unit, Source: AMEST (2016).

As the measurement system under consideration is also responsible for determining the shape (cylindricity) of axle seats, system's approach for calculating the cylinder is described in the following section.

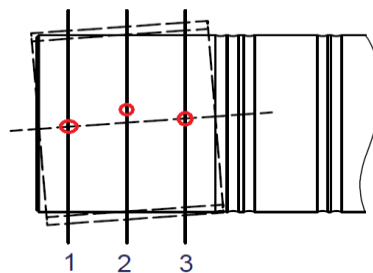


Figure 30: Cylinder determination, Source: Own illustration.

In this context, the axle seat is measured in three different sections (measuring planes), in which the diameters and the center points are calculated by means of the GG method. The center points C1 and C3 (red points), in section 1 and section 3 respectively, are used to determine the rotational axis of the axle seat (Figure 30). Then the distances between every single measuring point determined in the three measuring sections and the calculated axis are determined. The maximum and the minimum distance are taken into account for computation of the actual cylindricity shape error.

Described method of cylindricity evaluation should be compared with the standardized procedure presented in chapter 2.3.2.2. In supplier's approach, the maximum and minimum distances from the axis can be seen as the radii of coaxial cylinders. The difference to the standardized method is that the axis, and thus the location of the cylinders, is defined beforehand by the center points C1 and C3.

Furthermore, the way of determining the actual shape of the geometry element has to be analyzed and compared to standardized procedures.

According to DIN EN ISO 12180-2, four different approaches for determining the actual geometry element are available. As the geometry is captured in three parallel measuring planes along the axle journal, the roundness acquisition strategy is performed in supplier's measuring operation.⁴⁵

⁴⁵ Conf. DIN EN ISO 12180-2 (2011), p.11.

3.2 Measurement System Analysis

The investigated measurement system is used for final dimensional inspection of all machined parts and thus for the decision whether a product meets the requirements or not. Poor quality of gathered measuring data may therefore lead to wrong decisions which may have dire consequences. Furthermore, readings from this measurement system, as well as statistics calculated from them, are the basis for evaluation of the process performance.

These facts are the reason for preparing and performing a detailed measurement system investigation at Lucchini RS' production site in Lovere. The performed MSA is based on the procedures described in chapter 2.3.5. These procedures as well as formulas (3.1) to (3.12) are based on the "Measurement System Capability" Reference Manual⁴⁶.

For the investigations, the wheel seat diameter of the selected axle type is chosen as the reference characteristic. The specification states a required diameter value of $\varnothing XXX \text{ v}6$ for this axle section which implies a tolerance range of $25 \mu\text{m}$ for this characteristic.

3.2.1 Basic Assessment

In a first step of the MSA, a general assessment of the measurement system is performed. This inter alia includes the evaluation of system's resolution as well as the suitability of the measurement system for its intended use.

For this evaluation, the relation between measurement device's resolution and the tolerance range of the characteristic to be measured is taken into account. As the automated 3D measuring machine's resolution ($0.1 \mu\text{m}$) is short compared to characteristic's tolerance range ($25 \mu\text{m}$), the first evaluation step is completed with satisfactory results. Formula (3.1) is presented to confirm this statement.

$$\%RE = \frac{\text{Resolution } RE}{\text{Tolerance Range } TR} = \frac{0.1 \mu\text{m}}{25 \mu\text{m}} = 0.4\% \quad (3.1)$$

The requirement of $\%RE \leq 5\%$, in order to be able to reliably determine measurement values, is met.

3.2.2 Type-1 Study

As no measurement standard within characteristic's tolerance range is available, a production part is taken to perform this investigation. To get a trustable reference value for the selected part, it is measured by a coordinate measuring machine (CMM).

The study is conducted by repeated measurements (20 times) of the same characteristic on the selected production part in short time intervals under repeatable conditions. For each of the 20 measuring runs, the axle is unloaded and then reinserted in the measuring

⁴⁶ Conf. Audi AG et al. (2002), p. 20-22, 28-29.

position automatically. As the 3D measuring machine is placed in the automated finish machining line, the production has to be stopped for this investigation. Due to the fact that one axle measurement takes about five minutes (all axle characteristics are measured in each run; only measuring the desired characteristic is not possible due to the fully automated measuring program), the number of repeated measurements is reduced to the lower level of required repetitions.

After obtaining the results from the repeated measurements, gathered data is statistically analyzed. As a first step, the mean \bar{x}_g as well as the standard deviation s_g are determined by applying formulas (3.2) and (3.3) respectively.

$$\bar{x}_g = \frac{1}{l} \sum_{i=1}^l x_i \quad (3.2)$$

$$s_g = \sqrt{\frac{1}{l-1} \sum_{i=1}^l (x_i - \bar{x}_g)^2} \quad (3.3)$$

In formulas (3.2) and (3.3), l represents the number of determined readings (20 in the present case) and x_i stands for the individual readings from repeated measurements.

In a next step, the capability index C_g , which only considers a random component (repeatability), is determined by relation (3.4). In there, TR represents the characteristic's specified tolerance range.

$$C_g = \frac{0.2 TR}{4 s_g} \quad (3.4)$$

As the wheel seats on axle's A- and B-side are inspected by different measuring units, (the measuring device comprises four measuring units for the measurement of different axle sections) data for each axle side is analyzed. The results $C_{gA} = 2.06$ (capability index for wheel seat on A-side) and $C_{gB} = 2.27$ (for B-side) meet the requirement of $C_g \geq 1.33$. Obtained results imply that the repeatability, and thus the general appropriateness of the measuring technology for the measuring task at hand, is given.

After that, the capability index C_{gk} , which considers also a systematic error component beside a random one, has to be determined according to formula (3.5). In contrast to the C_g -index, C_{gk} also considers the true value of the measured characteristic by taking into account the bias Bi . This parameter represents the difference between the mean of observed data and the reference value. Stated relation is shown in formula (3.6), in which x_{ref} represents the reference value.

$$C_{gk} = \frac{0.1 TR - Bi}{2 s_g} \quad (3.5)$$

$$Bi = |\bar{x}_g - x_{ref}| \quad (3.6)$$

For C_{gk} , the same minimum value is required as for C_g , which leads to the specification $C_{gk} \geq 1.33$. The data from the wheel seat on the B-side provides a satisfactory result of $C_{gk B} = 1.77$. For the wheel seat diameter of the axle's A-side, calculated bias has a value of $2.5 \mu\text{m}$, which exactly is 10% of the tolerance range. Therefore, all ends up in a result of $C_{gk A} = 0$. This constitutes no satisfactory result when taking into account the requirement.

In conclusion, the results of the type-1 study show that the measuring device would basically be appropriate for the task at hand due to satisfying C_g -indices. That means, the variation of the measurement system (s_g) is on an acceptable level. Nevertheless, the measurement system capability is not given due to the present level of bias.

Further investigations are conducted because of the non-satisfactory result of C_{gk} -evaluation for the axle's A-side, especially due to the present level of bias as a systematic error component. The results of these investigations are presented in chapter 3.2.4.

3.2.3 Type-3 Study

In general, the type-2 or type-3 study should only be performed after a positive result of the type-1 study. As the basic appropriateness for the measurement system is given and main causes for the current level of bias are determined (further information in chapter 3.2.4), the investigation is continued.

As the investigated system contains a measuring device with an automated loading procedure, operator influence can be neglected. Therefore, the type-3 study is performed. As a first step, the conditions of the study have to be defined. This includes the definition of the quantity of different production parts n as well as the number of repeated measurements r of the same object. Requirements for each of these condition variables as well as the values selected for the present investigation are stated in Table 2.

Table 2: Conditions of type-3 study, Source: Own illustration.

	Requirement ⁴⁷	Value for investigation
No. of different objects n	≥ 5	7
No. of repeated measurements r	≥ 2	3
Product $n \cdot r$	≥ 20	21

The total number of taken measurements in the course of this study is close to the required limit due to time reasons, like it is for type-1 study.

The Reference Manual states that it is recommended to measure all the different objects n in one run and to repeat this run r times. As it is often not possible to strictly observe the recommended approach due to practical reasons, the sequence can be adapted to ones demand.⁴⁷ Since the measurement system is integrated in the production line, it is not

⁴⁷ Conf. Audi AG et al. (2002), p. 28.

possible to perform the investigation in the sequence recommended by the Reference Manual. It is performed in a way that each of the n parts is measured r times, before the next part enters the measuring machine. It has to be documented that each part is unloaded and reinserted before each of the r measuring rounds.

In a first step of data analysis, the range R of each measuring object has to be determined. The range R of a data set represents the difference between the highest and the lowest value of the underlying data and therefore shows the range in which the data is distributed. Formula (3.7) shows this relationship. In there, x_i stands for the individual values gathered in three repeated measurements of the same production part.

$$R = \max(x_i) - \min(x_i) \quad (3.7)$$

After determination of R for each of the seven different objects, the mean range \bar{R} is calculated by employing formula (3.8).

$$\bar{R} = \frac{1}{n} \sum_{j=1}^n R_j \quad (3.8)$$

After that, the index EV , which is taken into account for assessing the results of the type-3 study, is calculated by applying formula (3.9).

$$EV = K_1 \cdot \bar{R} \quad (3.9)$$

$$K_1 = \frac{5.152}{d_2^*} \quad (3.10)$$

Basic statistical background has to be given in the following three paragraphs for explanation of relations (3.9) and (3.10):^{48, 49}

In the procedures selected for the present measurement system analysis, the figure R is used to represent the variation in a data set. The factor K_1 should improve the value of the figure \bar{R} (determined from the present data) in a way that it gets close to the actual value of variation. This approach is known as unbiased estimation. When substituting relation (3.10) in (3.9), the ratio \bar{R}/d_2^* serves as estimation for the actual standard deviation $\sigma_{R\&R}$. The true or actual value of variation, respectively range, is unknown.

The factor 5.152 in formula (3.10) is utilized to represent 99% of the normal distribution. Historically, by convention, a 99% spread has been used to represent the “full” spread of measurement data, represented by a 5.152 multiplying factor. This means that $\sigma_{R\&R}$, which is estimated by \bar{R}/d_2^* in the present procedure, is multiplied by 5.152 to represent a total spread of 99%. The value of the multiplying factor originates in the fact that 99% of the surface under a normal distribution curve is located in a range of $\pm 2.576 \sigma$ around the mean. In contrast, it would also be possible to increase the multiplying factor to a value of

⁴⁸ Conf. Audi AG et al. (2002), p. 57;

⁴⁹ Conf. Chrysler Group LLC et al. (2010), p. iv.

6.0, which represents a 99.73% spread. This embodies a variation of $\pm 3\sigma$ around the mean and represents the full spread of a “normal” curve.

For the procedures within the scope of this project, the 99% spread was utilized for calculations due to the usage of this approach in several books.

The factor d_2^* depends on the number of trials r , on the number of different objects n as well as on the number of different operators k . As the operator influence is negligible for the automated measurement system, the value one is taken for the variable k in the present example. Relation (3.10) is a statistical formula, for which d_2^* is taken from a table (accessible in appendix). The lines of the table are represented by different manifestations of the product $k \cdot n$, which stands for the sample size. Different numbers of trials r build the columns. The number of trails represents how often the sample is taken.

Like it was done for the type-1 study, a differentiation between axle’s A- and B-side was made for the assessment of the equipment variation. In the end, the characteristic values EV_A (A-side) and EV_B (B-side) were calculated to be both 0.00211 mm. This was possible due to the same means of ranges \bar{R} , since the factor K_1 is the same for each side anyway.

$$EV = 2.97804 \cdot 0.00071 \text{ mm} = 0.00211 \text{ mm} \quad (3.11)$$

As this value for EV is not meaningful by itself, it is compared to a reference value. For this, the characteristic’s tolerance range is most commonly taken. A system in use is said to be appropriate, if the requirement $\%EV \leq 30\%$ is met. The calculation for Lucchini RS’ automated measuring machine is shown in formula (3.12).

$$\%EV = \frac{EV}{RF} = \frac{EV}{TR} = \frac{0.00211 \text{ mm}}{0.025 \text{ mm}} = 0.0844 = 8.44\% \quad (3.12)$$

This result implies, that the measurement system would be suitable for the measuring task at hand according to the requirements stated for the type-3 study. Furthermore, the low level of measurement system variation is confirmed by this result.

According to literature, the type-3 study is followed by the performance of a linearity investigation, which constitutes the final step to the acceptance of the measurement system. As neither a masterpiece with different diameters on various axle sections, nor other possibilities to cover the whole operating range of the measuring device were available, the linearity study could not be performed in the present case.

3.2.4 Root Cause Analysis

Similar to other production process steps, the measurement operation, and thus the measurement system, is impacted by both random and systematic sources of variation. These are due to common and special causes respectively. In order to control measurement system’s bias and variation, potential sources of these error components have to be identified. An Ishikawa diagram, which is theoretically described in chapter 2.1.1.3, is used for this task. The diagram prepared for the automated 3D measurement system is shown in Figure 31.

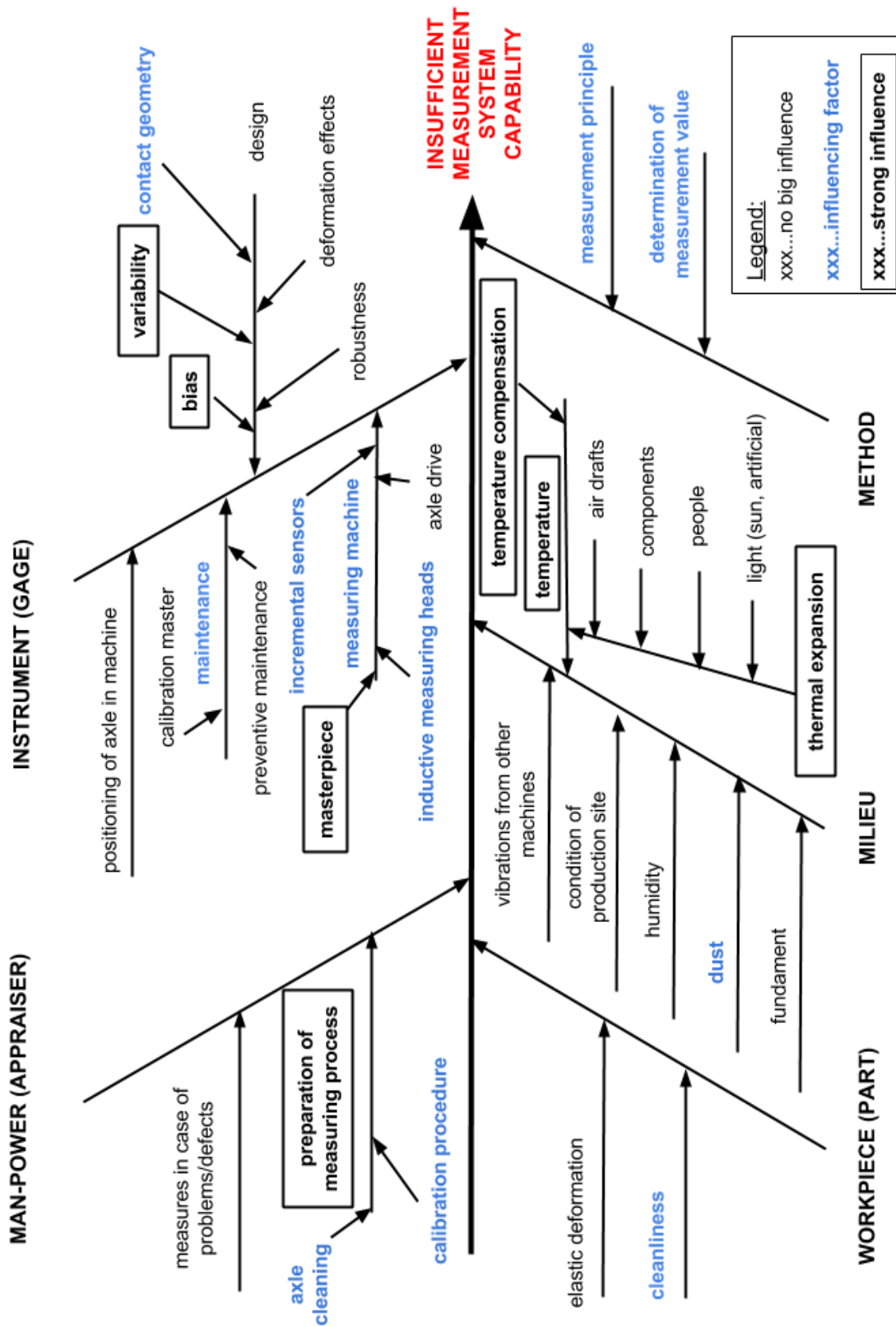


Figure 31: Ishikawa diagram for automated 3D measurement system, Source: Own illustration.

In there, the five categories appraiser (operator), gage, workpiece (part), milieu (environment) and method are used to categorize influencing factors and potential causes for insufficient measurement system capability.

The results of the measurement system analysis show that there is an offset (bias) between measurement values from the automated 3D measuring machine and values taken by the coordinate measuring machine.

The investigated measurement system is integrated in the automated finish machining line without any kind of housing around the measuring machine. Therefore, environmental conditions in the production hall have a great influence on the measuring process. Attention should be paid to the temperature (marked as main influencing factor in Figure 31) in the production site as no measures for direct temperature compensation are implemented in the control of the measuring machine. This circumstance plays a decisive role in the measuring process at hand, as no air condition system exists in the production site. Therefore, the room temperature changes in a certain range within a single day, especially in summer.

This problem can theoretically be overcome by measurement system's basic principle.

Following information about the measuring machine was obtained from the manufacturer via personal communication:

In order to compensate temperature changes, comparing measurements (mastering) between a masterpiece and the product to be measured are performed. The masterpiece is located under the bench of the measuring machine and therefore its temperature adapts to room temperature level. Furthermore, the measuring principle is based on the assumption that the product has also adapted to this temperature. According to this assumption, the measurement system is adjusted to the current room temperature and therefore to the actual temperature of the product which has to be measured after performing a calibration procedure on the masterpiece in a dedicated frequency.

As a next step, the actual situation in Lucchini RS' production site has to be considered. Based on not fully satisfying results of the type-1 study due to oversized bias, cross measurements between the automated 3D measuring machine and the coordinate measuring machine were performed in order to verify obtained results. Nine wheel seats of different axles were measured on the 3D measuring machine five times. The averages of those results were compared to reference values determined by the coordinate measuring machine. Obtained results are shown in Figure 32, in which the specification limits for the measured characteristic are represented by the two horizontal red lines. Furthermore, a vertical line is inserted in the diagram which separates the readings from two different lots. The first lot was produced in July, the second one in November. This information is of importance for further considerations.

It is evident that there is an offset at each axle between the values taken by the 3D measuring machine (black crosses in Figure 32) and the coordinate measuring machine (red crosses in Figure 32). For each of these axle seats, the bias according to formula (3.6) was determined. Obtained results were further analyzed and presented in Table 3.

Table 3: Bias of 3D measurement system, Source: Own illustration.

	A-Side	B-Side
Max. Bias $B_{i_{max}}$	6.5 μm	6.4 μm
Mean Bias $\overline{B_i}$	2.8 μm	3.9 μm

The results for the first lot show constantly lower measurements taken by the automated 3D measuring machine compared to the reference values. The situation for the second lot is mostly contrary. Up to a certain point, this phenomenon can be explained by the physical effect of thermal expansion (chapter 2.3.3). Before going into more detail about this issue, an introduction to this topic is given in the subsequent sections.

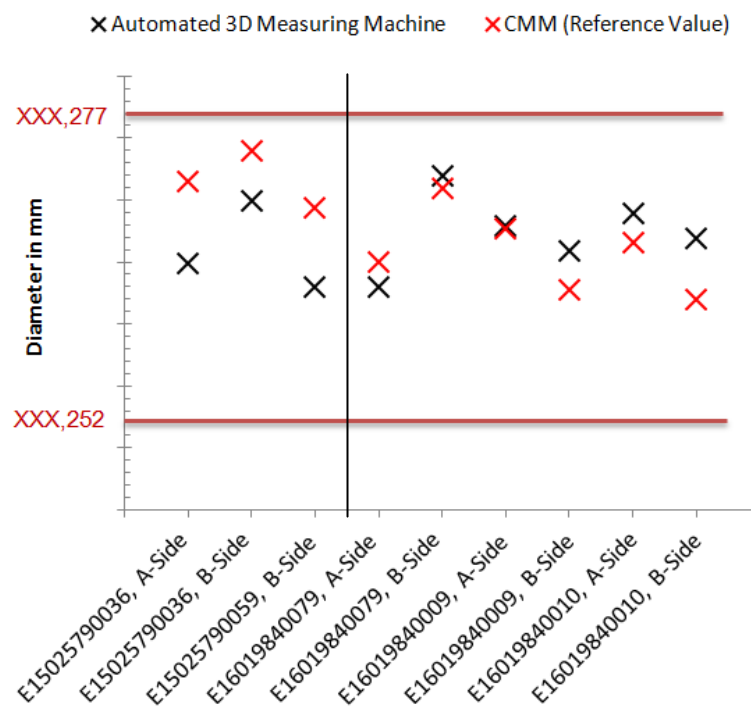


Figure 32: Comparing measurements between 3D measurement system and CMM, Source: Own illustration.

As the measuring principle is based on the assumption that the masterpiece and the product have the same temperature, the quality of gathered measuring data strongly depends on this assumption's accuracy for the present measuring operation. Therefore, temperature measurements on the masterpiece as well as on different axes are performed in order to verify the assumption. By means of a contact measurement device, the temperature is measured right before starting the dimension measurement operation.

Due to observed temperature differences between the masterpiece and production parts, the accuracy of the assumption, on which the measurement system's principle is based, is refuted. According to various measurements, the production part's temperature can be seen as nearly constant and as independent from room temperature. This is true for the state right after the grinding process. The time between the grinding and measuring

operation is quite short in most cases. Therefore, it can be assumed that the production part has a temperature which is a result of the machining operations performed in the automated finish machining line. In contrast, the temperature of the masterpiece is strongly influenced by the room temperature and thus changes in a certain range throughout one day as well as throughout the year. Additionally, exceptional cases, in which a buffer time between the grinding machining and the measuring operation occurs, also have to be taken into account. In these cases, the production part gets time to change its temperature towards the room temperature level.

These findings imply that a temperature difference between the masterpiece and the production part cannot be avoided in Lucchini RS' measuring process. Furthermore, a general quantification of the temperature difference is not possible.

Information given in the last sections enables the explanation of the result differences between the two lots presented in Figure 32 to a certain extent. In this context, it is important to mention that the explanation of the phenomenon (the 3D measurement system in the production line provides lower measurement values in summer and higher ones in winter compared to reference values) given in the following sections is restricted to the temperature influence. Further influencing factors to the measurement system (Figure 31) are not considered.

In summer months, the temperature in the production hall and thus the master piece temperature (between 30°C and 31.5°C for the three measured axes) are generally higher than the axle surface ones after the machining operation. The production part's temperature is determined to be in a range between 27.5°C and 29°C. This means, the measurement system is adjusted by a masterpiece which is a few degrees warmer than the part that is going to be measured. In other words, the measurement system is adjusted for measuring a production part which has the master piece's temperature. But as the axle temperature is a few degrees lower than expected, the readings provided by the automated measurement system are lower than the actual value. These results can be traced to the physical effect of thermal expansion up to a certain point and can be explained as follows:

Due to lower production part temperature compared to the masterpiece, the extent of thermal expansion of the axle is lower as it is expected after calibration at the reference piece (master). As the measurement system is adjusted to the masterpiece, which on average is 2.5°C warmer than the production part, the readings provided by the automated measuring machine are between 4 µm and 6.5 µm smaller than the actual value (Figure 32). The present magnitude of deviation from the actual value can be verified by calculating the diameter change caused by the temperature difference between the reference part and the axle by applying formula (2.17). For the present calculation, the linear expansion coefficient α_l of mild steel ($\alpha_l = 12 \cdot 10^{-6} \text{K}^{-1}$) is inserted⁵⁰.

$$\Delta D \approx \alpha_l \cdot D_0 \cdot \Delta T = 12 \cdot 10^{-6} \text{K}^{-1} \cdot 0. \text{XXXXXX m} \cdot 2.5 \text{ K} \approx 5.5 \text{ } \mu\text{m} \quad (3.13)$$

The calculation in (3.13) implies that the 3D measuring machine provides readings which are about 5.5 µm smaller than the actual ones if production part's temperature is 2.5 K

⁵⁰ Conf. Böge, Eichler (2008), p. 97.

lower than the one of the masterpiece. It is assumed for the calculation that the masterpiece has the same diameter as the production part, for which the middle of the specified tolerance range is taken. As Lucchini RS uses a masterpiece with a diameter value of about 70% of the production part's wheel seat diameter, an additional error component is present in the measurement system.

On the other hand, the temperature in the production site is generally lower than the production part ones right after termination of the machining operation in winter months. In this season, room temperature is nearly kept constant throughout the day on a value between 22°C and 23°C because of constant heating. That means, the measurement system is adjusted by a colder masterpiece compared to the actual product temperature. This furthermore results in a measuring value that is higher than the reference value for this characteristic. This phenomenon can be observed at readings to the right of the vertical separation line in Figure 32.

It has to be mentioned that the conditions for determining these measuring values by the automated 3D measuring machine were slightly different to the ones for the three readings determined in summer. A buffer time occurs between the grinding and measuring operation for these six axles. Therefore, the axle temperature changes somewhat towards room temperature level. This reduction of temperature difference between the masterpiece and the axle to be measured can be seen as explanation for generally lower offsets to the reference value.

Finally, it has to be pointed out again that the present offset between readings from the 3D measuring machine and reference values cannot be explained only by the influence of temperature differences. The measurement system is affected by a variety of other influences, whereby their impact on the measuring value cannot be quantified.

Nevertheless, presented explanation clearly showed that the temperature in the production hall, and thus the masterpiece's one, has a great influence on measurement results. Furthermore, the magnitude of actual offset can mostly be explained by theoretical considerations (formula (3.13)). Therefore, quality improvement of measuring data provided by this system is inevitably connected to a solution of the temperature difference issue. Potential measures regarding this topic are presented in the following chapter.

3.3 Interpretation of Results

To sum up, it can be said that the measuring device basically would be appropriate for the measuring task at hand. This statement is based on satisfying C_g - indices and thus on a low level of variation observed in the measuring process. Furthermore, the type-3 study, in which the repeatability is determined under actual operating conditions, provides acceptable results.

As variation is not the only statistical property which characterizes measuring data quality, measurement system's bias also has to be taken into account in this context. This is especially true for the investigated system, since its capability is not given due to the present level of bias. Investigations show that the systematic offset is mainly caused by the influence of environmental conditions in the production site, in particular by room

temperature. The impact of temperature conditions on measuring results can be traced to device's measuring principle. Present temperature differences between the masterpiece and the production part induce the systematic error. The masterpiece is used for device's calibration and adjustment.

As the temperature in the production hall, and thus masterpiece temperature, changes in a certain extent over time, present bias also varies in a specific range.

The results of the measurement system analysis show that readings taken by the automated 3D measuring machine cannot be fully trusted. In this context, different levels of bias are observed in various tests performed within the scope of this project. Bias in a range between $1\ \mu\text{m}$ and approximately $7\ \mu\text{m}$ is determined. Although this level of offset seems to be quite low, it can cause wrong product acceptance decisions. This is true for production parts whose determined diameter reading is located in a range of up to $\pm 7\ \mu\text{m}$ around a specification limit. In this range around LSL and USL respectively, there is a risk of calling a good production part "bad" or a bad one "good".

In the first situation, a product actually meeting the specified requirements is reworked in case of being close to USL or gets scrapped in case of lying close to LSL. In the second situation, a product which actually does not comply with the requirements is erroneously evaluated as one which meets the specification. Wrong decisions have adverse effects in both cases; in the first case for the producer, in the second and more severe one for the customer as well as for the end user of the product. Therefore, the investigated measurement system should not be further used for final dimensional inspection of production parts under present conditions.

In this context, potential measures for overcoming stated temperature influence issue are presented in the following section.

An improvement of the measuring device itself is one possible approach for enhancement of the measurement system. The idea is, to take into account the actual temperature difference between the masterpiece and the production part for determining product dimensions. In this context, the determination of the masterpiece temperature, as well as production part ones for each measuring operation, is indispensable. Therefore, the implementation of temperature sensors is required. Furthermore, an extension of device's software would be necessary for the process of temperature compensation.

Another possible approach is the avoidance of the temperature difference between the masterpiece and the production part. This could be managed by implementing an interim storage facility for axles between the grinding machines and the 3D measurement system. The underlying consideration is that the axle adapts to room temperature, and thus to masterpiece ones, during the storage time. Therefore, a temperature difference between the masterpiece and the axle can be avoided for the measuring process. It has to be mentioned that this potential measure is accompanied by various drawbacks. By applying stated interim storage concept, the production flow would be interrupted and the handling effort as well as the cycle time would be increased drastically.

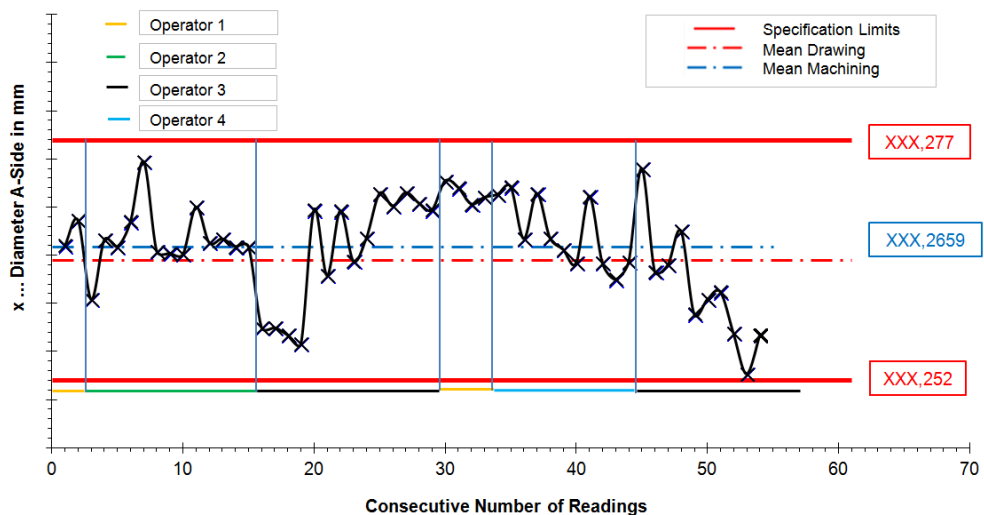
The upgrade of the measurement device constitutes the preferred solution for Lucchini RS. Detected temperature influence on the measuring process as well as the proposed improvement measure has already been discussed with measurement device's manufacturer. The fabricator is going to investigate the possibility of implementing the suggested solution as well as alternative ways to overcome the stated problem.

4 Machining Process Investigation

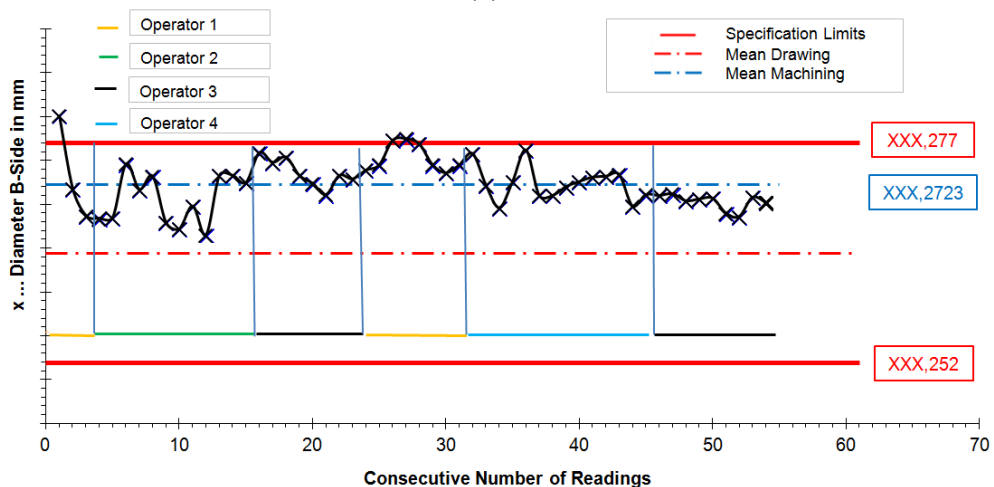
In this chapter, performed analyses and investigations of machining steps, on which the main focus of this Thesis lies, are described.

Before performing particular investigations of certain machining process steps, a great deal of information and data has to be gathered. In addition to manufacturing-related data, control charts with original values gathered by the automated 3D measurement system at the end of the finish machining line are created. This is done in order to gain basic information about the actual process performance. In this context, it has to be stated that the measurement system is capable of providing basic information about production process performance despite the non-satisfactory measurement system analysis results.

As an example, Figure 33 shows control charts of diameter readings of one production batch taken at the wheel seat on the A- and B-side respectively.



(a)



(b)

Figure 33: Original value charts for wheel seat diameter A-side (a) and B-side (b), Source: Own illustration.

The vertical lines in Figure 33 represent shift changes at the grinding machine which are associated with an operator change. The short and colored horizontal lines act as a code. Each color is associated to one specific operator.

A measuring data analysis of different production lots basically shows that the finish machining process is not stable over time and that currently a high level of variation is present. In other words, the process is out of statistical control and does not meet process capability requirements (chapter 2.1.2). Therefore, measures have to be taken in order to improve the machining process.

Overall, diameter (three wheel seat sections for each axle side) and cylindricity readings from seven different production batches of the selected axle type are statistically analyzed within the scope of the project. An example for stated analyses is presented in the appendix. In addition to above mentioned issues, further findings are gathered:

- Basic machining result differences between A- and B-side
- Jumps in time course of readings after shift changes
- Considerable amount of wheel seat diameter readings exceeding USL on the axle's B-side

Some of the stated issues can be observed in the $\bar{x} - R$ - charts in Figure 34.

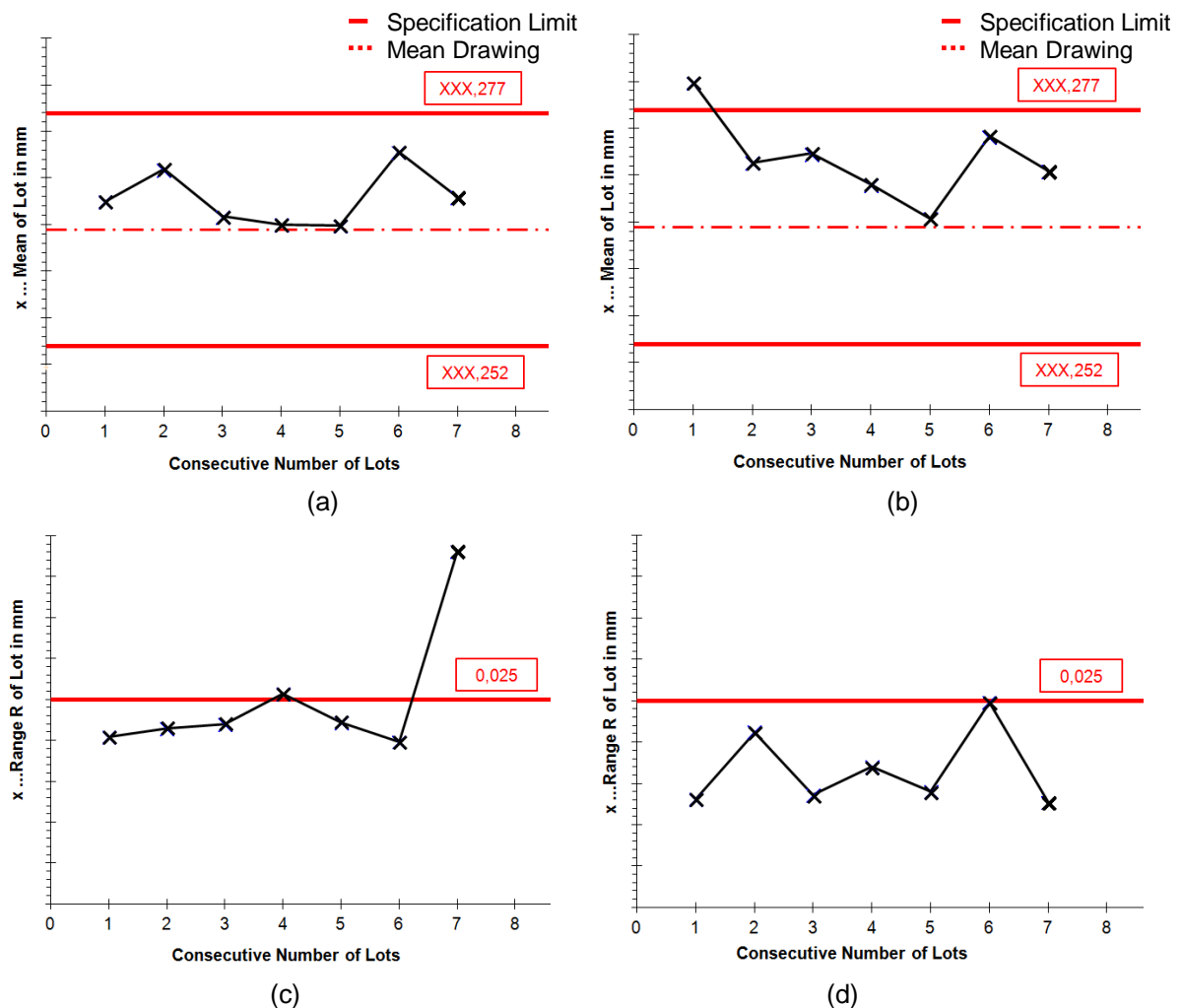


Figure 34: $\bar{x} - R$ - charts for axle's A- (left) and B-side (right), Source: Own illustration.

By means of Figure 34, the stated lack of process stability is illustrated. The requirements for a stable process (process under statistical control) - location \bar{x} and variation R are stable over time - are not met.

In this context, the term process stability has to be considered in more detail. Basically, the periods for evaluation of process stability have to be defined. For the present project, the two types, within-batch stability and between-batch stability respectively, can be distinguished. Within-batch stability refers to alteration of location and variation between different shifts and thus between different operators. An example for this situation is presented in Figure 33. Between-batch stability refers to changes of evaluated parameters between complete production lots, as it is depicted in Figure 34. The latter one is basically termed as “stability” in the course of this Thesis.

Furthermore, result differences between the axle’s A- and B-side are shown. In the \bar{x} - charts (diagram (a) and (b) in Figure 34), the means \bar{x} for A- and B-side of the seven lots under consideration are plotted. By comparing these two diagrams it is becoming clear that diameter readings gathered on axle’s B-side have higher values than ones from A-side in general.

Furthermore, it is evident that the means \bar{x} of all the batches are located in the upper half of the tolerance range. This finding can be put down to a general idea of safety. If the diameter of an axle seat undershoots LSL, the product has to be scrapped. This constitutes a great loss as the product has passed a huge number of production stages before it enters the grinding machining operation. Additionally, the production batch, and thus the number of saleable products, is down-sized. Contrary, an excess of USL has less dire consequences as the axle can be reworked. But it has to be considered that every kind of rework constitutes a loss of productivity and therefore should be avoided. The analysis showed that especially diameter values of the axle’s B-side frequently exceed USL. This issue is further considered in chapter 4.2.2.

Diagrams (c) and (d) represent R - charts in which the range of different production batches is plotted. In this context, it has to be referred to formula (3.7) regarding the definition of the parameter R . The comparison of these two diagrams shows that the range, and thus the variation, of the majority of lots have a higher value on A-side. On this side, the variation within a lot exceeds $20\ \mu\text{m}$ for each of the seven batches. Such a high level of variation in connection with a mean located in the upper half of the tolerance range does inevitable lead to a high rework ration. Thus, the actions should be focused on variation reduction.

The red horizontal lines in these diagrams represent the width of characteristic’s tolerance range ($25\ \mu\text{m}$) and are implemented as guide values.

As the project’s focus also lies on the cylindricity of the axle’s wheel seats, readings of these characteristics are also analyzed. In this context, original value charts are created for each lot. Examples of control charts for axle’s A- (a) and B-side (b) of one production batch are shown in Figure 35.

In the presented example, each wheel seat meets the specified shape requirement, which is represented by the red horizontal line in the diagrams. In this context, it has to be mentioned that only one axle seat from seven different batches does not meet the specified requirements.

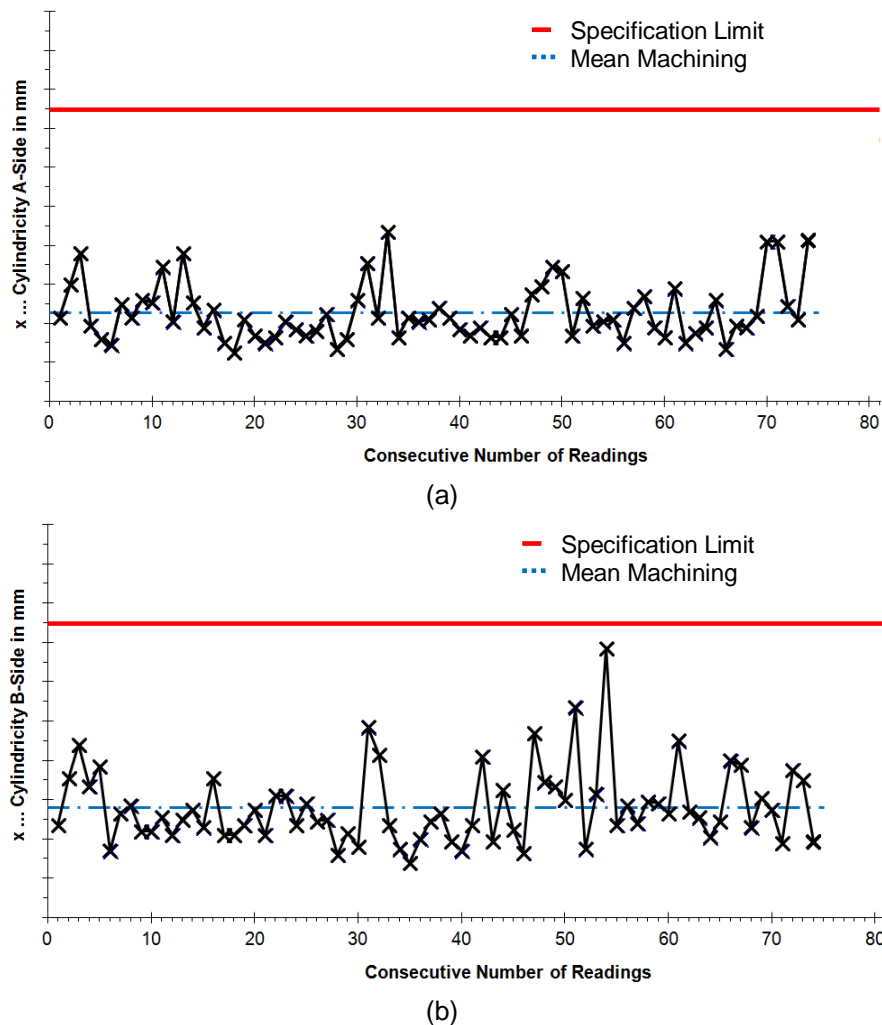


Figure 35: Cylindricity of A- and B-side's wheel seat, Source: Own illustration.

As no stable results are obtained for the wheel seat diameter in the machining process under consideration and as further conspicuities are detected (Figure 33 and Figure 34), research of influencing factors and potential causes for stated issues is conducted. Performed investigations of the centering and grinding process as well as associated results are presented in subsequent sections.

4.1 Axle Centering

The conformance of the centering process, which is performed in machine A03 as a part of journal machining, is essential for ensuring good quality of finished machined parts. This statement is based on the fact that in all subsequent process steps, which are performed in different machines, the axle is clamped between centers and thus on the surface of axle's centering bore.

As the axles are already hollow bored when they enter A03, there is no need to produce a centering bore as it is required for solid axles. In the present case, an operation similar to a countersinking procedure is performed. By doing this, a chamfer is produced which

serves as contact surface for the centering cone (2). This situation is shown in Figure 36, in which the setting of the axle (1) in the grinding machine is illustrated as an example for axle clamping in further machining steps. The chamfer is surrounded by red circles in order to mark the contact zone.

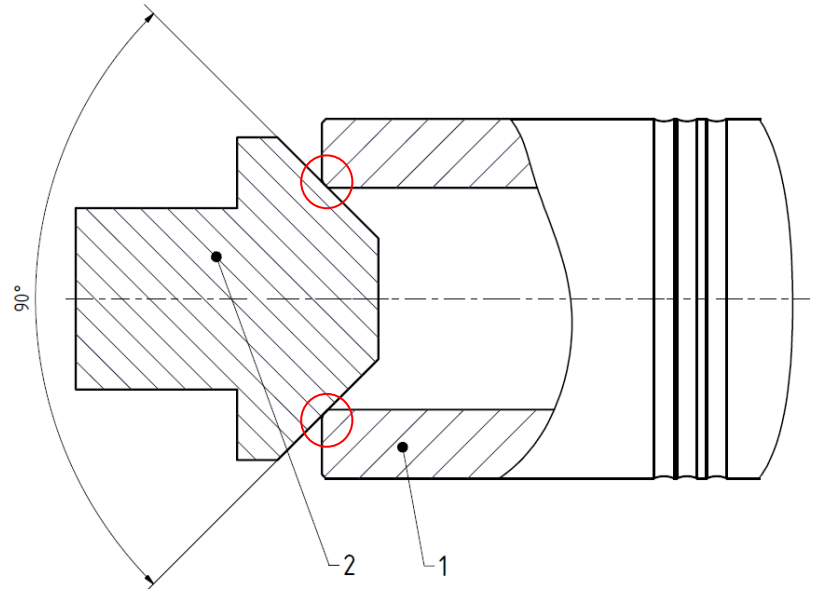


Figure 36: Axle Clamping in grinding machine, Source: Own illustration.

Figure 37 shows the setting in machine A03, in which both axle sides are machined simultaneously by rotating tools. The axle is fixed during the machining operation by clamping units (1). To ensure the correct alignment of the axle relative to the rotational axes of the machining tools, the axle is positioned by two separate units before it is clamped (2).

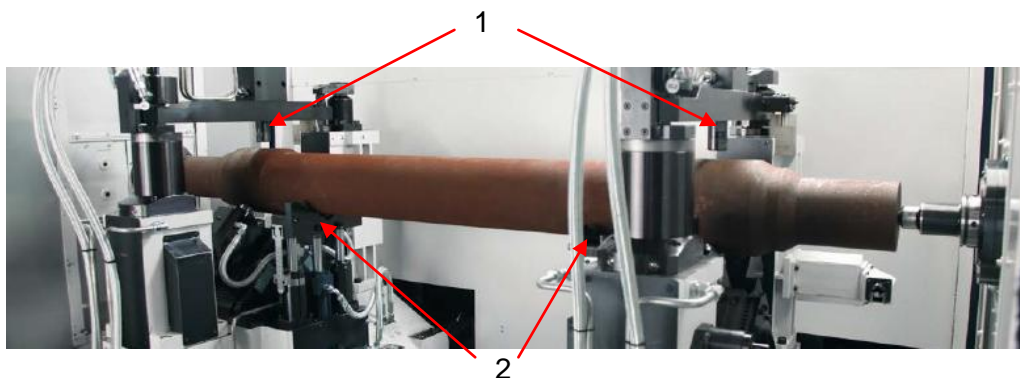


Figure 37: Machining of axle's centering bore, Source: DANOBAT (n.d.).

Potential failures made in this clamping operation inevitably lead to shape errors of the centering chamfer which furthermore result in different types of non-conformances at finish machined parts. In this context, shape deviations of axle seats due to uneven rotation of the axle in subsequent machining operations would not be avoidable.

In order to prevent described irregularities, the positioning procedure in advance of the centering process is based on a sensing operation performed on the hollow bore surface

at each axle face by a sensing device. By this approach, the actual rotational axis of the production part is determined. In the actual positioning operation, the axle's rotational axis, and thus the product itself, is aligned to the tool ones, which is exactly defined by tool holder's position. Before starting the machining operation, axle's alignment relative to the centering tool is rechecked by a repeated sensing operation. If the current axle position is not accurate, the positioning procedure is repeated.

The result of centering process evaluation is satisfying. Furthermore, the analysis of measuring data gives no indication that supplier's centering process has any type of adverse consequences for the final product quality. Due to this result, no further analysis and investigation of the centering process is required.

In conclusion it can be said, that the centering process provides satisfactory results and therefore meets the stated requirements.

In contrast to the centering process, the investigation of the grinding machining operation points out some weak points. Stated research and associated results are presented in the subsequent chapter.

4.2 Grinding Machining

The grinding machining operation, which is performed in machines A07 and A08, has the highest impact on the final product quality.

Whether important characteristics of axle seats meet the specification requirements or not, strongly depends on the performance of the grinding process. In this context, characteristics which are essential for subsequent assembly operations, or generally for the safety of the rail vehicle in use, are considered. Such attributes are the diameter and the cylindricity as well as the roughness of the wheel-, bearing-, sealing- and gear seats of the axle.

As the grinding process has a high impact on the final product quality, the grinding system is analyzed in detail. Thereby, it is intended to find out the most influencing factors as well as potential causes for the present level of process variation and the lack of process stability. For this investigation, an Ishikawa diagram, which is based on theoretical considerations in chapter 2.1.1.3, is used. The created diagram for the grinding machining process is shown in Figure 38. In this diagram, the six categories man power, machine, material, milieu (environment), measurement and method are used to classify influencing factors.

In an initial step, potential influencing factors of the grinding process, which are derived from theoretical considerations, are inserted in the diagram. The stated chart serves as a basis for further process investigation. Each potential influencing factor is evaluated and categorized regarding its relevance for the present process (legend in the bottom right corner of Figure 38). In following chapters, potential causes for detected quality issues are described.

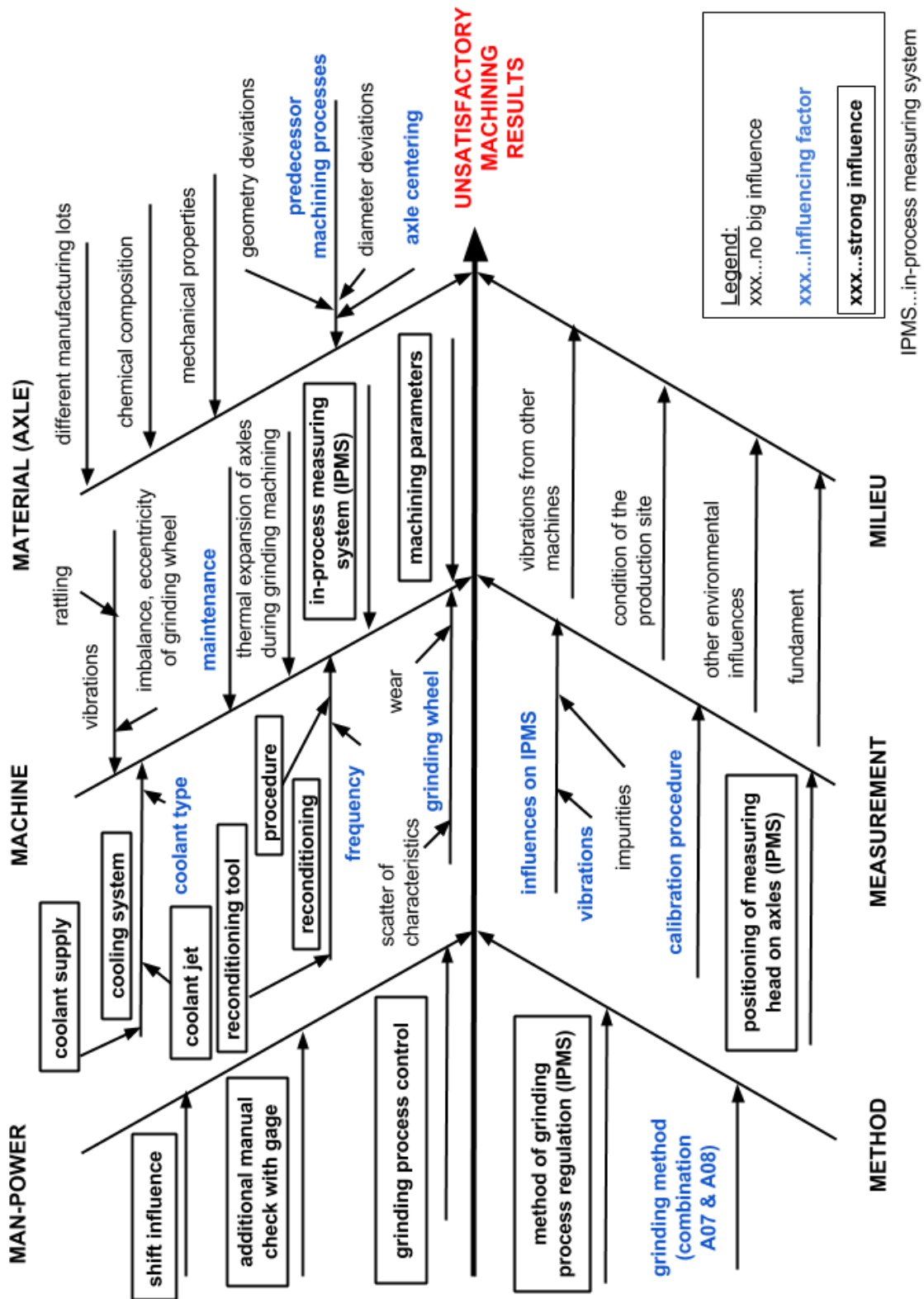


Figure 38: Ishikawa diagram for grinding process, Source: Own illustration.

4.2.1 Operator Influence

In Lucchini RS' highly automated finish machining line, one operator is responsible for operation and supervision of the two grinding machines A07 and A08. Contrary to expectations, the investigations showed that a high level of operator influence is present in the process.

Since the machining line in Lucchini RS' site in Lovere runs three shifts per day, the grinding machining process is operated by three different operators within 24 hours. This circumstance cannot be avoided, but brings along different causes for the lack of within-batch stability. Figure 33 illustrates different issues which are described in the following paragraphs.

The main cause for obtaining no stable results over time is the fact that different operators obviously have different strategies or different approaches to grinding process operation and grinding process control respectively. This situation refers to different frequencies of manual dimensional checks and process parameter adjustments as well as to different target values of single operators. One operator likes to have a big safety padding to LSL. Therefore, he runs the process near USL. As there is a certain level of variation in the process, USL is frequently exceeded in some lots at axles which are machined by applying the safety strategy. Another operator has the target to produce axles which are near to the middle of the tolerance range. Observed changes in the time course of readings after shift changes can mainly be traced to different process control approaches of various operators.

In order to achieve a stable process, a uniform strategy of process control has to be implemented. Further information regarding this topic is presented in chapter 4.2.3.

As the operators perform manual dimensional checks on axles in a certain frequency, and as these measurements are taken into account for potential changes to the machining process, another factor has to be considered. A certain level of operator influence is introduced by these manual diameter checks due to the fact that different operators very likely measure different values on the same part. This influence was investigated by means of an R&R-analysis. This investigation allows the quantification of measuring variation between different operators as well as the suitability of this measurement system for the intended use. This study is described in more detail in the following chapter.

4.2.1.1 R&R-Analysis

The approach for the performed R&R-investigation is based on chapter 2.3.5, in particular on the type-2 study.

For manual diameter checks, mechanical dial comparators with a graduation value (resolution) of 1 μm are used. As 1 μm constitutes four percent of characteristic's tolerance range (25 μm), the requirements for sufficient resolution stated in chapter 2.3.4 are met.

In a first step, the study's basic conditions have to be defined. In this context, the number of different appraisers (in this case machine operators) k , quantity of different measuring objects n as well as the number of measurements per appraiser r are termed. Table 4

gives an overview of stated requirements and the conditions selected for the present investigation. Five finish machined axles were taken from the production lot and their wheel seat diameter was measured by the operators with manual gage in the scope of this investigation.

Table 4: Conditions R&R-analysis, Source: Own illustration.

	Requirement ⁵¹	Value for investigation
No. of different appraisers k	≥ 2	3
No. of different objects n	≥ 5	5
No. of measurements per appraiser r	≥ 2	3
Product $k \cdot n \cdot r$	≥ 30	45

Three blue-collar workers, which are responsible for operating the grinding machines in three different shifts, are selected as appraisers for this study. It is intended to find out potential differences between them which can occur in the process of performing manual dimension measurements. The first appraiser measures the five different production parts in sequence, before he repeats this run two times. The second one measures the objects in the same order before the study is completed by performing the same measurements by the third appraiser. For this study, the measuring positions on the five different axles are clearly marked, in order to ensure that each measurement is taken from the same position. In the end, 45 different readings are available for assessing the repeatability and reproducibility of the measurement system for manual diameter check. A Microsoft Excel based form, which can be seen in the appendix, was used for recording the readings during the study as well as for statistical analysis of gathered data.

Part Number	Appraiser 1 (Operator 1)					Appraiser 2 (Operator 2)					Appraiser 3 (Operator 3)				
	Measurements			\bar{X}	R	Measurements			\bar{X}	R	Measurements			\bar{X}	R
1	XXX,275	XXX,276	XXX,274	XXX,275	0,002	XXX,278	XXX,276	XXX,278	XXX,277	0,002	XXX,275	XXX,275	XXX,276	XXX,275	0,001
2	XXX,265	XXX,265	XXX,265	XXX,265	0,000	XXX,267	XXX,265	XXX,267	XXX,266	0,002	XXX,265	XXX,264	XXX,265	XXX,265	0,001
3	XXX,271	XXX,274	XXX,272	XXX,272	0,003	XXX,275	XXX,273	XXX,275	XXX,274	0,002	XXX,273	XXX,272	XXX,272	XXX,272	0,001
4	XXX,272	XXX,274	XXX,271	XXX,272	0,003	XXX,275	XXX,276	XXX,276	XXX,276	0,001	XXX,274	XXX,271	XXX,272	XXX,272	0,003
5	XXX,266	XXX,270	XXX,265	XXX,267	0,005	XXX,270	XXX,267	XXX,270	XXX,269	0,003	XXX,265	XXX,265	XXX,267	XXX,266	0,002
6															
7															
8															
9															
10															
Average	X1= XXX,2703					X2= XXX,273					X3= XXX,2701				
Range of Appraiser !!!!	R1= 0,0026					R2= 0,0020					R3= 0,0016				

Figure 39: Extract from the R&R-analysis form, Source: Own illustration.

The procedure of the study as well as mathematical relationships used in its context, are shortly described hereunder:⁵²

For easier explanation, an extract from the R&R-analysis form is shown in Figure 39.

⁵¹ Conf. Audi AG et al. (2002), p. 25 ;

⁵² Conf. Audi AG et al. (2002), p. 24-27.

In a first step of data analysis, the ranges R and the means \bar{X} for each appraiser and each measuring object are determined. This step is marked by a red frame around the data from appraiser 1 in Figure 39. The mathematical relationship for calculating these figures are presented in formulas (3.2) and (3.3). After that, the means X_1 , X_2 and X_3 from the individual results of the three different appraisers as well as the average ranges R_1 , R_2 and R_3 from each appraiser's measurement series are calculated. For transparency reasons, this step is marked by a green frame around measuring data from appraiser 2 in Figure 39.

After determining stated figures, the repeatability of the measurement system could be evaluated by means of EV (formula (4.1)). This index stands for equipment variation, which is also called within-system variation.

$$EV = K_1 \cdot \bar{R} \quad (4.1)$$

A similar assessment was made regarding the repeatability of the automated measurement system integrated in the finishing line (chapter 3.2.3). Like it is described there, K_1 is a statistical factor (formula (3.10)) calculated by means of d_2^* , which is taken from a table (appendix) and is a function of k, n and r . \bar{R} represents the average of the average ranges R_1 , R_2 and R_3 .

As a next step, the reproducibility of the measurement system, which represents the appraiser variation AV or between-system variation, has to be calculated by applying formula (4.2).

$$AV = K_2 \cdot X_{diff} \quad (4.2)$$

The factor K_2 is also calculated from d_2^* , but for the AV-analysis it only depends on the number of different appraisers. The factor X_{diff} represents the range of the means X_1 , X_2 and X_3 (formula (4.3)).

$$X_{diff} = MAX(X_1, X_2, X_3) - MIN(X_1, X_2, X_3) \quad (4.3)$$

The figure $R\&R$ can be calculated by applying formula (4.4). It is a combination of EV and AV .

$$R\&R = \sqrt{EV^2 + AV^2} = \sqrt{(0.00623 \text{ mm})^2 + (0.00665 \text{ mm})^2} = 0.00911 \text{ mm} \quad (4.4)$$

Finally, the index $\%R\&R$ can be determined by considering the ratio between $R\&R$ and a reference value. It is taken for the decision whether the measurement system is suitable for its intended use. Measured characteristic's tolerance range was taken as reference value due to practical reasons.

$$\%R\&R = \frac{R\&R}{RF} = \frac{R\&R}{TR} = \frac{0.00911 \text{ mm}}{0.025 \text{ mm}} = 0.3645 = 36.45\% \quad (4.5)$$

The value obtained in formula (4.5) has to be compared to the requirement $\%R\&R \leq 30\%$. This comparison implies that the repeatability and reproducibility is not given by manual diameter checks performed by different operators. The obtained result is not extremely poor as the $\%R\&R$ -index has a value close to the acceptance limit. Nevertheless, this study confirms the presumption that manual diameter checks performed by different operators provide no reproducible results.

Beside the R&R-analysis, the ranges R of the nine taken measurement values for each object are determined. Table 5 shows the results. In the course of the study, each selected production part is measured three times by each of the three appraisers. Therefore, nine different readings for each object are available.

Table 5: Range of measurement values for different axles, Source: Own illustration.

	Range R in μm
Object 1	4
Object 2	3
Object 3	4
Object 4	5
Object 5	5

Table 5 shows, that the nine measurement values taken from the same position at the same measuring object vary in a range of up to $5 \mu\text{m}$. This value constitutes 20% of the characteristic's tolerance range. These result differences in manual measurements for one and the same object may lead to different decisions regarding process control and consequently to different machining results.

In addition to the confirmed operator influence on the machining process, the extent of in-process measurement system's impact on obtained machining results is considered in the following chapter.

4.2.2 In-Process Measurement System

The grinding machining operation is controlled by an in-process measurement system which permanently monitors the diameter value of the currently machined axle seat. Furthermore, this system is responsible for terminating the machining process. Once the target diameter, which is stored in the machine control, is reached the first time, the feed motion of the grinding wheel is stopped automatically and the spark-out operation begins. When the defined spark-out time is over, the grinding wheel moves away from the machined seat and the process is finished for this axle section. Simultaneously, the measuring head of the in-process measurement system (shown in Figure 40 and 41) swings away from the axle surface into its initial position in order to be ready for axial movement to the axle seat which is machined next. Figure 40 shows the mentioned in-process measurement system. In this picture, the thick red arrows show the movements performed by the measuring device. These are the axial movement of the whole device to

the desired axle section as well as the swinging movement of device's head from the initial position to the axle surface and vice versa. In addition, the diagonal red straight represents the rotational axis of the product which is going to be machined.

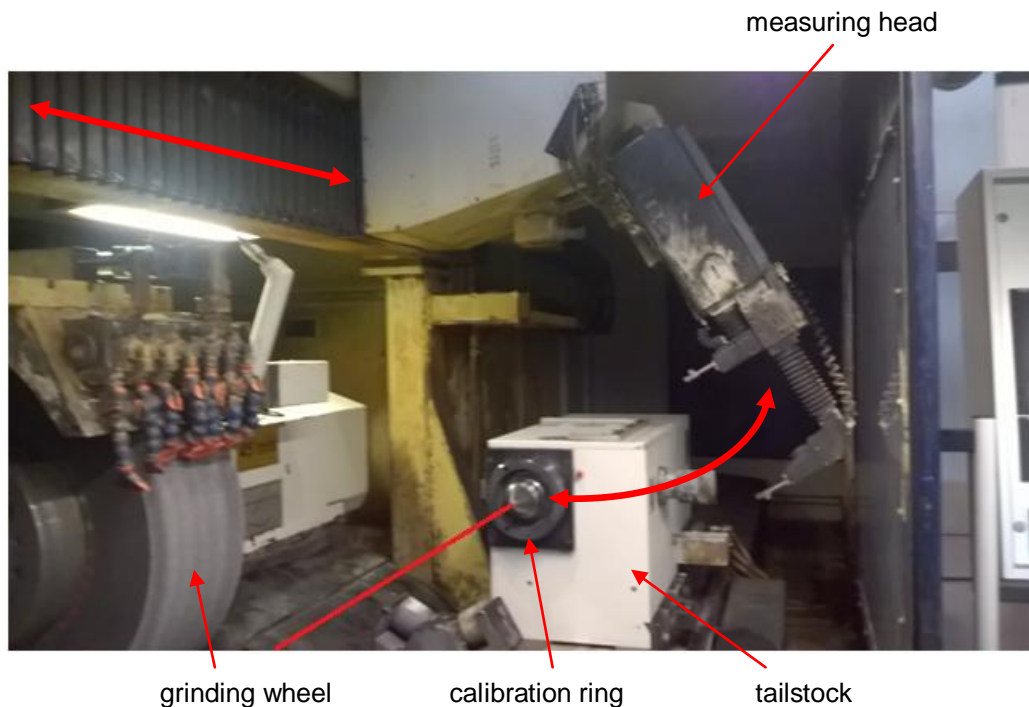


Figure 40: In-process measurement system, Source: Own illustration.

As the system is responsible for terminating the grinding process, it has a great influence on the machining results. Therefore, different investigations of the in-process measurement system are performed, which are described in the following paragraphs. Before going into more detail about performed investigations, the system itself as well as the underlying measuring principle, has to be described. This is done in the following four paragraphs, for which the information was obtained from the manufacturer of the in-process measurement system (personal communication).

Figure 41 shows the head of the measurement system, which is comprised of a main body (1), two inductive measuring cells (2) as well as two hard faced contacts (probes) (3), which are permanently touching the axle's surface, and two mobile arms (4).

The diameter measurement given by the system is a combination of the value detected by the inductive measuring cells and the position of optical incremental transducers inside the head body.

In the system's initial state, which is shown in Figure 40, the probes are in a safety position (maximum opening of the measuring device). After the measuring head had swung into measuring position (shown in Figure 41), the mobile arms drive the probes towards the axle surface. Once the surface is touched, the position of each mobile arm is fixed and the measuring cells are determining the deviation from this position during the machining action. This is done by means of the LVDT method described in chapter 2.3.1.1. Each of the measuring cells has a measuring range of $\pm 500 \mu\text{m}$, which is about twice the machining allowance, and a measuring precision of some hundredths of a micron.

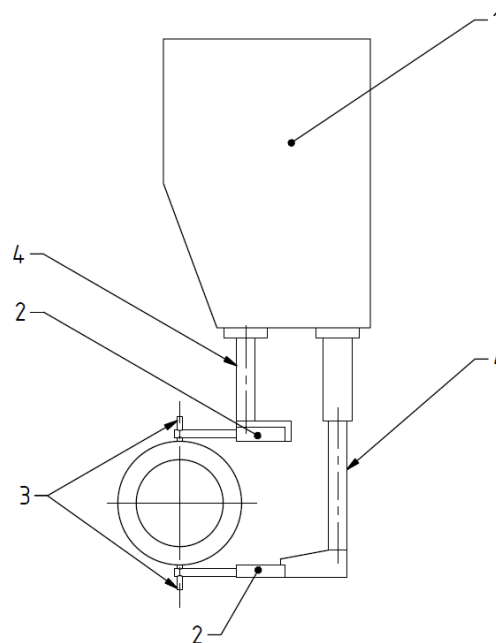


Figure 41: In-process measuring device, Source: Own illustration.

The mobile arms' fixed position is determined precisely by means of incremental measuring technology, which is described in chapter 2.3.1.2. In this context, a calibration action has to be performed in a dedicated frequency (about every 20 axes). This is done by using a calibration ring which is fixed to the tailstock. This calibration ring can be seen in Figure 40.

The in-process measurement system's basic principle is the same as for the automated 3D measurement system described in chapter 3.1. The measurement value is the result of combining a value from an inductive and one from an optical incremental device, but the method of determining a diameter value is totally different. On the one hand, the automated 3D measuring machine determines the diameter from a set of points around the circumference by means of the GG method (chapter 2.3.2.1). On the other hand, the in-process measurement system determines a diameter value by a point-to-point distance between the two probes. This implies that the LP method (chapter 2.3.2.1) is applied.

In a first investigation step, the way of machining process control performed by the integrated measurement system has to be considered. Furthermore, the conditions in which it is used have to be analyzed. Since the probes continuously gather measurement values during the machining operation, the system is exposed to machine vibrations, grinding process residuals, the cooling lubricant and further disturbing factors. Therefore, the measuring task at hand constitutes a great challenge.

As the system determines the diameter value by a point-to-point distance on a rotating axle, small shape errors (in particular circularity errors in the measuring plane) can have a big impact on the machining process control. Stated circumstance is shown in Figure 42. This is especially true for the system at hand as the feed motion of the grinding wheel is stopped when the diameter target value is reached the first time. Due to deviations from the perfect circle form, the measurement system determines different diameter values within one revolution of the axle.

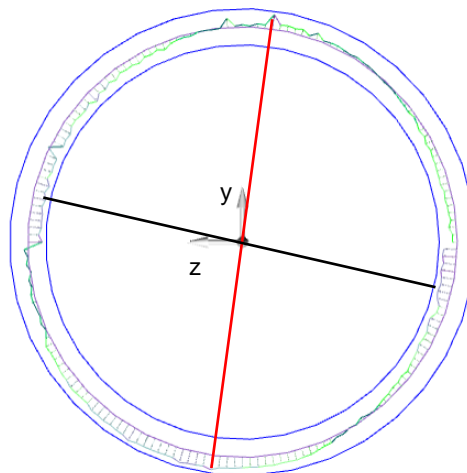


Figure 42: Shape error in measuring plane, Source: Own illustration.

In this context, Figure 42 has to be explained. It shows an extract of a measuring protocol from the coordinate measuring machine. The purple circle constitutes the least square circle. In other words, this is the one which was determined from all the measuring points around the circumference by means of the GG method. On the other hand, the two blue circles represent the limits of the specified cylindricity tolerance for the wheel seat. In the present case, 180 points around the circumference of an axle wheel seat were taken. In this figure, deviations from the desired circle form in the measuring plane are evident. The comparison of the red and black straight, whereby each represents a point-to-point distance, illustrates the stated issue of different diameter readings within one axle revolution.

By performing stated kind of machining process control, grinding process termination at wrong times and thus dimensional deviations on finish machined parts, cannot be totally excluded.

In order to gain further insights about potential reasons for dimensional deviations and high level of variation of grinded parts, different investigations of the in-process measurement system are performed on finish machined production parts. This means that no material is removed during these investigations. As a first step, a repeatability study of the in-process measurement system is performed under real process conditions. This is done in order to get an idea about the magnitude of measurement system's variation and its contribution to the process variation respectively.

4.2.2.1 Repeatability Study

This study is performed in each of the two grinding machines under repeatable process conditions. Before each of the ten measuring runs, the measuring head is moved into its initial position near the tailstock (Figure 40). In particular, the procedure of each measuring run is the following:

At the beginning, the measuring head is moved in axial direction in order to get to the desired axle section. Once this section is reached, the measuring head swings into measuring position on the rotating axle. In each round, measurement values taken

throughout 30 seconds are recorded. To simulate real process conditions, the cooling system is activated for this investigation.

Figure 43 shows obtained results from the ten measuring runs performed in machines A07 (a) and A08 (b). In there, the ranges of gathered readings throughout 30 seconds are plotted for each measuring run. Additionally, the means of the measuring ranges are indicated by points.

It is obvious that the measurement system integrated in machine A07, which is responsible for machining the axle's B-side, provides a better repeatability result compared to A08's system. In general, the machining process variation is much smaller in machine A07 (Figure 33). This circumstance is inter alia a consequence of better repeatability of its in-process measurement system compared to the one integrated in machine A08.

Regarding variation, it can be said in conclusion that a variation reduction in A08's machining process is inevitably connected to an improvement of its in-process measurement system. A more detailed analysis of this issue would go far beyond the scope of this Thesis. Therefore, a solution has to be found in cooperation with the manufacturer of the system.

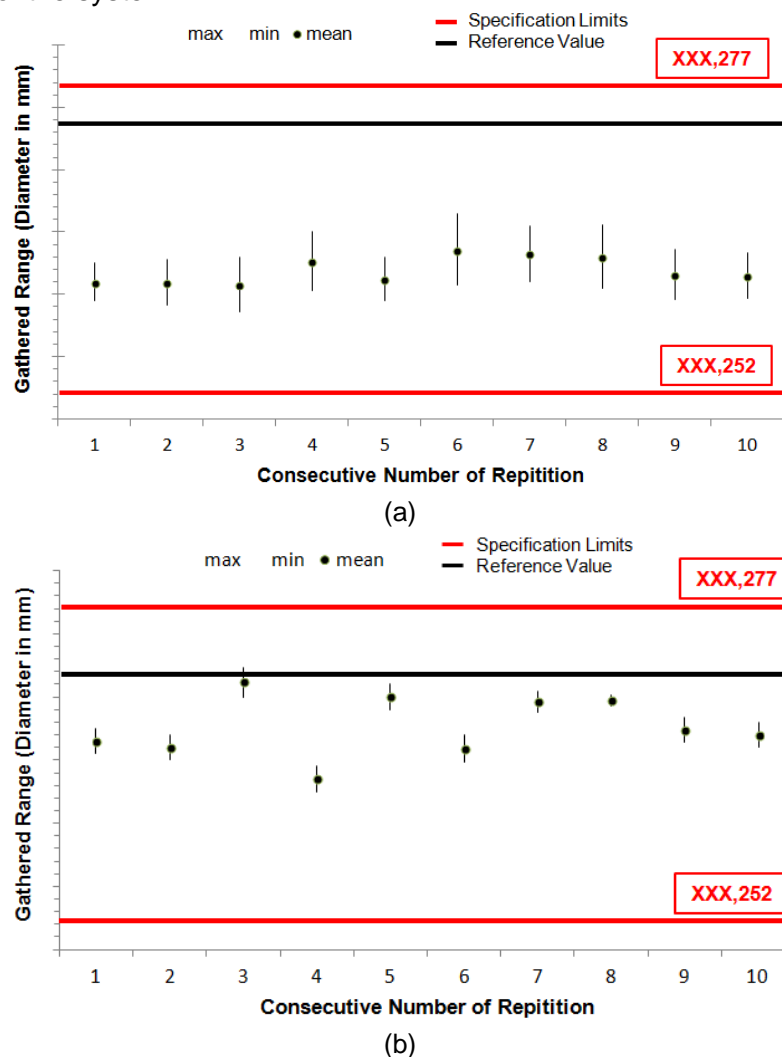


Figure 43: Repeatability test results for machine A07 (a) and machine A08 (b), Source: own illustration.

Furthermore, the bias of the measurement systems has to be considered. For the system in A07, a bias of about $12\ \mu\text{m}$ was determined (formula (3.6)). This constitutes nearly half of the tolerance range. On the other hand, the systematic error of machine A08's system has a magnitude of about $4\ \mu\text{m}$. These results are further considered and analyzed in chapter 4.2.2.3.

It also has to be mentioned that the measurement values change in a wider range within one measuring run in machine A07. This circumstance was confirmed by performing comparison measurements on non-rotating axles, which is further described in the subsequent chapter.

4.2.2.2 Stability in Face of Machining Conditions

In the scope of investigations, also non-rotating axles are measured by the in-process measurement systems in both grinding machines. These analyses show that the diameter value of one axle seat taken by the in-process measurement system in A07 varies in a range of about $2\ \mu\text{m}$ over time within the 30 seconds of measuring. This variation may be caused by vibrations of the grinding machine and the measuring arm. The same experiment performed in machine A08 shows a constant measurement value for seats on non-rotating axles throughout the investigation period of 30 seconds.

This finding is in line with the results shown in Figure 43. As the measurement value determined in each run in machine A07 (Figure 43 (a)) changes in a range of up to $6\ \mu\text{m}$ when measuring a rotating axle seat, it is most likely that the target diameter is not exactly reached in the end. This issue can be seen as a systematic error component of the system.

A potential cause for stated variation magnitudes within a measuring run of A07's measurement system may be the probe geometry. Since a point contact is used in A07, only very small movements of the probe relative to the axle surface caused by vibrations have noticeable consequences. On the other hand, A08's system uses a line contact for measuring. This design is able to compensate small probe movements, which has a positive impact on systems stability.

4.2.2.3 Impact of Contact Geometry on Machining Results

Beside its impact on the stability within a measuring run, the contact geometry also influences the systematic deviation from the reference value (bias). This fact is shown in Figure 43. The circumstance, that both systems provide readings which are smaller than the reference value, is based on potentially wrong measuring head positioning after swinging into measuring position at the axle surface. This leads to a situation, in which the probes do not exactly touch the highest and the lowest point of the circle in the measuring plane. This incident is shown in Figure 44. The magnitude of the positioning error is the same for both contact geometries in this example. This fact is shown by the red lines.

The significant difference in the results from the two systems is caused by the different severities of the positioning error consequences. When using a probe with a point contact, no error compensation is present. That means, the distance represented by the red line is actually measured (Figure 44 (a)).

When a line contact is employed, the positioning error can be compensated up to a certain point. In this case, the distance represented by the green line is measured instead

of the red one (Figure 44 (b)). This leads to a measurement value which is closer to the actual one.

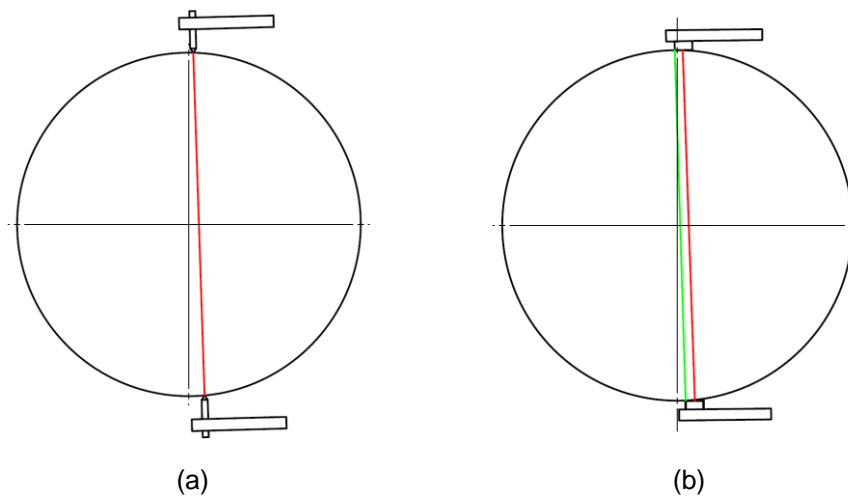


Figure 44: Comparison of contact geometries, Source: Own illustration.

As already described, the variation between different measuring runs at A07's measurement system is on a low level. Therefore, the offset from the reference value is nearly constant. This in turn suggests that a systematic deviation from the perfect measuring head position is present in the system. To gain insights into the magnitude of this systematic positioning error, a calculation is set up for determining the measuring error as a function of the angle error α . By performing this investigation, it is intended to determine the angle between the actual measuring head position and the intended, completely vertical alignment which results in a bias of about $12 \mu\text{m}$. Described situation (b) as well as the course of measuring error as a function of the angle error (a) is shown in Figure 45.

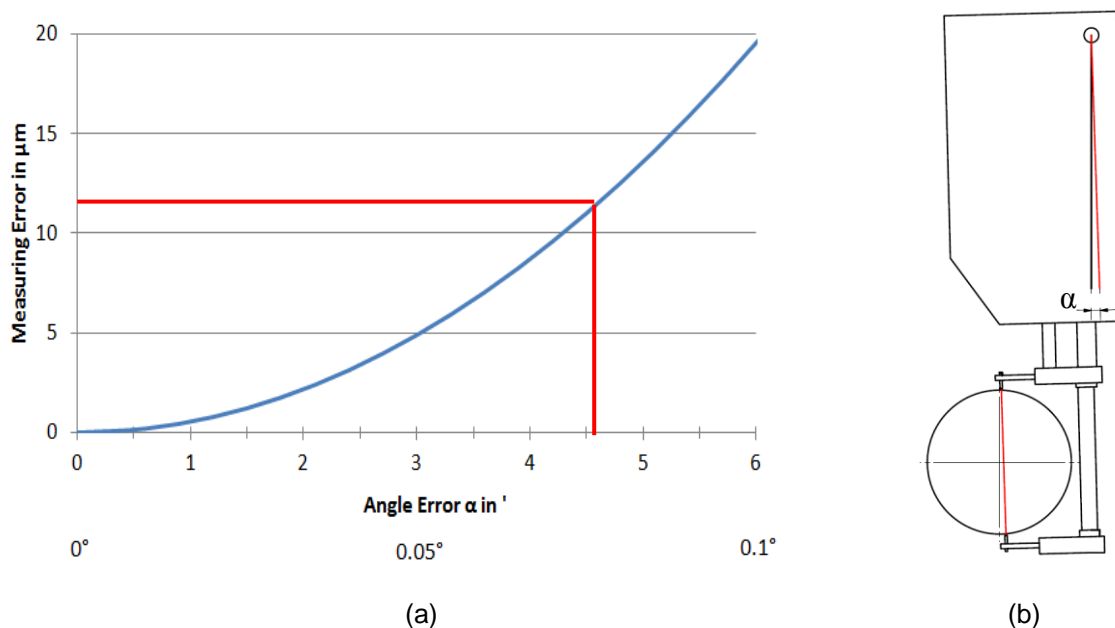


Figure 45: Course of measuring error (a) and angle error definition (b), Source: Own illustration.

This calculation provides a systematical angle error of about 0.075° , which corresponds to 4.5' (angular minutes). This result is also indicated by red lines in Figure 45 (a).

This systematic positioning error of the measuring head has a significant impact on grinding process results. As the system apparently does not determine the distance between the highest and the lowest point of the circle in the measuring plane, gathered value is systematically smaller than the actual one. Therefore, the grinding process is terminated too early by the machine control. This leads to finished part dimensions which are likely to be bigger than required by specification. That state of affairs is proven by analyzing measuring results of different lots, taken at the final dimensional inspection. Thereby, a great number of diameters exceeding USL on the axle's B-side are detected. Furthermore, the B-side's means, determined for different production lots, are basically on a higher level than the A-side ones. These facts are shown in Figure 34.

In this context, a correction of the systematic positioning error of machine A07's measuring head by the manufacturer of the system is strongly recommended. Furthermore, a change of the probe geometry to a line contact can be proposed in order to overcome stated problem.

When seeking to improve a production process, the process control approach also has to be taken under consideration.

4.2.3 Machining Process Control

In order to overcome present stability problems, supplier's machining process control approach has to be improved. As stated in chapter 4.2.1, various operators have different machining strategies. Furthermore, the specified tolerance range is exploited completely, as the "Goal Post Mentality" (chapter 2.1.2.1) is present.

In order to achieve a stable machining process, a uniform strategy of process control has to be implemented. In this context, a specification has to be set up which contains important information regarding process control and which has to be followed by various operators.

Inter alia, requirements for the set target diameter at the in-process measurement system, for frequency of manual diameter checks and specific ranges of machining and reconditioning parameters have to be set. For the latter aspect, reference is made to chapter 4.2.4 and 4.2.5. This specification could be set up in form of a document similar to a production control plan (explained in chapter 2.1.2.2), which serves as an instruction for process control for the operators.

When thinking about machining strategy, reference should be made to Taguchi's loss function approach, which is explained theoretically in chapter 2.1.2.1. According to this concept, each deviation from the target value constitutes a deterioration of the overall result. The risk of producing non-conformance parts, which results in additional costs and an increased failure risk for the final product, grows by the deviation from the target value. In the present example, the middle of the tolerance range can be seen as the target.

It can be said in conclusion, that safety strategies, in which the process is run near USL in order to prevent scrap, should be avoided. By this approach, a great amount of production

parts, on which diameters are exceeding USL, are produced. The result is a high rework ratio which means a productivity loss.

The creation of parts with characteristic values in the middle of the tolerance range has to become the general goal of the process control strategy. By this approach, productivity can be increased and the achievement of the main goal, avoidance of scrap due to smaller dimensions than required, can be ensured. This statement is based on the fact that the variation in the machining process itself (without taking into account the operator influence) is on a relatively low level. Figure 33 exemplary shows this circumstance in which the great peaks are caused by interference actions of operators.

After considering the influence of operators and the in-process measurement system as well as the present process control strategy, grinding technology aspects are presented in the following three chapters.

4.2.4 Reconditioning

In the two grinding machines A07 and A08, different reconditioning procedures are performed. Two separate dressing spindles equipped with form rolls are deployed for grinding wheel reconditioning in machine A07. On the other hand, a non-rotating dressing tool, in particular a dressing plate with inserted diamond grains, is used in A08.

Basically, the dressing operation has a great impact on the obtained surface roughness of machined parts. Therefore, roughness measurements are performed on all axles of one production lot directly after the grinding machining operation at Lucchini RS' production site. In this context, roughness values of the A- and B-side's wheel seat from 80 axles are taken. Obtained results are presented in Figure 46. The two black horizontal lines represent the specification limits for surface roughness. It has to be mentioned, that this specific roughness range for the axle's wheel seat ($Ra\ 0.8 - 1.6$) is required for the wheelset assembly which is performed by Siemens MO MLT BG in Graz.

Orange squares around some measurement values from the A-side's wheel seat, as well as green ones around specific values from the B-side, mark adjustments of reconditioning parameters by the machine operator. In particular, these are adjustments of the feed rate v_{fad} (in this context, see Figure 15).

Mentioned adjustments are carried out after performing the roughness check of the marked axles. This means, the effect of the parameter changes can be observed at the subsequent axle. When taking a look at Figure 46, the effect of different feed rate adjustments is clearly noticeable by jumps in the time course of roughness readings. The direction of the wheel seat roughness change (changing to a lower or a higher value) as a consequence of parameter adjustment can be explained theoretically. A significant roughness change to a higher value is caused by an increase of the dressing tool's feed rate v_{fad} , which leads to a higher cutting ability and effective roughness of the grinding wheel. On the other hand, lower roughness values are obtained by a decrease of v_{fad} .

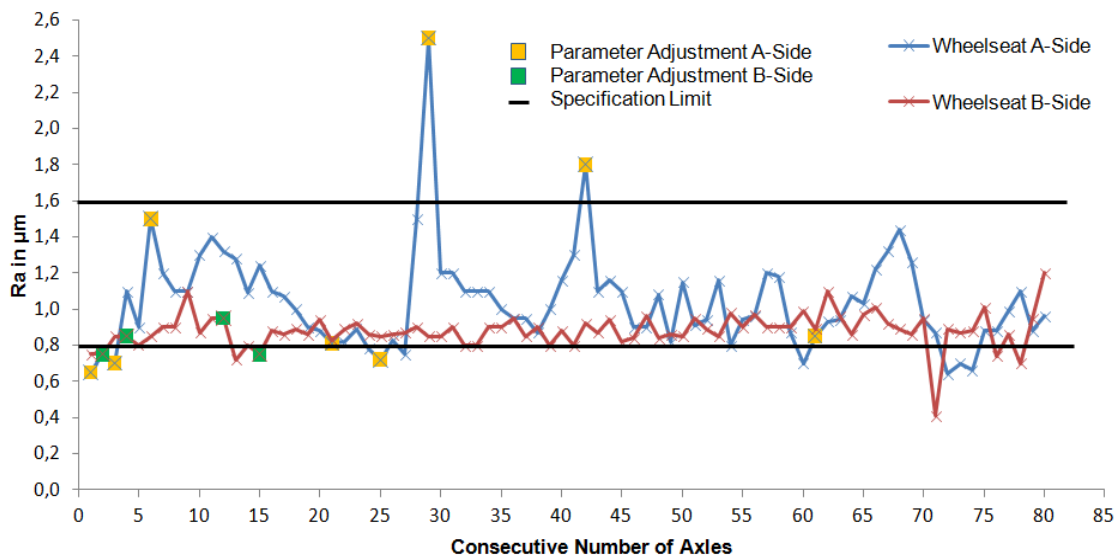


Figure 46: Roughness of A- and B-side's axle seats, Source: Own illustration.

The results show that the roughness is much more stable over time at the axle's B-side, which is machined in A07. This further implies that the rotating dressing system provides more stable reconditioning results compared to the non-rotating tool integrated in machine A08.

The information given in the following paragraph was obtained in a personal meeting with a technician of Dr. Kaiser Diamantwerkzeuge:

It can be said in general, that rotating dressing tools should be preferred to non-rotational ones. This statement is mainly based on the fact that rotating dressing tools provide a significantly higher number of different diamond cutting edges. Therefore, a breakout or damage of a single diamond edge has considerably less impact on reconditioning results. On the other hand, it has to be mentioned that non-rotational dressing tools constitute an inexpensive alternative which is also able to provide satisfactory results. To accomplish this, the device type and the reconditioning parameters have to be perfectly adapted to the dressing task at hand.

Stated points are further considered in the next chapters.

In order to find out potential root causes for the present level of dressing process variation in machine A08, the implemented reconditioning system is extensively investigated.

- Dressing Tool

Dressing plates with inserted diamond grains are currently deployed in machine A08's reconditioning operation.

The grains are made of natural diamond and have a diameter of about 1 mm. The structure of such a dressing tool is shown in Figure 47. The grains are held by bonding material, for which tungsten or hard metal is used in most cases. This thin layer of bonding material with inserted diamond grains (1) is implanted in the main body of the tool (2).⁵³

⁵³ Conf. Dr. Kaiser Diamantwerkzeuge (2012), p. 8, 9.

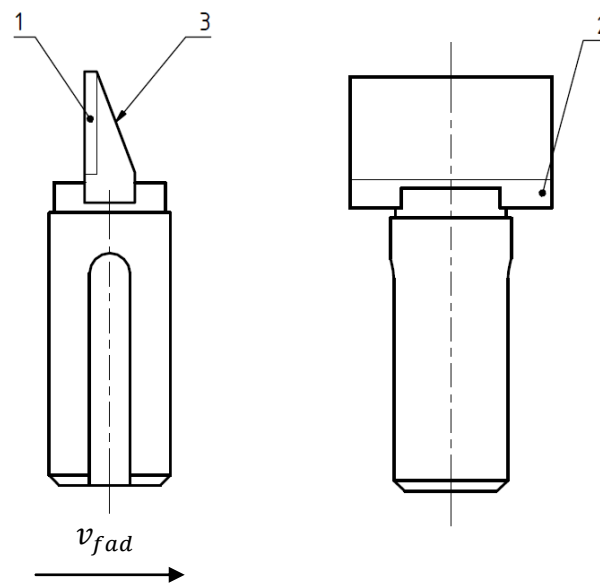


Figure 47: Dressing plate with inserted diamond grains, Source: Own illustration.

The information presented in the following paragraph was obtained in a personal meeting with a technician of Dr. Kaiser Diamantwerkzeuge:

The device is used in a way that the diamond-free back (3) of the tool firstly touches the grinding wheel surface. In this context, the feed direction of the tool is indicated in Figure 47. By this approach, the grains come into operation after removing a thin layer of the tool's main body. Therefore, this type can be allocated to the category of self-sharpening dressing tools. If the grains at the top of the tool are exhausted, new ones come into operation. This self-sharpening procedure works quite well if required ranges of dressing parameters are applied in the process and if the device is matched to the grinding wheel in use.

When taking into account deployed grinding grain material (corundum) and further conditions, the currently utilized dressing tool (Figure 47) does not constitute the best solution. In this context, the usage of dressing plates with set diamond sticks (1) is recommended by a technician of Dr. Kaiser Diamantwerkzeuge. Such a tool is shown in Figure 48. Mono-crystalline diamond (MCD) as stick material can be recommended. The number and the geometry of diamond sticks depend on grinding wheel dimensions.

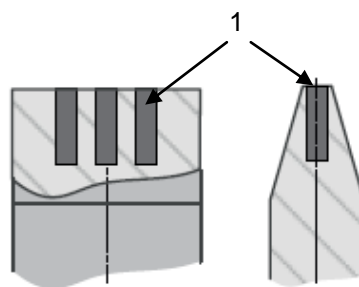


Figure 48: Dressing plate with set diamond sticks, Source: Dr. Kaiser Diamantwerkzeuge (2012), p. 9.

- Dressing Parameters

As described in chapter 2.2.2.1, the cutting depth a_{ed} plays a decisive role in the reconditioning process. For dressing plates, a value between $5\ \mu\text{m}$ and $30\ \mu\text{m}$ for a_{ed} is recommended. Such small values for the depth of cut have to be set in the process in order to ensure a high removal rate as well as a good surface quality.⁵⁴

Furthermore, reference values for the overall cutting depth $a_{ed\ ges}$ are available in literature.

In many industrial grinding applications, more than one dressing stroke is performed per dressing operation. That means, the dressing tool is moved along the grinding wheel several times. After completion of one stroke, the tool is set in radial direction by a_{ed} . In many cases, the cutting depth a_{ed} changes from stroke to stroke, whereby the parameter value decreases stepwise. The overall cutting depth $a_{ed\ ges}$ constitutes the sum of the individual a_{ed} -values for different dressing strokes. In general, reference values for this parameter are individually stated for different grinding wheel materials. For corundum grinding wheels, a parameter range for $a_{ed\ ges}$ of $20 - 40\ \mu\text{m}$ is proposed.⁵⁵

The supplier currently performs the dressing operation with a cutting depth a_{ed} which is higher than the recommended maximum value for the deployed dressing tool. Furthermore, only one dressing stroke per reconditioning operation is currently performed. The set value of a_{ed} as well as the current number of dressing strokes could be the root cause for the present level of dressing process variation.

When taking into account present conditions (grinding wheel type, dressing tool), following improvement measures can be recommended:

The cutting depth a_{ed} has to be decreased to a range of $5 - 30\ \mu\text{m}$ per dressing stroke. Furthermore, the overall cutting depth $a_{ed\ ges}$ has to be reduced to a maximum value of $40\ \mu\text{m}$. In this context, a procedure with two dressing strokes and values for the depth of cut $a_{ed1} = 30\ \mu\text{m}$ and $a_{ed2} = 10\ \mu\text{m}$ can be advised. This proposal is derived from theoretical considerations.

In this context, a test procedure has been set up in order to verify the effectiveness of the proposed parameter change. The results of a preliminary investigation are satisfying. Further studies have to be performed by Lucchini RS in order to gain further insights.

- Cooling Liquid Supply Throughout Reconditioning Operation

In order to ensure proper function as well as a long service life of the dressing tool, a strong and uninterrupted coolant supply is required as diamonds are highly heat-sensitive. This information was obtained in a personal meeting with a technician of Dr. Kaiser Diamantwerkzeuge. The relatively low flow rate of cooling lubricant in machine A08, compared to the one in A07, may also have adverse effects on reconditioning results.

This topic is further considered in chapter 4.2.6.

After analysis of the situation in machine A08, the dressing operation in the second grinder has to be considered as well. Despite the evident stability and predominant conformance of the reconditioning process in A07, the axle surface roughness results are

⁵⁴ Conf. Winterthur Technology Group (2006), p. 72;

⁵⁵ Conf. Saint-Gobain (2014/2015), p. 109.

not fully satisfactory due to its closeness to LSL. This finding is confirmed by measurement of further axles in delivery condition at Siemens MO MLT BG site in Graz. When taking a look on these results, it seems that this issue can easily be solved by adjusting the reconditioning parameters in order to obtain a higher effective roughness of the grinding wheel. This for instance could be done by increasing the axial feed ratio v_{fad} in the reconditioning process, which results in a decrease of the coverage ratio u_d . But it has to be taken into account that different roughness values on various axle seats have to be met. This situation is shown in Figure 49. Beside the required roughness range $Ra\ 0.8 - 1.6$ for the wheel seat, a maximum roughness value of $Ra\ 0.8$ is required for the bearing seats on each axle side's journal as well as for the gear seat.

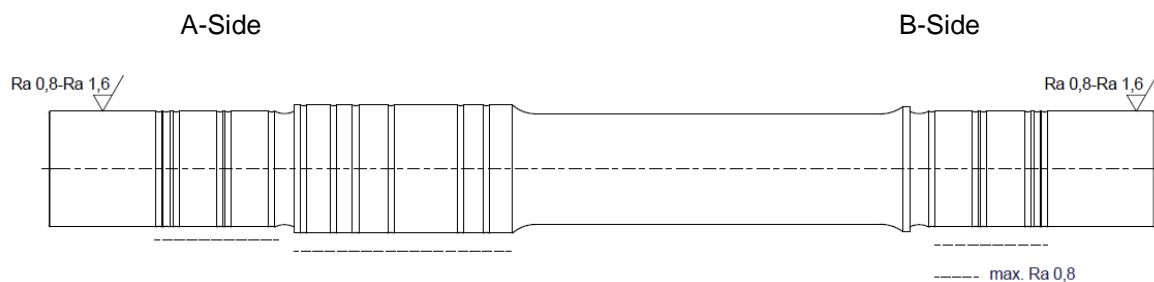


Figure 49: Roughness requirements for different axle seats, Source: Own illustration.

In this context, the current machining approach has to be considered. As already mentioned, the two axle sides are grinded in different machines due to cycle time reasons. In each case, one grinding wheel is used for machining of various seats with different roughness requirements on one axle side (Figure 49). The machining process is performed without an intermediate reconditioning operation. Different surface roughness requirements are currently met by the strategy of beginning the grinding process on the seat for which a high figure is required, as well as by different spark-out times for various axle seats. The first approach is based on the fact that the grinding wheel is less aggressive after a certain time of operation compared to the condition directly after dressing. The second part of the grinding strategy is derived from the point that a longer spark-out operation results in a smoother axle surface.

Instead of meeting roughness requirements by different spark-out times, an additional dressing procedure between grinding of axle seats with different roughness requirements would be advisable. Additionally, it has to be mentioned that the current procedure may have adverse effects on shape properties in case of very short spark-out times. By the proposed approach, two separate dressing operations with parameters exactly coordinated to particular requirements can be performed. Thereby, specified roughness values on various axle seats can be ensured. In this context, the spark-out times for the bearing-, sealing- and gearwheel seat can be reduced drastically as they are currently quite long. Due to this time saving, the grinding process will not be strongly extended by the implementation of an additional reconditioning operation. Furthermore, it is recommended to slightly increase the spark-out time for the wheel seat in order to avoid potential shape deviations.

Besides reconditioning parameters and the spark-out time, surface roughness can also be influenced by grinding machining parameters. In particular, these are the specific metal removal rate Q'_w as well as the velocity ratio q_s . These possibilities are considered in more detail in the following chapter.

4.2.5 Grinding Parameters

As machining parameters have a high level of impact on obtained machining results, the set parameter values in the investigated grinding process are analyzed. Before going into more detail about specific values, it has to be mentioned that certain parameter values slightly differ between the grinding machines A07 and A08. Nevertheless, considerations presented in this chapter refer to both machines since differences between the values are insignificant.

Set machining parameters of the investigated process are compared to rough reference values provided by literature as well as by suppliers of grinding system components. Advisable measures were derived from this comparison. These are presented in Table 6.

Table 6: Grinding machining parameters, Source: Reference values based on Winterthur Technology Group (2006), p. 41, 45.

Parameter	Advisable Measure
Q'_w rough machining	↑ (increase)
Q'_w finishing	↑ – (slight increase)
Q'_w fine finishing	– (no adjustment)
q_s	↓↓ (strong decrease)

In a first step, the specific metal removal rate Q'_w and thus the radial feed rate v_{fr} (formula (2.6)) is considered. In this context, also the machining approach has to be taken into account. The supplier performs a multistage grinding process. This means, the radial feed rate v_{fr} decreases stepwise by getting closer to the desired target dimension. Therefore, the grinding operation is split up into a rough machining, finish machining, fine finishing and spark-out stage.

Literature provides rough reference values for Q'_w in the different stages of a grinding process. Comparison of set values to these reference rates lead to the result that there is a potential for productivity improvement. This statement is based on the fact that the set feed ratio in radial direction and thus the removal rate is low compared to the reference values. This is especially true for the removal rate in the rough machining stage at the beginning of the grinding operation.⁵⁶

In reference books, values of the velocity ratio q_s for the different stages of a grinding process are provided. Generally, it is recommended to increase the velocity ratio when

⁵⁶ Conf. Winterthur Technology Group (2006), p. 45;

getting closer to the end of the grinding operation in order to obtain high surface quality.⁵⁷ In the process at hand, a constant velocity ratio is used throughout machining of an axle section. The value for q_s in supplier's process is about two times higher than the recommended one for fine finishing. This fact can be reduced to a very small rotational speed of the axle which leads to a smooth surface on the machined part. Such results are desirable in general, but a problem for the machining task at hand due to the required roughness range. Therefore, it is recommended to decrease q_s for seats with a higher required roughness value by increasing the rotational speed of the axle.

As the multistage grinding process is finished by a spark-out operation, this process stage is also taken under consideration. In this context, the spark-out time, more precisely the number of revolutions of the machined part during the spark-out operation, is of major interest. As the supplier currently adjusts the surface roughness of machined parts by different spark-out times, there are great differences between values of this characteristic for different axle sections. This leads to the situation, that the spark-out time for the wheel seat is quite low in order to obtain a surface roughness value which meets the specified range of Ra 0.8 – 1.6. Nevertheless, it has to be kept in mind that elastic deformations of the system caused by grinding forces should dissipate by performing a spark-out procedure. Furthermore, the spark-out stage has the task of improving the shape accuracy. It has to be doubted that these targets are met by the spark-out procedure currently performed for axle's wheel seat. Therefore, it is strongly recommended to follow up the proposal of implementing different spark-out operations for axle seats with various roughness requirements.

Beside an appropriate dressing operation and the right selection of machining parameters, the application of a suitable cooling liquid as well as an efficient coolant supply of the grinding zone is of great importance in order to ensure satisfying machining results. This topic is considered in the subsequent section.

4.2.6 Cooling System

Due to its impact on machining results, supplier's cooling system is also examined. In this context, the focus is on the design of the cooling liquid nozzle and on coolant jet's characteristics, like volume flow and pressure.

It has to be stated, that the present design of the cooling liquid supply (shown in Figure 40) does not meet the requirements for the principle of equal velocity fluid delivery, which is described in chapter 2.2.3.2. In this context, a straight line supply instead of the present one can be recommended (Figure 19) in order to ensure sufficient coolant supply of the grinding zone.

Additionally, coolant jet's characteristics should be adapted to following reference values. In general, the values for coolant's specific volume flow \dot{V}' and pressure p are depending on the circumferential speed of the grinding wheel v_s . Table 7 shows the recommended figures for \dot{V}' (volume flow per mm grinding wheel width) and p for the supplier's process.

⁵⁷ Conf. Winterthur Technology Group (2006), p. 41.

Table 7: Required volume flow and pressure of coolant jet, Source: Based on Winterthur Technology Group (2006), p. 100.

Volume Flow \dot{V}' in $l \cdot \text{min}^{-1} \cdot \text{mm}^{-1}$	Pressure p in bar
1.5 – 2	2 – 4

5 Summary and Outlook

In this chapter, a summary of important findings as well as a collection of proposals for production process improvement is given. These measures are presented as recommendations for the supplier in order to ensure further improvement of the process performance (process quality) and the productivity.

As the centering operation provides satisfying results, considerations are focused on the final dimensional inspection (automated 3D measurement system) and the grinding machining process.

5.1 Measurement System for Final Inspection

The performed measurement system analysis (MSA) revealed that the system for final dimensional inspection is not capable due to a certain level of bias. Under current conditions, the measurement system is not suitable for the measuring task at hand. The systematic error can mainly be traced to temperature differences between the masterpiece (used for calibration) and the inspected product.

Different measures are worked out in order to overcome this problem. The consideration of the temperature difference between the masterpiece and the production part in the process of dimension measurement constitutes the preferred solution. In this context, the determination of the masterpiece temperature, as well as production part ones, for each measuring operation is indispensable. Therefore, the implementation of temperature sensors is required. Furthermore, an extension of device's software would be necessary for the process of temperature compensation.

Detected temperature influence on the measuring process as well as the proposed improvement measure has already been discussed with measurement device's manufacturer. The fabricator is going to investigate the possibility of implementing the suggested solution as well as alternative ways to overcome the stated problem.

5.2 Grinding Machining Process

Various aspects of the grinding system are considered in this section.

- Machining Process Control

Analyses showed that currently no uniform machining process control strategy exists in the supplier's production area. Various operators have different approaches of machining process control. This issue has to be overcome in order to achieve a stable process. The implementation of a uniform process control strategy by provision of instructions for the operators in form of a control plan is strongly recommended. This measure should be accompanied by operator trainings regarding process control.

Furthermore, it is of great importance to get away from the "Goal Post Mentality". The focus should be set on reaching the target value, which means the middle of the specified tolerance range. Not every part within the tolerance range can be seen as equally good,

as the risk of producing non-conformance parts increases, the further a particular characteristic gets from the target value. (Taguchi Loss Function, chapter 2.1.2.1)

- In-Process Measurement Systems in Grinding Machines

Machine A07's in-process measurement system provides acceptable repeatability results. Contrary, a certain level of bias was observed, as all measurements taken by this system in the course of an investigation were considerably smaller than the corresponding reference value (actual value). These facts are reflected in the machining process results; the distribution of process output shows a low level of variation but is located near the upper specification limit (USL).

The systematic offset (bias) can be traced to a small positioning error of the measuring head in combination with the contact geometry of measurement system's probes. Due to the point contact, small positioning errors of the measuring head cannot be compensated and therefore, the highest and the lowest point of the circle in the measuring plane are not touched. This ends up in measurement values provided by the in-process measurement system which are smaller than the actual dimensions.

As measurement system's offset is stable over time, it can be taken into account in the process control strategy. The target diameter for the in-process measurement system can be adjusted by the value of this offset. This action should only be seen as an immediate measure. As a sustainable solution, the correction of the systematic positioning error as well as a change of the probe geometry (line contact) is strongly recommended.

Investigations of machine A08's in-process measurement system showed a certain extent of variation and thus no satisfying repeatability results. This circumstance is reflected in the machining process' output as the present level of variation is higher than in machine A07 ones.

A solution has to be found by the manufacturer of the system because a variation reduction in A08's machining process is inevitably connected to an improvement of its in-process measurement system.

- Grinding Machining Parameters

Analysis of grinding machining parameters showed some potential for improvement. Generally, an increase of the specific metal removal rate Q'_w , especially in early stages of the grinding process, can be recommended. This statement is based on the fact that currently set values are on a low level compared to ones stated in literature. Furthermore, the grinding machining operation constitutes the longest lasting process step in the finish machining line. Therefore, this step can be seen as a bottleneck. By an increase of Q'_w , grinding machining time could be saved which would result in a cycle time reduction and an overall productivity increase.

Additionally, an adjustment of the velocity ratio q_s is proposed. As this parameter has an impact on obtained surface roughness, values should be adjusted to roughness requirements of various axle seats.

Present strategy of meeting different surface roughness requirements of various axle seats only by different spark-out times should not be further applied. The roughness has to be adjusted by other means like an additional dressing procedure. It is strongly recommended to implement a uniform spark-out operation for various axle seats. A spark-

out operation which lasts for three to five axle rotations is advisable in order to ensure the degradation of elastic system deformations caused by grinding forces.

- Grinding Wheel Reconditioning

It can be said, that rotating dressing tools generally should be preferred to non-rotating ones. On the other hand, non-rotational dressing tools constitute an inexpensive alternative which is also able to provide satisfactory results. To accomplish this, the device type and the reconditioning parameters have to be perfectly adjusted to the dressing conditions at hand.

Investigations of machine A08's reconditioning system revealed that the dressing parameters have to be adapted. For dressing plates, a value between $5\ \mu\text{m}$ and $30\ \mu\text{m}$ for a_{ed} is recommended. Furthermore, the overall cutting depth per dressing process $a_{ed,ges}$ has to be decreased to a range of $20 - 40\ \mu\text{m}$. Currently, only one dressing stroke per reconditioning operation is performed.

In this context, a procedure with two dressing strokes and values for the depth of cut $a_{ed1} = 30\ \mu\text{m}$ and $a_{ed2} = 10\ \mu\text{m}$ can be advised. A test procedure has been set up in order to verify the effectiveness of the proposed parameter adjustment which is derived from theoretical considerations. The results of a preliminary investigation are satisfying. Further studies have to be performed by the supplier in order to gain further insights.

When taking into account deployed grinding grain material and further conditions, the current dressing tool (dressing plate with natural diamond grains) does not constitute the best solution. A tool change to dressing plates with set diamond sticks is advisable in order to improve dressing process stability. Mono-crystalline diamond (MCD) as stick material can be recommended.

Furthermore, the coolant supply has to be improved in order to ensure, that the contact zone is sufficiently provided with cooling liquid. More information regarding that topic is presented in the following section.

In order to be able to meet different surface roughness requirements of various axle seats, the implementation of an additional dressing operation is strongly advisable. Currently deployed strategy of different spark-out times should be replaced by a reconditioning step between machining of axle seats with different roughness requirements.

- Cooling Systems in Grinding Machines

The cooling liquid supply of the grinding zone (contact between workpiece and grinding wheel) is of great importance for satisfying machining results. The same is true for the reconditioning process as diamond material is highly heat sensitive. The contact zone (grinding wheel and reconditioning tool) has to be provided with a sufficient amount of cooling liquid.

A state of equal velocity fluid delivery has to be ensured by adapting coolant jet's parameters to proposed values (Table 7). Furthermore, the implementation of a straight line supply with a setting angle of about 20° (Figure 19 (b)) is strongly recommended.

6 Bibliography

AMEST (publ.) (2008): *Maßkontrolle von finalen Eisenbahnachsen*, retrieved from <http://www.amest.cz/neuheiten/makontrolle-von-finalen-eisenbahnachsen> [accessed April 10, 2017]

AMEST (publ.) (2016): *Measuring Unit (Drawing)*, obtained from customer service after inquiry [received December 5, 2016]

Audi AG; BMW AG; Robert Bosch GmbH; Daimler Chrysler AG; Fiat Auto S.p.A.; Ford-Werke AG; Adam Opel AG; Q-DAS GmbH; T.Q.M. Itaca s.r.l. & Volkswagen AG (publ.) (2002): *Leitfaden zum „Fähigkeitsnachweis von Messsystemen“*, retrieved from http://www.q-das.com/uploads/tx_sbdownloader/Leitfaden_v21_me.pdf [accessed April 10, 2017]

Böge, Alfred; Eichler, Jürgen (2008): *Physik für technische Berufe*, 11th ed., Wiesbaden: Vieweg + Teubner Verlag

Bredner, Barbara (2014): *Prozessfähigkeit bei technisch begrenzten Merkmalen - Fähigkeitskennzahlen und Berechnungsmethoden*, retrieved from http://www.drsteuer.de/vorlagen/Prozessfaehigkeit_bei_technisch_begrenzten_Merkmale_n_Jan_14.pdf [accessed April 10, 2017]

Carl Zeiss Industrielle Messtechnik (publ.) (2017): *GPS zur Spezifikation geometrischer Anforderungen und messtechnischer Prüfungen in der industriellen Produktion*, n.p.

Chernov, Nikolai; Lesort Claire (2005): *Least Squares Fitting of Circles*, in: Journal of Mathematical Imaging and Vision, no. 23, p. 239-252, retrieved from <http://link.springer.com/article/10.1007/s10851-005-0482-8> [accessed April 10, 2017]

Chrysler Group LLC; Ford Motor Company & General Motors Corporation (publ.) (2010): *Measurement System Analysis: Reference Manual*, 4th ed., n.p.

Daimler Chrysler Corporation; Ford Motor Company & General Motors Corporation (publ.) (2005): *Statistical Process Control (SPC): Reference Manual*, 2nd ed., n.p.

Danzer, Hans Heinz (2013): *Advanced Product Quality Planning*, in: Kamiske, Gerd F.: *Handbuch QM-Methoden, Die richtige Methode auswählen und erfolgreich umsetzen*, München: Hanser Verlag, p. 81-95

Danzer, Hans Heinz (2016): *Qualitätsorientiertes Management*, Graz: n.p.

DANOBAT (publ.) (n.d.): *End Machining Centre*, retrieved from <http://railways.danobatgroup.com/media/uploads/solutions/axle-ends-facing-machine-railways-sm1.pdf> [accessed April 10, 2017]

Dillinger, Josef et al. (2007): *Fachkunde Metall, Mechanische Technologie*, 55th ed., Haan-Gruiten: Verlag Europa Lehrmittel

DIN Deutsches Institut für Normung e.V. (publ.) (2008): DIN EN ISO 1101: Geometrische Produktspezifikation (GPS) – Geometrische Tolerierung – Tolerierung von Form, Richtung, Ort und Lauf

DIN Deutsches Institut für Normung e.V. (publ.) (2011): DIN EN ISO 8015: Geometrische Produktspezifikation (GPS) – Grundlagen – Konzepte, Prinzipien und Regeln

DIN Deutsches Institut für Normung e.V. (publ.) (2011): DIN EN ISO 14405-1: Geometrische Produktspezifikation (GPS) – Dimensionelle Tolerierung – Teil 1: Längenmaße

DIN Deutsches Institut für Normung e.V. (publ.) (2011): DIN EN ISO 12180-2: Geometrische Produktspezifikation (GPS) – Zylindrizität – Teil 2: Spezifikationsoperatoren

Dr. Kaiser Diamantwerkzeuge (publ.) (2012): *Abrichten von Schleifscheiben*, Celle

Haigermoser, Andreas (2002): *Schienerfahrzeuge*, Graz: n.p.

Hehenberger, Peter (2011): *Computerunterstützte Fertigung*, Berlin/Heidelberg: Springer-Verlag

Heisel, Uwe et al. (2014): *Handbuch Spanen*, 2nd ed., München: Hanser Verlag

Klocke, Fritz; König Wilfried (2005): *Fertigungsverfahren: Schleifen, Honen, Läppen*, 4th ed., Berlin/Heidelberg: Springer-Verlag

Klocke, Fritz (n.d.): *Cutting with geometrically undefined cutting edges I*, retrieved from http://www.wzl.rwth-aachen.de/de/f786439a4c53fb78c125709f0055702f/l09_grinding_i.pdf [accessed April 8, 2017]

Keferstein, Claus P.; Marxer, Michael (2015): *Fertigungsmesstechnik: Praxisorientierte Grundlagen, moderne Messverfahren*, 8th ed., Wiesbaden: Springer Vieweg Verlag

Parthier, Rainer (2008): *Messtechnik*, 4th ed., Wiesbaden: Friedrich Vieweg & Sohn Verlag

Saint-Gobain (publ) (2014/2015): *Katalog 5: Abrichtwerkzeuge - WINTER Diamantwerkzeuge für das Abrichten von Schleifkörpern*, retrieved from http://www.winter-superabrasives.com/uploadedFiles/SGwintersuperabrasives/Documents/WINTER_Abrichtwerkzeuge_Nr5_2247.pdf [accessed April 10, 2017]

Siemens Mobility (publ.) (2016): *Neue Züge von Siemens für Thameslink-Strecke*, retrieved from http://www.siemens.com/press/pool/de/pressebilder/2016/mobility/300dpi/IG2016060041MODE_300dpi.png [accessed April 7, 2017]

Siemens AG (publ.) (2013): *SF 7000 das innovative Fahrwerkskonzept als Antwort auf Whole Life Cost Modelle*, retrieved from http://www.schienerfahrzeugtagung.at/download/PDF2013/21_Hirtenlechner.pdf [accessed April 7, 2017]

Studer AG (publ.) (n.d.): *Auswahl des richtigen Abrichtwerkzeuges*, retrieved from <https://www.studer.com/de/ueber-studer/newsinformationsmaterial/newsletters/2012-11/abrichtwerkzeuge.html> [accessed April 10, 2017]

Tränkler, Hans-Rolf; Fischerauer, Gerhard (2014): *Das Ingenieurwissen: Messtechnik*, Heidelberg: Springer Vieweg Verlag

Uhlmann, Eckert (2014(a)): *Schleifen: Allgemeines*, in: Heisel, Uwe et. al: *Handbuch Spanen*, 2nd ed., München: Hanser Verlag, p. 531-535

Uhlmann, Eckert (2014(b)): *Rundschleifen*, in: Heisel, Uwe et. al: *Handbuch Spanen*, 2nd ed., München: Hanser Verlag, p. 538-539

Uhlmann, Eckert (2014(c)): *Konditionieren*, in: Heisel, Uwe et. al: *Handbuch Spanen*, 2nd ed., München: Hanser Verlag, p. 569-583

Uhlmann, Eckert (2014(d)): *Schleifen: Berechnungsverfahren*, in: Heisel, Uwe et. al: *Handbuch Spanen*, 2nd ed., München: Hanser Verlag, p. 546-560

Winterthur Technology Group (publ.) (2006): *Leitfaden Rundschleifen*, n.p.

7 List of Figures

Figure 1: Integration of wheelset axle in complete rail vehicle, Source: Rail Vehicle: Based on Siemens Mobility (2016); Bogie: Siemens AG (2013), p. 11; Wheelset: Own illustration; Axle: Own illustration.	2
Figure 2: Automated finish machining line, Source: Own illustration.....	3
Figure 3: Axle finish machining process (top view), Source: Own illustration.....	5
Figure 4: Interaction of Q7-Tools, Source: Based on Hehenberger (2011), p. 211.	6
Figure 5: Original value chart, Source: Based on Hehenberger (2011), p. 212.....	7
Figure 6: Check sheet, Source: Based on Hehenberger (2011), p. 212.	8
Figure 7: Ishikawa diagram, Source: Based on Hehenberger (2011), p. 215.....	9
Figure 8: Process control, Source: Daimler Chrysler Corporation et al. (2005), p. 18.....	9
Figure 9: Process capability, Source: Daimler Chrysler Corporation et al. (2005), p. 18...10	10
Figure 10: Normal distribution of process output, Source: Based on Danzer (2016), p. 127.	11
Figure 11: Comparison “Goal Post Mentality” and Taguchi Loss Function, Source: Based on Daimler Chrysler Corporation et al. (2005), p. 148.	12
Figure 12: Grinding wheel, Source: Based on Dillinger et al. (2007), p. 175.....	13
Figure 13: Straight line cylindrical plunge grinding, Source: DIN 8589-11 (2003), n.p., quoted from Uhlmann (2014(b)), p. 539.	14
Figure 14: Parameters of grinding system, Source: Based on Klocke, König (2005), p. 186	15
Figure 15: Non-rotational dressing tool, Source: Klocke, König (2005), p. 158.	18
Figure 16: Rotating dressing tool (form roll), Source: Klocke, König (2005), p. 160.	19
Figure 17: Contact conditions of a form roll dressing procedure, Source: Based on Klocke, König (2005), p. 177,178.....	20
Figure 18: Relation between velocity ratio qd and effective grinding wheel roughness R_{ts} , Source: Saint-Gobain (2014/2015), p. 111.....	21
Figure 19: Coolant supply, Source: Winterthur Technology Group (2006), p. 98.....	23
Figure 20: Linear variable differential transducer, Source: Based on Keferstein, Marxer (2015), p. 142.	26
Figure 21: Relation between measuring pin displacement x and induced voltage ΔU , Source: Based on Tränkler, Fischerauer (2014), p. 24.....	26
Figure 22: Optical incremental transducer, Source: Based on Keferstein, Marxer (2015), p. 144.....	27
Figure 23: Approaches for diameter determination, Source: Carl Zeiss Industrielle Messtechnik (2017), p. 8.....	28
Figure 24: Cylindricity evaluation, Source: DIN EN ISO 1101 (2008), p. 60.	30
Figure 25: Systematic error of measurement system, Source: Based on Chrysler Group LLC et al. (2010), p. 6.	32

Figure 26: Variation of a measurement system, Source: Based on Chrysler Group LLC et al. (2010), p. 7.....	33
Figure 27: Approach for measurement system analysis, Source: Based on Audi AG et al. (2002), p. 18.	34
Figure 28: 3D measuring machine, Source: AMEST (2008).	36
Figure 29: Measuring unit, Source: AMEST (2016).	37
Figure 30: Cylinder determination, Source: Own illustration.	37
Figure 31: Ishikawa diagram for automated 3D measurement system, Source: Own illustration.	43
Figure 32: Comparing measurements between 3D measurement system and CMM, Source: Own illustration.	45
Figure 33: Original value charts for wheel seat diameter A-side (a) and B-side (b), Source: Own illustration.	49
Figure 34: $\bar{x} - R$ - charts for axle's A- (left) and B-side (right), Source: Own illustration.	50
Figure 35: Cylindricity of A- and B-side's wheel seat, Source: Own illustration.....	52
Figure 36: Axle Clamping in grinding machine, Source: Own illustration.	53
Figure 37: Machining of axle's centering bore, Source: DANOBAT (n.d.).....	53
Figure 38: Ishikawa diagram for grinding process, Source: Own illustration.	55
Figure 39: Extract from the R&R-Analysis form, Source: Own illustration.....	57
Figure 40: In-process measurement system, Source: Own illustration.	60
Figure 41: In-process measuring device, Source: Own illustration.	61
Figure 42: Shape error in measuring plane, Source: Own illustration.	62
Figure 43: Repeatability test results for machine A07 (a) and machine A08 (b), Source: own illustration.	63
Figure 44: Comparison of contact geometries, Source: Own illustration.....	65
Figure 45: Course of measuring error (a) and angle error definition (b), Source: Own illustration.	65
Figure 46: Roughness of A- and B-side's axle seats, Source: Own illustration.	68
Figure 47: Dressing plate with inserted diamond grains, Source: Own illustration.	69
Figure 48: Dressing plate with set diamond sticks, Source: Dr. Kaiser Diamantwerkzeuge (2012), p. 9.	69
Figure 49: Roughness requirements for different axle seats, Source: Own illustration.	71

8 List of Tables

Table 1: Reconditioning of grinding wheels, Source: Uhlmann (1994), n.p., quoted from Uhlmann (2014(c)), p. 570.	17
Table 2: Conditions of type-3 study, Source: Own illustration.....	40
Table 3: Bias of 3D measurement system, Source: Own illustration.....	45
Table 4: Conditions R&R-analysis, Source: Own illustration.	57
Table 5: Range of measurement values for different axles, Source: Own illustration.	59
Table 6: Grinding machining parameters, Source: Reference values based on Winterthur Technology Group (2006), p. 41, 45.	72
Table 7: Required volume flow and pressure of coolant jet, Source: Based on Winterthur Technology Group (2006), p. 100.	74

9 Appendix

1. Table for Values of d_2^*
2. Calculation Form for MSA
3. Example of Evaluation Results (Wheel Seat Diameter B-Side; Batch May 2016)
4. Example of Cylindricity Evaluation (Wheel Seat B-Side; Batch May 2016)
5. Machining Process Optimization Measures (Recommendations for Lucchini RS)

1. Table for Values of d_2^*

Source: Audi AG et al. (2002), p. 56.

		Sample Size: No. of Repetitions (r) for K_1 or No. of Operators (k) for K_2													
		Stichprobenumfang: Anzahl Wiederholungen (r) für K_1 oder Anzahl Prüfer (k) für K_2													
d_2^*		2	3	4	5	6	7	8	9	10	11	12	13	14	15
Anzahl Stichproben: $k \cdot n$ Anzahl Prüfer (k) * Anzahl Teile (n)	1	1.41	1.91	2.24	2.48	2.67	2.83	2.96	3.08	3.18	3.27	3.35	3.42	3.49	3.55
	2	1.28	1.81	2.15	2.40	2.60	2.77	2.91	3.02	3.13	3.22	3.30	3.38	3.45	3.51
	3	1.23	1.77	2.12	2.38	2.58	2.75	2.89	3.01	3.11	3.21	3.29	3.37	3.43	3.50
	4	1.21	1.75	2.11	2.37	2.57	2.74	2.88	3.00	3.10	3.20	3.28	3.36	3.43	3.49
	5	1.19	1.74	2.10	2.36	2.56	2.73	2.87	2.99	3.10	3.19	3.28	3.35	3.42	3.49
	6	1.18	1.73	2.09	2.35	2.56	2.73	2.87	2.99	3.10	3.19	3.27	3.35	3.42	3.49
	7	1.17	1.73	2.08	2.35	2.55	2.72	2.87	2.99	3.10	3.19	3.27	3.35	3.42	3.48
	8	1.17	1.72	2.08	2.35	2.55	2.72	2.87	2.98	3.09	3.19	3.27	3.35	3.42	3.48
	9	1.16	1.72	2.08	2.34	2.55	2.72	2.86	2.98	3.09	3.18	3.27	3.35	3.42	3.48
	10	1.16	1.72	2.08	2.34	2.55	2.72	2.86	2.98	3.09	3.18	3.27	3.34	3.42	3.48
	11	1.16	1.71	2.08	2.34	2.55	2.72	2.86	2.98	3.09	3.18	3.27	3.34	3.41	3.48
	12	1.15	1.71	2.07	2.34	2.55	2.72	2.85	2.98	3.09	3.18	3.27	3.34	3.41	3.48
	13	1.15	1.71	2.07	2.34	2.55	2.71	2.85	2.98	3.09	3.18	3.27	3.34	3.41	3.48
	14	1.15	1.71	2.07	2.34	2.54	2.71	2.85	2.98	3.08	3.18	3.27	3.34	3.41	3.48
	15	1.15	1.71	2.07	2.34	2.54	2.71	2.85	2.98	3.08	3.18	3.26	3.34	3.41	3.48
	> 15	1.128	1.693	2.059	2.326	2.534	2.704	2.847	2.970	3.078	3.173	3.258	3.336	3.407	3.472

2. Calculation Form for MSA (Used in Type-2 Study for Manual Diameter Measurement)

Meßsystemfähigkeitsanalyse

Measurement System Analysis (MSA)

Part Number & Name : Thameslink Trailer Axle
 Characteristics : Wheel Seat
 Specification Limits : XXX.252 - XXX.277

Gage Name : Micrometer
 Gage No. :
 Gage Type : +, - 50 µm

Gage Display Exactness: 1 µm
 Date : November 23, 2016
 Performed By : Rosenberger Lukas

Part Number	Appraiser 1 (Operator 1)			Appraiser 2 (Operator 2)			Appraiser 3 (Operator 3)			Part Average		
	1	2	3	1	2	3	1	2	3			
1	.275	.276	.274	.278	.276	.277	.275	.275	.276	.275	0.001	.276
2	.265	.265	.265	.267	.265	.266	.265	.264	.265	.265	0.001	.265
3	.271	.271	.272	.275	.273	.274	.272	.272	.272	.272	0.001	.273
4	.272	.274	.271	.275	.276	.276	.274	.271	.272	.272	0.003	.273
5	.266	.270	.265	.270	.267	.269	.265	.265	.267	.266	0.002	.267
6												
7												
8												
9												
10												
Average	X1 = .2703			X2 = .2725			X3 = .2701			X̄ = .2710		
Range of Appraiser !!!!	R1 = 0.0026			R2 = 0.0020			R3 = 0.0016			Rp = 0.0106		
R = (R1 + R2 + R3) / No. of Appraisers =	0.0021											
X _{diff} = (Max. of X1, X2, X3 - Min. of X1, X2, X3) =	0.0025											
UCLR = R * D4 (D4 = 3.27 OR 2.58 for 2 and 3 measurements) =	0.0053											
LCLR = R * D3 (D3 = 0 for up to 7 trials) =	0.0000											

If R & R as % of Tolerance is required, enter Tolerance Range ----> 0.0250

Repeatability - Equipment Variation (EV) = (R * K1) = 0.0063
 (K1 = 4.56 OR 3.05 for 2 and 3 Measurements respectively)

Reproducibility - Appraiser (AV) = $\sqrt{\frac{(X_{diff} * K2)^2 - (EV^2 / n * r)}{n}}$
 Variation AV = 0.0065 (K2 = 3.65 OR 2.70 for 2 or 3 Appraisers)
 n = Number of Parts, r = Number of Measurements

Repeatability & Reproducibility, R & R = $\sqrt{(EV^2 + AV^2)}$
 R & R = 0.0090

Part Variation (PV) = Rp * K3 = 0.0220
 (Value of K3 taken from the given table)

Parts	K3
5	2.08
6	1.93
7	1.82
8	1.74
9	1.67
10	1.62

Total Process Variation, TPV is determined from Sample Values

$$TPV = \sqrt{(R \& R^2 + PV^2)}$$

TPV = 0.0237

% Gauge R & R:

	Tolerance	% of Total Process Variation (TPV)
EV =	25.21	26.55
AV =	25.83	27.21
PV =	87.82	92.49
R & R =	36.10	38.02

Note 1 : Data can be entered only in the columns marked 1, 2, 3 and Cell for Tolerance Range and top header section. (All those cells which are shaded light yellow)

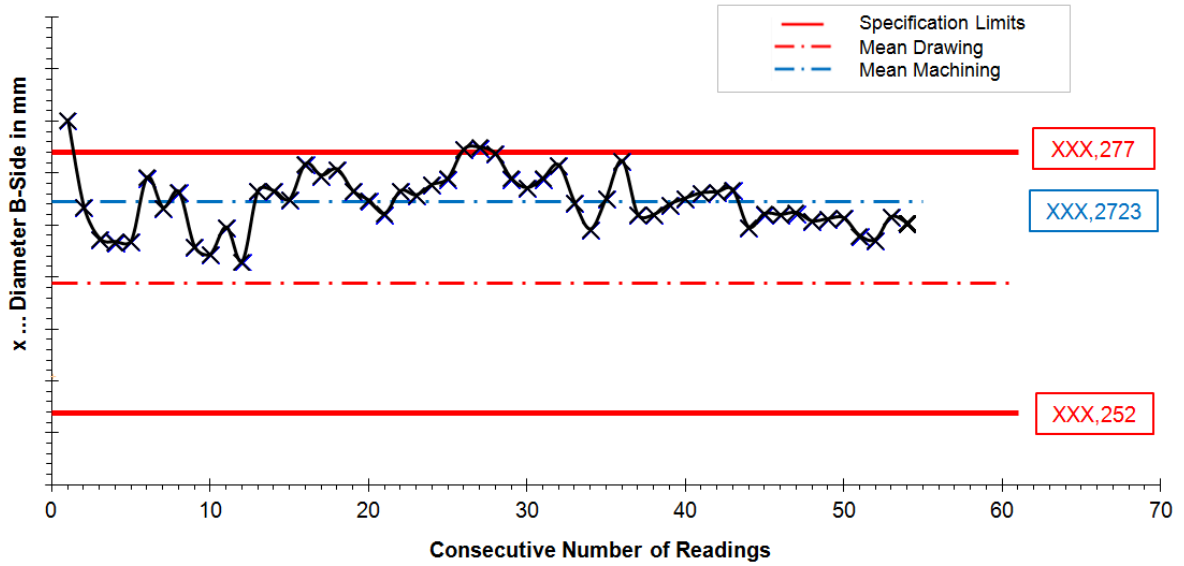
Note 2 : Study require any combination of 2 or 3 Appraisers, 2 or 3 Measurements and any parts from 5 to 10 .

Note 3 : (% R & R Interpretation - Lower of % Tolerance and % Total Process Variation- TPV)
 Under 10% error - Measurement system is acceptable;
 Between 10 - 30 % error - Marginal (May be acceptable based upon importance of application, cost of gage, cost of repairs, etc.;
 More than 30% error - Needs improvement. Make every effort to identify the problems and have them corrected

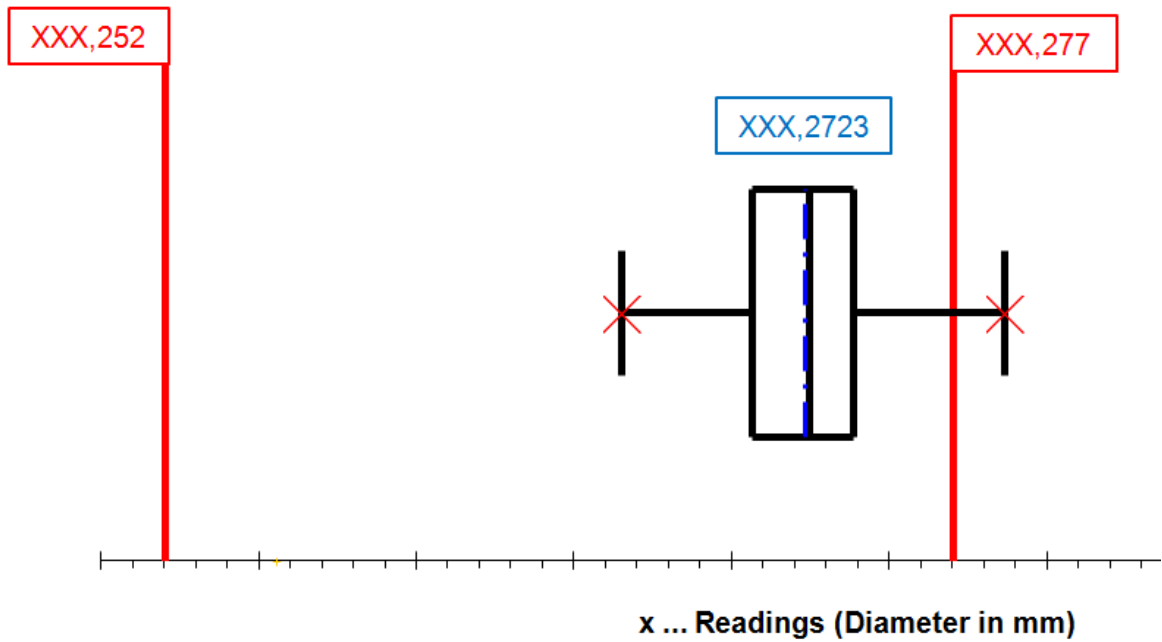
Results of this Gage R & R : MEASUREMENT SYSTEM IS UNACCEPTABLE AND NEEDS IMPROVEMENT

3. Example of Evaluation Results (Wheel Seat Diameter B-Side, Section B1; Batch May 2016)

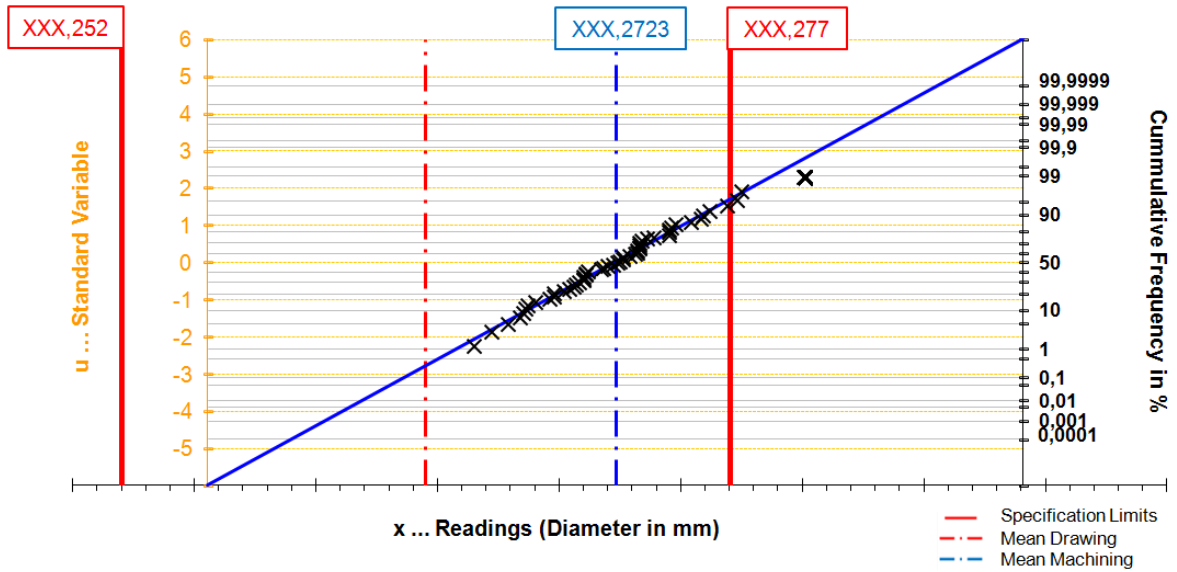
Control Chart



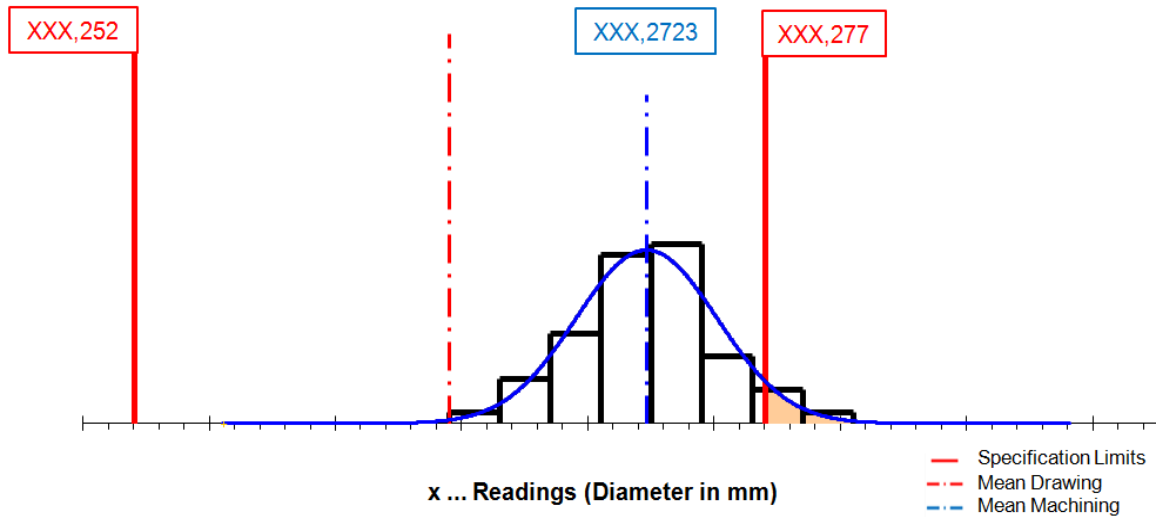
Box Plot



Probability Plot

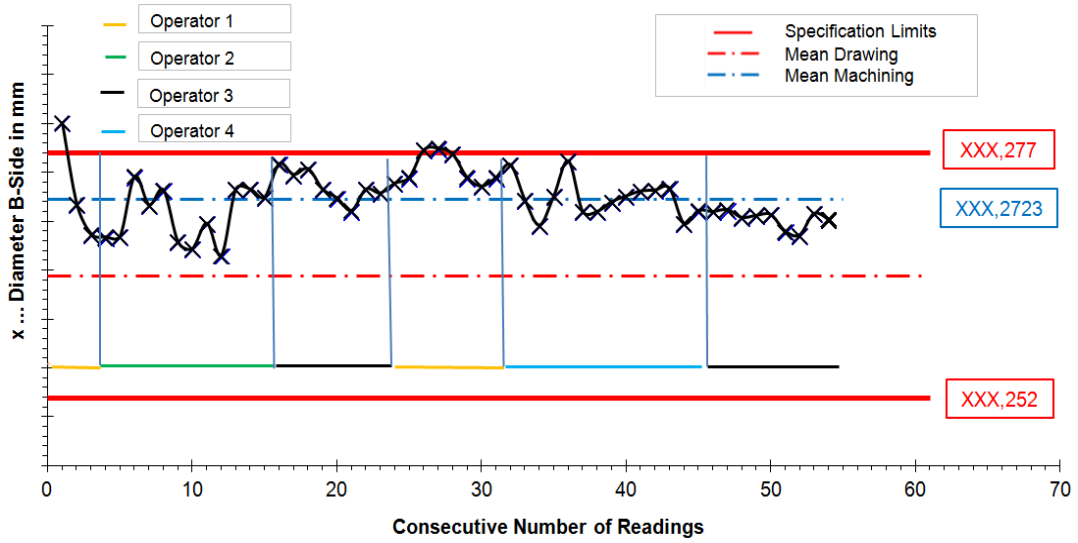


Distribution Curve

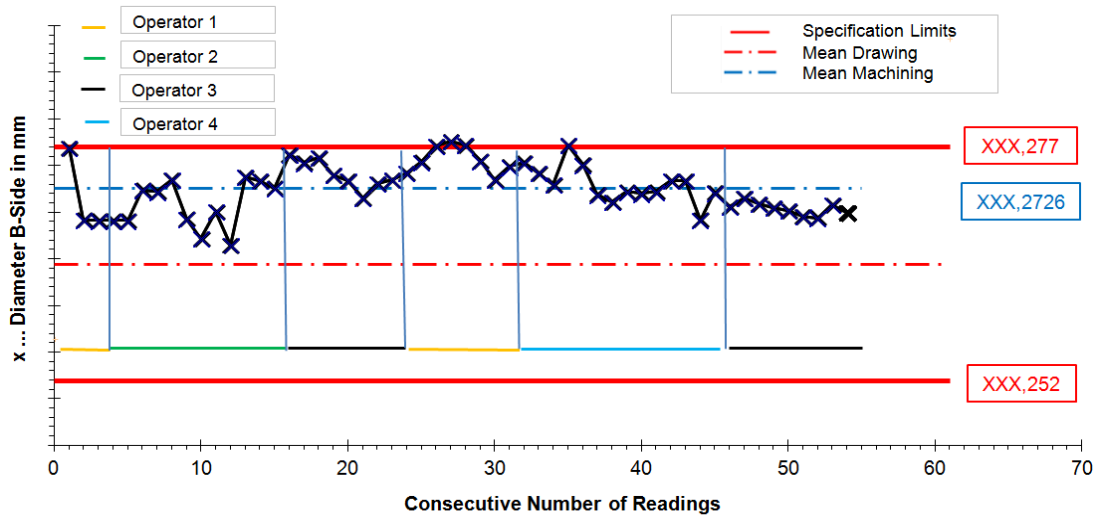


Control Charts with Shift Allocation for Wheel Seat Section 1, 2 & 3

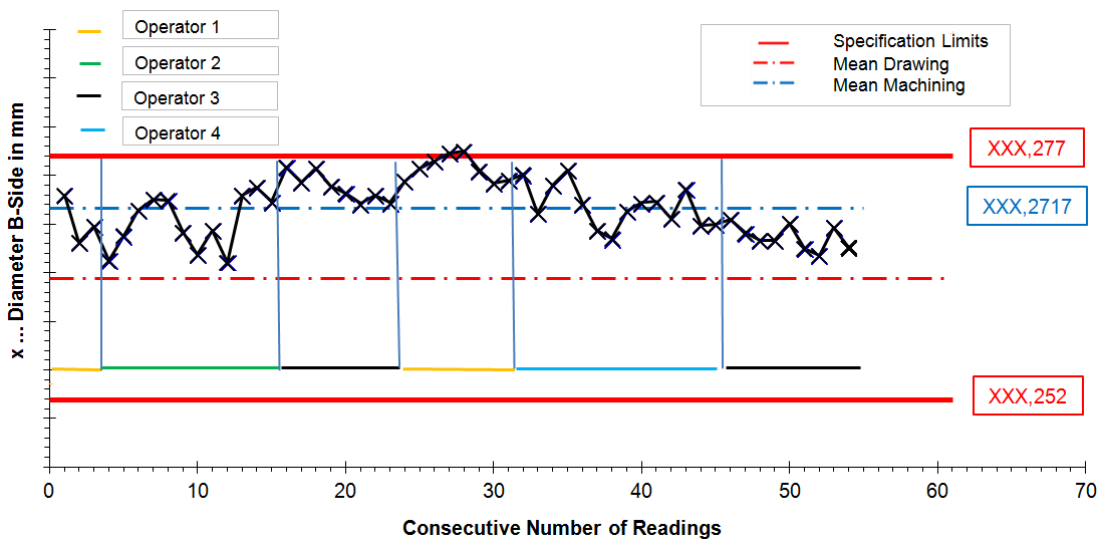
Section B1



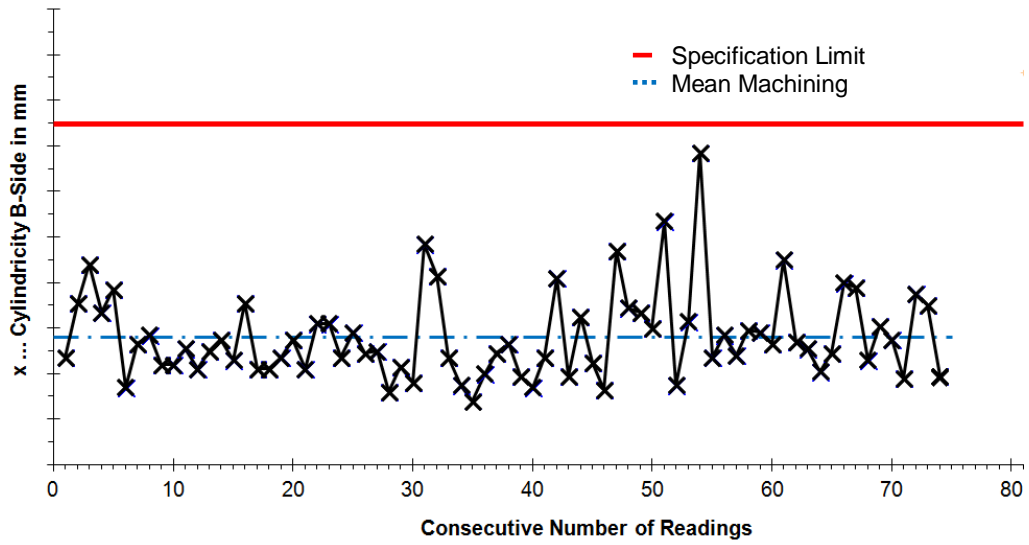
Section B2



Section B3



4. Example of Cylindricity Evaluation (Wheel Seat B-Side; Batch May 2016)



Machining Process Optimization Measures

Recommendations for Lucchini RS

n°	Process Step, Machine, System Element	Findings	Action	Responsible
1	Machining Process Control	<p>1) No uniform machining process control strategy (different operators have different approaches of process control)</p> <p>2) "Goal Post Mentality" is present (every part within tolerance range is seen as equally good)</p>	<p>1) Implementation of uniform process control strategy by provision of instruction for process control (control plan) in combination with operator training</p> <p>2) Get away from "Goal Post Mentality" and take Taguchi's Loss Function as role model</p>	Lucchini RS (LRS)
2	Grinding Machining, Machine A07, In-Process Measuring System (IPMS)	<p>1) High level of bias (big offset between measuring values taken by IPMS and actual value; IPMS measuring value is smaller than actual value); → this leads to part dimensions (diameter) which are close to upper specification limit (USL)</p> <p>2) High level of variation within one measuring run</p> <p>3) Good repeatability results (small variation in measuring results from repeated measurements on same part)</p>	<p>1) Correction of systematic positioning error of measuring head; Implementation of line contact probes → partial error compensation</p> <p>2) Usage of line contact provides more stability in measuring operation (better insensibility against vibrations)</p>	LRS & Manufacturer of IPMS (ongoing) LRS
3	Grinding Machining, Machine A08, In-Process Measuring System (IPMS)	<p>Unsatisfying repeatability results (high level of variation in measuring results from repeated measurements on same part) → causes high level of variation in machine A08's machining process</p>	Variation reduction of IPMS; Investigation of end stop (responsible for positioning of measuring head)	LRS & Manufacturer of IPMS (ongoing)

Machining Process Optimization Measures

Recommendations for Lucchini RS

n°	Process Step, Machine, System Element	Findings	Action	Responsible
4	Grinding Machining, Machine A07 & A08, Machining Approach	<p>Current approach: Machine A07: machining of B-side Machine A08: machining of A-side Different surface roughness requirements only met by different spark-out times → surface roughness close to specification limits (high risk of producing non-conformance parts)</p>	<p>Two possible improvement alternatives: 1) Retention of current approach (best solution in terms of cycle time); Implementation of different dressing procedures for seats with different roughness requirements; Implementation of uniform spark-out procedure for all axle sections 2) Change of machining approach: Machining of all seats with same roughness requirement (Ra max. 0.8 on both axle sides) in one machine and all seats with other requirement (Ra 0.8-1.6 on both axle sides) in other machine</p>	LRS (investigations ongoing)
5	Grinding Machining, Machines A07 & A08, Machining Parameters	<p>1) Metal removal rate $Q'w$ is on a low level (especially in early stages of multistage grinding process) → potential for machining time reduction 2) Velocity ratio qs up to 5 times higher than recommended literature</p>	<p>1) Increase of radial feed ratio vfr 2) Decrease of qs by increase of axle rotational speed</p>	LRS
6	Grinding Machining, Machine A08, Dressing System	<p>1) Dressing parameters are not perfectly adjusted to dressing tool in use (dressing plate with diamond grains) → unstable dressing results and therefore unstable surface roughness at production parts</p>	<p>1) Adjustment of cutting depth aed and number of dressing strokes (investigations ongoing) Alternative Solution: Change of dressing tool (dressing plate with set diamond sticks)</p>	LRS & Manufacturer of Dressing Tool (investigations ongoing)

Machining Process Optimization Measures Recommendations for Lucchini RS

n°	Process Step, Machine, System Element	Findings	Action	Responsible
7	Grinding Machining, Machines A07 & A08, Cooling System	<p>For satisfying machining and dressing results, the contact zone (grinding wheel/axle or grinding wheel/dressing tool) has to be sufficiently supplied with coolant;</p> <p>Influencing factors:</p> <ul style="list-style-type: none"> i) Nozzle geometry/design ii) Volume flow of coolant iii) pressure of coolant jet 	<ul style="list-style-type: none"> i) Replace current coolant supply (plugable plastic elements) by a straightline supply ii & iii) Change Volume flow and pressure of supplied coolant to proposed values (chapter 2.2.3.2 and 4.2.6 in Thesis) 	LRS
8	Final Inspection, Machine A10	<p>Automated 3D measuring system not capable due to a high level of bias (systematic offset between determined measuring values and actual values).</p> <p>Bias mainly caused by temperature difference between masterpiece and axle</p>	<p>Consideration of temperature difference between masterpiece and axle in measuring process.</p> <p>Implementation of probes for determination of axle and production part temperature.</p> <p>Extension of system's software for consideration of temperature difference.</p>	LRS & Manufacturer of measurement system (ongoing)